University of Nevada, Reno

Genetic Analyses of Ca^{2+} Circuits in Arabidopsis Vegetative and Reproductive Development

A dissertation submitted in partial fulfillment of the requirements for the degree of

Doctor of Philosophy in

Biochemistry

By:

Maryam Rahmati Ishka

Dr. Jeffrey F. Harper/Dissertation Advisor

December, 2015

THE GRADUATE SCHOOL

We recommend that the dissertation
prepared under our supervision by

MARYAM RAHMATI ISHKA

Entitled

Genetic Analyses Of Calcium Circuits In Arabidopsis Vegetative And Reproductive Development

be accepted in partial fulfillment of the
requirements for the degree of

DOCTOR OF PHILOSOPHY

Jeffrey F. Harper, Advisor

John C. Cushman, Committee Member

David K. Shintani, Committee Member

Grant R. Cramer, Committee Member

William E. Courchesne, Graduate School Representative

David W. Zeh, Ph. D., Dean, Graduate School

December, 2015

Abstract

Calcium homeostasis is maintained by the action of different calcium transporters including channels, antiporters, and calcium pumps. Calcium channels provide an influx pathway whereas calcium antiporters and pumps provide an efflux system. Together, influx and efflux systems create a calcium circuit. One of the calcium circuits operating in plant cells is associated with the endoplasmic reticulum (ER). In chapter II, results are presented on the functional characterization of three calcium pumps in Arabidopsis with ER and ER-like localization. In chapter III and IV, Arabidopsis pollen transcriptome data are presented, which compare heat-stress induced changes in the pollen transcriptomes of wild type and a mutant harboring a knockout of a *cyclic nucleotide gated channel* (*cngc16*).

Calcium pumps ACA1, 2, and 7 belong to the type IIB subfamily of Ca^{2+}-ATPases. In a comparison of protein sequences for all ten ACA Ca^{2+}-pumps in Arabidopsis, ACA1, 2, and 7 cluster as a distinct subgroup. Members of this subgroup all appeared to localize to the ER or ER-like structures when expressed in stably transformed plants with a YFP tag and imaged with confocal microscopy. A loss-of-function for all three ACAs, *ACA1*, *2*, and *7*, resulted in plants showing a lesion-like phenotype in the leaves. This phenotype was suppressed by the expression of a *NahG* transgene, which encodes an enzyme that degrades salicylic acid, indicating that the lesion phenotype is dependent on salicylic acid. In addition, a triple knockout of *aca1/2/7* resulted in a decrease in pollen transmission efficiency when assayed in competition with wild type pollen. This pollen transmission deficiency was exacerbated when crosses were done under temperature stress conditions. Both phenotypes could be rescued by the expression of any of the three

ACA1, 2 or *7* genes, suggesting that all three genes encode Ca^{2+}-pumps that are functionally interchangeable. Together, these results establish ACA1, 2, and 7 as a subgroup of ER-localized autoinhibited Ca^{2+}-ATPases that normally function to suppress an SA-dependent programmed cell death pathway in leaves, and are also important for pollen fitness under normal and temperature stress conditions.

Under temperature stress conditions, pollen harboring a *cngc16* knockout are nearly sterile, and show a greater than 10-fold decrease in pollen transmission efficiency compared to wild-type pollen. To gain further insight into mechanisms underlying this hypersensitivity, an RNA-Seq experiment was performed to compare the stress-dependent changes in the pollen transcriptomes from wild-type and a *cngc16* knockout parent. In response to a heat stress, the wild-type pollen transcriptome showed 2,612 changes (≥2-fold changes and adjusted $p<0.01$). Of these, 641 changes (~ 25%) failed to occur in the *cngc16* knockout, identifying a subset of failed responses that might contribute to the poor stress tolerance displayed by *cngc16* pollen. At the same time, the mutant displayed 2,733 changes that were not seen in wild-type pollen. Of these differences between wild type and *cngc16*, 148 were associated with transcription factors, suggesting that a primary defect in the *cngc16* mutant lies in its inability to properly reprogram the transcriptome in response to a heat stress. Overall, the RNA-Seq experiment here provides a great resource for research community to explore genes function of potential importance to pollen thermotolerance.

Acknowledgements

I would first like to thank my excellent advisor Dr. Jeff Harper for allowing me to work under his supervision. I would like to appreciate Jeff for all of his efforts to mentoring and supporting me during these five years. I have learned a lot from Jeff, but the most importantly, I have learned to do not give up.

I would also like to appreciate my committee members Dr. John C. Cushman, Dr. David K. Shintani, Dr. Grant R. Cramer, Dr. William E. Courchesne for being part of my dissertation committee members and for their guidance. I would like to thank Dr. John C. Cushman especially for proofreading of the entire of my dissertation. I also would like to thank Dr. David K. Shintani for his support during these five years to make sure my dissertation moving forward. I would like to especially thank Dr. Grant R. Cramer for hosting me in his lab until I found new lab to work.

I would also like to thank to Harper lab former and present members for being great labmates. I would like to thank Liz Brown especially for all of her help and supports. I would like to thank Dr. Meral Tunc-Ozdemir and Dr. Kelly Zinn for their friendship and scientific advices. Also I would like to thank Taylor Cohen, Alexa Rosenberg, and Olivia Alexander-Leeder for their technical assistance.

I would also like to thank my friends Supakan Rattanakon and Richard Lohaus for their friendship and for all wonderful time we had spent together.

Lastly, I would like to thank my parents Alireza Rahmati Ishka and Sekineh Mehdipour for their unconditional love and supports. Without their hard works, I would not be the person I am right now. Special thanks to my husband Mohammad Yazdani for being so nice and patient to me and for his love and special thanks to my lovely sons, Danial and Aryan, who always make me happy and busy.

Table of Contents

List of Tables

List of figures

Chapter I.
Introduction: Auto-inhibited Ca^{2+} ATPases and pollen transcriptome

In this work we present two main topics: Functional analysis of Arabidopsis Ca^{2+} ATPases 1, 2, and 7 (ACA1, 2, and 7), which will be covered in chapter II, and transcriptome comparison of wild-type pollen and *cngc16* knockout pollen under hot/cold stress condition, which will be discussed in chapters III and IV. This RNA-Seq experiment was done to compare the transcriptomes of wild-type pollen with that from a cyclic nucleotide gated channel 16 (*CNGC16*) mutant under hot/cold stress condition.

Functional analysis of Arabidopsis Ca^{2+}-ATPases

Plants are sessile. To combat environmental stimuli, plants developed several adaptive mechanisms. Ca^{2+} as a universal second messenger is required for cell survival. Cytosolic Ca^{2+} concentration is usually maintained at sub-micromolar levels (ranging from 200 nM to 0.1-1 μM; Poovaiah and Reddy 1993). There are transient increases in cytosolic Ca^{2+} concentrations in response to different stresses or developmental signals. Different stimuli can trigger the release of Ca^{2+} from subcellular locations such as Endoplasmic Reticulum (ER), vacuole, or trigger an influx of Ca^{2+} across the plasma membrane from the extracellular space (White 2000). Ca^{2+} homeostasis is maintained by Ca^{2+} influx and efflux transport systems, which in turn create Ca^{2+} circuits in different parts of a cell. Ca^{2+} circuits operate within plant cells at least in three subcellular locations including vacuole, the endoplasmic reticulum (ER), and the plasma membrane. How these Ca^{2+} circuits interact to regulate Ca^{2+} homeostasis is important.

Ca^{2+} signaling in plants

Many aspects of plant growth and development that are regulated by the Ca^{2+} signaling including stomata closure and opening, symbiosis in legumes, pathogen responses, programmed cell death, and polarized tip growth in roots and pollen tubes (Kudla et al., 2010).

Ca^{2+} transport systems

There are at least three types of Ca^{2+} transport systems including Ca^{2+} channels, Ca^{2+} antiporters, and Ca^{2+} pumps. Ca^{2+} channels release Ca^{2+} into the cytosol from either the apoplast or cellular organelles such the vacuole and the ER. They move Ca^{2+} across membranes without energy consumption (referred to as passive transport). Ca^{2+} channels are located in different membranes from plasma membrane to endo-membranes such as the tonoplast and the ER. There are at least three different types of Ca^{2+} channels: depolarization-activated, hyper-polarization-activated, and voltage-independent (White 2002).

Ca^{2+}/H^{+} exchangers/antiporters (also known as cation exchanger or CAX) are another type of Ca^{2+} transport system. They move Ca^{2+} (or other cations such as cadmium) and H^{+} in opposite direction across the membrane. The Arabidopsis genome encodes at least six CAX genes encoding transporters that are localized to the plasma membrane and organellar membranes such as the tonoplast (Kudla et al., 2010).

Ca^{2+} pumps belong to a large family of P-type ATPases (Geisler et al., 2000). Using the energy from ATP hydrolysis, they transport Ca^{2+} across a membrane against its concentration gradient.

Ca^{2+} ATPases are a subfamily of P-type ATPases

Plant P-type ATPases are encoded by a large superfamily of genes consisting of 5 subfamilies. Type I ATPases include heavy metals pumps. Type II ATPases contain Ca^{2+} ATPases, Na^{+} and K^{+} ATPases, and H^{+} and K^{+} ATPases. Type III ATPases are H^{+} ATPases and Mg^{2+} ATPases. Type IV ATPases contain phospholipid ATPases, and lastly type V ATPases are a group of ATPases without specificity for transport (Geisler et al., 2000).

Plants utilize two types of Ca^{2+} ATPases: PIIA or ER-type Ca^{2+} ATPases (referred to as ECAs; with four gene family members in Arabidopsis) and PIIB or Auto-inhibited Ca^{2+} ATPases (referred to as ACAs; with 10 gene family members in Arabidopsis) (Geisler et al., 2000). These two types of Ca^{2+} pumps have different regulatory features. ECAs have low affinity for Ca^{2+} while ACAs have high affinity. ACAs and ECAs Ca^{2+} pumps also utilize different regulatory mechanisms. The mechanism by which ECA type Ca^{2+} pumps are regulated is unknown (Geisler et al., 2000). Based upon analogy to related pumps in animal systems, ECAs are potentially inhibited by an accessory protein such as phospholamban, which can physically interact with the pump. Phospholamban binding site is close to the aspartylphosphate-forming active site, which in turn can inhibit the pump activity. The inhibitory effects of phospholamban can be released upon phosphorylation followed by dissociation from the pump (Geisler et al., 2000).

ACA-type Ca^{2+} pumps contain an auto-inhibitory region located in either the N- or C-terminal domains. In plants, this auto-inhibitory region is located at the N-terminal end of the pump (Geisler et al., 2000). Auto-inhibition can be released upon Ca^{2+}/CAM binding to the auto-inhibitory region. In the case of ACA2, a phosphorylation of a site within this

auto-inhibitory region was shown to inactivate the Ca^{2+} pumps (Hwang et al., 2000; Geisler et al., 2000).

Biochemical and biological characterization of Ca^{2+} ATPases

Among the four ECAs, isoforms 1 and 3 have been functionally characterized. ECA1 has been shown to be required for plant growth under conditions of Ca^{2+} deficiency and high Mn^{2+} (Wu et al., 2002). ECA3 has been demonstrated to be involved in secretory pathway (Li et al., 2008). This was the first evidence in plants showing a role for a specific Ca^{2+} ATPase in the plant secretory pathway. A loss-of-function analysis showed ECA3 is required for root growth and also tolerance to elevated concentration of Mn^{2+} (Li et al., 2008; Mills et al., 2008). Under the same growth conditions as ECA3, Mills et al. (2008) did not observe any phenotype for *eca1* knockout when grown under condition of low Ca^{2+} and high Mn^{2+}, suggesting that it may have a different function or is redundant with other types of Ca^{2+} pumps.

Biological functions have been proposed for most of the ACA pumps in Arabidopsis except for ACA1, 2, and 12. In chapter II, we present results on a triple knockout of pumps ACA1, 2, and 7. ACA2 was the first ACA that was biochemically characterized as a Ca^{2+}/CAM activated Ca^{2+} pump (Harper et al., 1998).

ACA9 was the first plasma membrane Ca^{2+} pump identified in Arabidopsis (Sciott et al., 2004) with a role in pollen tube growth and fertilization. ACA9 is almost specifically expressed in pollen with minor expression in roots. A T-DNA knockout analysis showed three types of defects are associated with the *aca9* knockout. The mutant has slow

growing and short pollen tubes, which fail to discharge sperm cells into ovules. As a result, the *aca9* knockout is partially male sterile.

A disruption of vacuole Ca^{2+} pump, ACA4 and 11 has been shown to activate a salicylic acid (SA)-dependent programmed cell death (PCD, Boursiac et al., 2010). Expression of ACA11 reversed the double mutant phenotype, providing evidence for functional redundancy of ACA4 and 11. The *aca4/11* lesion phenotype was suppressed by a *sid2* mutation, which disrupts a gene involved in SA biosynthesis, or the introduction of a *NahG* transgene, which encodes an enzyme that degrades SA. This result provided evidence for a role of ACA4 and 11 in regulating the propagation of an SA-dependent PCD pathway. In addition, application of high concentrations of anions such as 15mM NO_3^- was also observed to suppress the *aca4/11* lesion phenotype. The underlying mechanism for this conditional suppression has not understood.

An RNA silencing experiment in tobacco identified a Ca^{2+} pump referred to as NbCA1 with evidence for its function in a plant immune response (Zhu et al., 2010). Silencing of the tobacco Ca^{2+} pump resulted in an accelerated cell death in response to the Tobacco Mosaic Virus. While the authors suggested that NbCA1 was an ER-localized ACA, its amino acid sequence is more similar to those of the Arabidopsis ACA4 and 11, which are localized to the vacuole. This raises the potential that the authors actually silenced the vacuolar pumps, resulting in a phenotype similar to the lesion mimic phenotype describe for *aca4/11*. In chapter II, we show the results from the analysis of a triple knockout of the ER Ca^{2+} pumps which indicate a role in regulating a SA-dependent lesion phenotype, but with a knockout phenotype that is much less severe than that observed for the loss of the vacuolar *aca4/11* pumps.

ACA7 in conjunction with ACA2 and ACA1 forms the subgroup third of ACAs in Arabidopsis. Among this group, ACA7 was the first isoform for which a knockout phenotype was published (Lucca and Leon, 2012). A T-DNA insertion experiment showed 20-50% dead pollen associated with the *aca7* knockout, based upon Alexander staining method. In this method, live pollen were stained as pink, and dead pollen stained turquoise. However, no genetic analysis was done to corroborate the lethal phenotype suggested by the staining result. In chapter II we will present the results of our genetic analyses that indicate that an *aca7* knockout does not result in a pollen autonomous cell-death phenotype.

ACA8 and its homologue ACA10 have been shown to have partial overlapping functions (Frei dit Frey et al., 2012). These two ACAs are involved in plant immune response by limiting bacterial growth. ACA8 interacting with FLS2, flg22 receptor, results in initiation of the plant immune response.

Of the 10 different ACAs in Arabidopsis, ACA12 and 13 are unique in that they are missing a sequence in the N-terminal domain that is proposed to function as an autoinhibitor. A biochemical characterization of ACA12 (Limonta et al., 2014) provided evidence that the pump has a constitutive Ca^{2+}-pump activity that is not further activated by Ca^{2+}/CAM. In contrast to other ACAs, which require a disruption of their autoinbitors in order to rescue a Ca^{2+}-pump deficient yeast mutant, a rescue was observed using the wild-type form of ACA12, indicating this pump has a de-regulated Ca^{2+}-pump activity. Overall, this result suggests that in plants that the requirement for ACA12 activity might be regulated at the level of transcription or translation.

ACA13 has been shown to be highly induced in stigma right after compatible pollination (Iwano et al., 2014). A *T-DNA* insertion experiment showed ACA13 is required for the compatible pollen tube growth into the stigma, and thus fertilization by exporting Ca^{2+} to the pollen tube.

Distribution of Ca^{2+} ATPases in cellular compartments

Among the four ECAs, isoforms 1 is distributed to ER membrane (Liang et al., 1997). ECA3 has dual subcellular locations, Golgi (Mills et al., 2008) and endosomes (Li et al., 2008).

ACA1 subcellular localization is proposed to be at the chloroplast inner envelop (Huang et al., 1993), based upon evidence from membrane fractionation and immuno-detection studies. However, the polyclonal antibody used in this study showed cross-reactivity with other types of Ca^{2+} pumps such as the plasma membrane (Bonza et al., 1998). In a recent study conducted by Dunkley et al. (2006), in an effort for isolating organelle proteome, ACA1 was found in the ER compartment similar to ACA2. Based upon these contradictory results, and a phylogenetic analysis showing ACA1 and ACA2 (along with ACA7) as a distinct subfamily of pumps, we decided to reexamine ACA1 localization, which is discussed in chapter II.

Immunological approach and confocal microscopy have been used to provide evidence that ACA2 is localized to the ER (Harper et al., 1998; Hong et al., 1999), ACA4 to the vacuole (Geisler et al., 2000), ACA8 to the plasma membrane (Bonza et al., 2000), and ACA13 with dual localization as plasma membrane and Golgi bodies (Iwano et al., 2014).

Localization of ACA9 and ACA12 within the plasma membrane (Sciott et al., 2004; Limonta et al., 2014) was determined using YFP- or GFP-tagged proteins in stable transgenic lines, respectively. For GFP-ACA7, a transient expression in tobacco epidermal cells suggested plasma membrane localization (Lucca and Leon 2012).

As evidenced by the phylogenetic analysis, ACA1, 2, and 7 branch together away from other types of ACAs. Thus the speculation is that they target the same subcellular location. In chapter II, the results of subcellular localization of ACA1 and 7 will be presented.

Transcriptome comparison of Arabidopsis wild-type pollen with *cyclic nucleotide gated channel 16* (*cngc16*) knockout under the hot/cold stress condition

Pollen as a cell-autonomous model for research purposes

Arabidopsis pollen is comprised of two sperm cells inside a mother cell that forms a tube and delivers the sperm cells to an ovule. Being able to grow independently from other cell types, pollen provides a model to study the physiology and growth processes as a single cell-autonomous unit.

Pollen and temperature stresses

Climate change is a global threat for all living organism. As a sessile organism, plants have evolved several adaptive mechanisms to face environmental fluctuation. Upon stress application, accumulation of stress responsive proteins such as heat shock proteins, osmo-protectants, and antioxidant enzymes have been reported to protect cells from stresses.

While temperature stresses including heat will affect whole plant, the reproductive organs are one of the most vulnerable parts. Temperature stress can affect flowering time depending on species (Craufurd and Wheeler 2009). For example, a mild temperature stress can accelerate flowering time (Zinn et al., 2010). While a temperature stress can impact both male and female reproductive structures, the male gametophyte might in many cases be the most sensitive. A study conducted by Young et al. (2004) showed that heat stress applied to the pollen of the donor plant before and during pollen release decreased seed number (in both tomato and canola) and fruit set (in tomato) more severely than heat stress applied to the developing ovule and to the style. Several studies have now shown that the most temperature-sensitive process in pollen is during pollen development (Peet et al., 1998; Porch and Jahn, 2001; Sato et al., 2002). So understanding how pollen responds to stresses would help us to gain insight into understanding mechanisms underlying the pollen stress response.

Transcriptome analyses of heat stressed pollen

Compared to heat stress responses in vegetative tissues, information on pollen is still lacking. For example, *HsfA2* and *Hsp 17-CII* are shown to be highly expressed in tomato mature pollen under heat stress (Giorno et al., 2010). Increased level of transcripts associated with ER resident proteins such as *Hsp60*, *BiP*, and *Bzip60* was also reported in heat stressed pollen (Iwata et al., 2008). In heat stress tolerant tomato, higher expression levels of *HsfA2* and *LeHsp17.4-CII* were detected (Frank et al., 2009).

In Arabidopsis pollen, cyclic nucleotide gated channel 16 (CNGC16) has been shown as a critical component for pollen heat stress tolerance, in which *cngc16* knockout showed a

decrease in transcript abundance of heat stress marker genes such as *HsfA2*, *HsfB1*, and *Bag6*.

Recently, an RNA-Seq study was done with heat stressed tomato pollen to identify heat stress regulated small non-coding RNAs (sncRNAs, Bokszczanin et al., 2015). As a result, they identified two miRNAs and 6 tRNAs showing differential expression in mature pollen. In contrast to reproductive systems, many studies have shown the importance of miRNAs in plant vegetative tissues adaptation to stresses (Stief et al., 2014; Sunkar et al., 2012). To establish a system in which genetics can be used to determine the role of stress-dependent changes in the transcriptome, we used RNA-Seq to compare the stress-dependent changes that occur in a wild-type pollen with those that occur in a mutant (*cngc16*) that has pollen that are hypersensitive to multiple stress conditions, including a heat stress. In chapter III and IV, we present the results of our RNA-Seq experiment, and outline follow-up experiments to better understand the role of selected genes of potential importance to the stress response.

References

Bokszczanin KL, Krezdorn N, Fragkostefanakis S, Müller S, Rycak L, Chen Y, Hoffmeier K, Kreutz J, Paupière MJ, Chaturvedi P, Iannacone R, Müller F, Bostan H, Chiusano ML, Scharf K, Rotter B, Schleiff E, Winter P, SPOT-ITN Consortium (Solanaceae Pollen Thermotolerance Initial Training Network Consortium) SPOT-ITN Consortium (Solanaceae Pollen Thermotolerance Initial Training Network Consortium) (2015) Identification of novel small ncRNAs in pollen of tomato. BMC Genomics 16: 714-733.

Bonza MC, Carnelli A, De Michelis MI, Rasi-Caldogno F (1998) Purification of the Plasma Membrane Ca-ATPase from Radish Seedlings by Calmodulin-Agarose Affinity Chromatography. Plant Physiology 116: 845–851.

Bonza MC, Morandini P, Luoni L, Geisler M, Palmgren MG, Michelis MID (2000) *At*-ACA8 encodes a plasma membrane-localized calcium-ATPase of Arabidopsis with a calmodulin-binding domain at the N-terminus. Plant Physiology 123: 1495-1506.

Boursiac Y, Lee SM, Romanowsky S, Blank R, Sladek C, Chung WS, Harper JF (2010) Disruption of the vacuolar calcium-ATPases in Arabidopsis results in the activation of a salicylic acid-dependent programmed cell death pathway. Plant Physiology 154: 1158-1171.

Craufurd PQ, Wheeler TR (2009) Climate change and the flowering time of annual crops. Journal of Experimental Botany 60: 2529–2539.

Delaney TP, Uknes S, Vernooji B, Friedrich L, Weymann K, Negrotto D, Gaffney T, Gut-Rella M, Kessmann H, Ward E, Ryals J (1994) A central role in salicylic acid in plant disease resistance. Science 266: 1247-1250.

Dit Frey NF, Mbengue M, Kwaaitaal M, Nitsch L, Altenbach D, Häweker H, Lozano-Duran R, Njo MF, Beeckman T, Huettel B, Borst JW, Panstruga R, Robatzek S (2012) Plasma Membrane Calcium ATPases Are Important Components of Receptor-Mediated Signaling in Plant Immune Responses and Development. Plant Physiology 159: 798-809.

Dunkley TPJ, Hester S, Shadforth IP, Runions J, Weimar T, Hanton SL, Griffin JL, Bessant C, Brandizzi F, Hawes C, Watson RB, Dupree P, Lilley KS (2006) Mapping the Arabidopsis organelle proteome. Proceedings of the National Academy of Sciences of the United States of America 103: 6518-6523.

Frank G, Pressman E, Ophir R, Althan L, Shaked R, Freedman M, Shen S, Firon N (2009) Transcriptional profiling of maturing tomato (*Solanum lycopersicum* L.) microspores reveals the involvement of heat shock proteins, ROS scavengers, hormones, and sugars in the heat stress response. Journal of Experimental Botany 60: 3891-3908.

Gaffney T, Friedrich L, Vernooij B, Negrotto D, Nye G, Uknes S, Ward E, Kessmann H, Ryals J (1993) Requirement of salicylic acid for the induction of systemic acquired resistance. Science 261: 754-756.

Geisler M, Axelsen KB, Harper JF, Palmgren MG (2000) Molecular aspects of higher plant P-type Ca^{2+}-ATPases. Biochimica et Biophysica Acta 1465: 52-78.

Geisler M, Frangne N, Gomès E, Martinoia E, Palmgren MG (2000) The ACA4 gene of Arabidopsis encodes a vacuolar membrane calcium pump that improves salt tolerance in yeast. Plant Physiology 124: 1814-1827.

Giorno F, Wolters-Arts M, Grillo S, Scharf KD, Vriezen WH, Mariani C (2010) Developmental and heat stress-regulated expression of HsfA2 and small heat shock proteins in tomato anthers. Journal of Experimental Botany 61: 453–462.

Hong B, Ichida A, Wang Y, Gens JS, Pickard BG, Harper JF (1999) Identification of a Calmodulin-Regulated Ca^{2+}-ATPase in the Endoplasmic Reticulum. Plant Physiology 119: 1165-1175.

Huang L, Berkelman T, Franklin AE, Hoffman NE (1993) Characterization of a gene encoding a Ca^{2+}-ATPase-like protein in the plastid envelope. Proceedings of the National Academy of Sciences of the United States of America 90: 10066–10070.

Hwang I, Sze H, Harper JF (2000) A calcium-dependent protein kinase can inhibit a calmodulin-stimulated Ca2+ pump (ACA2) located in the endoplasmic reticulum of Arabidopsis. Proceedings of the National Academy of Sciences of the United States of America 97: 6224-6229.

Involvement of heat shock proteins, ROS scavengers, hormones, and sugars in the heat stress

Iwano M, Igarashi M, Tarutani Y, Kaothien-Nakayama P, Nakayama H, Moriyama H, Yakabe R, Entani T, Shimosato-Asano H, Ueki M, Tamiya G, Takayama S (2014) A pollen coat-inducible autoinhibited Ca2+-ATPase expressed in stigmatic papilla cells is required for compatible pollination in the Brassicaceae. The Plant Cell 26: 636-649.

Iwata Y, Fedoroff NV, Koizumi N (2008) *Arabidopsis* bZIP60 is a proteolysis-activated transcription factor involved in the endoplasmic reticulum stress response. The Plant Cell 20: 3107–3121.

Kudl J, Batistič O, Hashimoto K (2010) Calcium Signals: The Lead Currency of Plant Information Processing. The Plant Cell 22: 541-563.

Li X, Chanroj S, Wu Z, Romanowsky SM, Harper JF, Sze H (2008) A distinct endosomal Ca^{2+}/Mn^{2+} pump affects root growth through the secretory process. Plant Physiology 147: 1675-1689.

Liang F, Cunningham KW, Harper JF, Sze H (1997) ECA1 complements yeast mutants defective in Ca^{2+} pumps and encodes an endoplasmic reticulum-type Ca^{2+}-ATPase in Arabidopsis thaliana. Proceedings of the National Academy of Sciences of the United States of America 94: 8579-8584.

Limonta M, Romanowsky S, Olivari C, Bonza MC, Luoni L, Rosenberg A, Harper JF, De Michelis MI (2014) ACA12 is a deregulated isoform of plasma membrane Ca^{2+}-ATPase of Arabidopsis thaliana. Plant Molecular Biology 84: 387-397.

Lucca N, León G (2012) Arabidopsis ACA7, encoding a putative auto-regulated Ca^{2+}-ATPase, is required for normal pollen development. Plant Cell Reports 31: 651-659.

Mills RF, Doherty M, Lopez-Marques RL, Weimar T, Dupree P, Palmgren MG, Pittman JK, Peet MM, Sato S, Gardner RG (1998) Comparing heat stress effects on male-fertile and male-sterile tomatoes. Plant Cell Environment 21: 225–231.

Poovaiah BW, Reddy ASN (1993) Calcium and signal transduction in plants. Critical Review in Plant Science 12: 185-211.

Porch TG, Jahn M (2001) Effects of high-temperature stress on microsporogenesis in heat-sensitive and heat-tolerant genotypes of *Phaseolus vulgaris*. Plant Cell Environment 24: 723–731.

Sato S, Peet MM, Thomas JF (2002) Determining critical pre- and post-anthesis periods and physiological processes in *Lycopersicon esculentum* Mill. exposed to moderately elevated temperatures. Journal of Experimental Botany 53: 1187–1195.

Sunkar R, Li Y, Jagadeeswaran G (2012) Functions of microRNAs in plant stress responses. Trends in Plant Cell 17: 196-203.

White PJ (2000) Calcium channels in higher plants. Biochimica et Biophysica Acta 1465: 171–189.

Williams LE (2008). ECA3, a Golgi-localized P2A-type ATPase, plays a crucial role in manganese nutrition in Arabidopsis. Plant Physiology 146: 116-128.

Wu Z, Liang F, Hong B, Young JC, Sussman MR, Harper JF, Sze H (2002) An Endoplasmic Reticulum-Bound Ca^{2+}/Mn^{2+} Pump, ECA1, Supports Plant Growth and Confers Tolerance to Mn^{2+} Stress. Plant Physiology 130: 128-137.

Young LW, Wilen RW, Bonham-Smith PC (2004) High temperature stress of Brassica napus during flowering reduces micro- and megagametophyte fertility, induces fruit abortion, and disrupts seed production. Journal of Experimental Botany 55: 485-495.

Zhu X, Caplan J, Mamillapalli P, Czymmek K, Dinesh-Kumar SP (2010) Function of endoplasmic reticulum calcium ATPase in innate immunity-mediated programmed cell death. The EMBO Journal 29: 1007-1018.

Zinn KE, Tunc-Ozdemir M, Harper JF (2010) Temperature stress and plant sexual reproduction: uncovering the weakest links. Journal of Experimental Botany 61: 1959-1968.

Chapter II

Loss of function of *Arabidopsis thaliana* Ca^{2+}-ATPases 1, 2, and 7 results in plants with lesion-like phenotype and defects in pollen fitness

Abstract

Cytosolic Ca^{2+} homeostasis is maintained by the action of both Ca^{2+} channels and Ca^{2+} transporters (including Ca^{2+}/H^{+} antiporters and Ca^{2+}-ATPases). Plants utilize two types of Ca^{2+}-ATPase pumps: ER-type Ca^{2+}-ATPase, with four gene family members in *Arabidopsis thaliana*, and autoinhibited Ca^{2+}-ATPase, with ten gene family members in *Arabidopsis thaliana*. ECAs and ACAs have different regulatory features and affinity for Ca^{2+}, and therefore, are expected to make different contributions to cellular functions. Here we show a triple knockout of autoinhibited Ca^{2+}-ATPases 1, 2, and 7 (*aca1*$^{-/-}$/*2*$^{-/-}$/*7*$^{-/-}$) results in plants with a mild frequency of lesion in leaf tissues as well as deficiencies in pollen fitness. The lesion phenotype was fully suppressed by the expression of a *NahG* transgene encoding an enzyme that degrades salicylic acid, indicating a role of *ACA1*, *2*, and *7* in the suppression of salicylic acid-dependent programmed cell death pathway. Genetic segregation analyses in which the *aca1/2/7* plants segregating a wild-type *ACA2* showed reduced transmission efficiency for pollen harboring a triple knockout of *aca1/2/7*. This deficiency could be reversed by the pollen expression of transgenes encoding either *ACA1*, *ACA2* or *ACA7* individually, suggesting that each of the three ACAs possess biochemically redundant function. Together, these results provide evidence for the involvement of ACA1, 2, and 7 in the control of programmed cell death and in normal pollen fitness.

Introduction

In plants like animals, cytosolic Ca^{2+} is maintained at the submicromolar level, and is increased after the perception of various stimuli. There are three different types of Ca^{2+} transporters: Ca^{2+} channels, Ca^{2+} antiporters (Ca^{2+}/H^{+} antiporters), and Ca^{2+} pumps (Ca^{2+}-ATPases). Ca^{2+} channels release Ca^{2+} into the cytosol in the same direction as the concentration gradient without energy consumption. Ca^{2+} antiporters move Ca^{2+} and protons in the opposite direction. Lastly, Ca^{2+} pumps remove Ca^{2+} from the cytosol and return Ca^{2+} to either apoplast or organelles such as ER. Because Ca^{2+} pumps move Ca^{2+} against concentration gradient, they utilize energy from ATP hydrolysis. In plants, there are two types of Ca^{2+}-ATPases; type IIA or ECA (ER-type Ca^{2+}-ATPase, with four gene family members in *Arabidopsis thaliana*), and type IIB or ACA (autoinhibited Ca^{2+}-ATPase, with ten gene family members in *Arabidopsis thaliana*). ECAs and ACAs have affinity for Ca^{2+}, and different regulatory features, and thus are expected to have different contributions to cellular functions.

In *Arabidopsis thaliana*, there are ten isoforms of ACAs, which can be divided into three subgroups based upon protein sequence similarity (Figure 1A). Subgroup I contains five isoforms including ACA8, 9, 10, 12, and 13, all with plasma membrane localizations (Bonza et al., 2000; Schiot et al., 2004; Limonta et al., 2013; Iwano et al., 2014). Subgroup II includes two isoforms, ACA 4 and 11, with both targeting vacuole, and functioning as suppressor of Programmed Cell Death (PCD) (Boursiac et al., 2010). A double knockout of *aca4/11* results in a high frequency of salicylic acid-dependent lesions in leaf tissues. This lesion phenotype can be inhibited either by a *sid2* mutation (to

stop the major source for SA production) or the expression of a *NahG* transgene (to degrade SA).

ACAs subgroup III comprised of three isoforms; ACA1 (At1g27770), 2 (At4g37640), and 7 (At2g22950). ACA2 has been demonstrated to localize to the endoplasmic reticulum (ER, Harper et al., 1998), whereas ACA1 and 7 have been reported to localize to the plastid envelope (Huang et al., 1993) and plasma membrane (Lucca and Leon 2012), respectively.

ACA1 or PEA1 (stands for Plastid Envelop ATPase) was the first putative Ca^{2+}-ATPase to be identified in plants and was proposed to be important for exporting Ca^{2+} from chloroplast to the cytosol (Huang et al., 1993). Evidence for a plastid localization was based upon immunological evidence with an antisera raised against a long region of ACA1 starting from glutamate 714 to serine 950 (Glu^{714}-Ser^{950}). However, the polyclonal antibody used in this study showed cross-reactivity with other types of Ca^{2+} pumps such as plasma membrane (Bonza et al., 1998). Although there are some possible candidates for Ca^{2+} transport into the chloroplast such as Ca^{2+}/H^{+} antiporter, so far efforts for showing Ca^{2+}-dependent ATPase activity or ATP-dependent Ca^{2+} uptake in chloroplast has failed (Huang et al. 1993; Roh et al. 1998). Using "localization of organelle proteins by isotope tagging" (LOPIT) technique, Dunkley et al. (2006) found ACA1 and ACA2 associated with the ER. Based upon these two controversial results, ACA1 localization still remains to be determined.

Harper et al. (1998) identified ACA2 in Arabidopsis. ACA2 has been functionally expressed in yeast and shown to have Ca^{2+}/CaM-dependent ATPase activity. Using both

immunological and GFP-tagging approaches, the authors demonstrated that ACA2 localized to the ER.

For ACA7, Lucca and Leon (2012) provided evidence for a plasma membrane localization, based upon transient expression of ACA7 with an N-terminal GFP tag in tobacco epidermal cells. However, no control was done to ensure that the GFP-ACA7 was not over-expressed.

Of these three ACAs in Arabidopsis, the only knockout phenotype published so far was for *ACA7* (Lucca and Leon 2012). The *aca7-1* knockout was reported to result in a high frequency of dead pollen grains ranging from 20% to 60%, as detected by Alexander staining of pollen grains. However, a pollen transmission assay was not done to corroborate an expected segregation distortion.

Using an RNA silencing approach, Zhu et al. (2010) provided evidence in tobacco leaves that the silencing of a tobacco ACA (NbCA1) can result in a high frequency of salicylic acid-dependent lesions. Based upon transient expression of a GFP-tagged enzyme, the tobacco NbCA1 was reported to be localized to the ER. However, the protein sequence of NbCA1 is more similar to two vacuolar ACAs (ACA4 and 11) that have been demonstrated to be localized to the vacuole using GFP-tagged enzymes expressed in stable transgenic plants (Boursiac et al., 2010). Thus, it is not yet clear if the silencing experiment in tobacco resulted in a lesion phenotype because of the loss of ACAs associated with the ER, vacuole, or both.

A similarity analysis showed that ACA1, 2 and 7 have high sequence similarity at the protein level; ACA1 and ACA2: 81%, ACA1 and ACA7: 84%, ACA2 and ACA7: 93%. This high degree of similarity raises the possibility for these genes to be (partially) functionally redundant, and to target the same subcellular location. Here we provide two lines of evidence (confocal microscopy and genetic approaches) that both ACA1 and ACA7 localizes to the ER and a ER-like structure, respectively, and not to the chloroplast envelope or plasma membrane, as previously published. In addition, we show a triple knockout of *ACA1*, *2*, and *7* results in plants with lesion-like phenotype and defects in transmission efficiency of male gametophyte. Expression of any of the three ACA isoforms reverse the mutant phenotype, indicating that ACA1, 2, and 7 are functionally redundant.

Material and methods

Plant growth conditions

Seeds from both wild-type and mutants after sterilization were grown on 0.5x Murashige and Skoog (MS) medium containing 1% sucrose, 0.05% MES, and 1% agar. After 48 h vernalization at 4 ˚C, the seeds were exposed to 130-150 μmol m^{-2} s^{-1} constant light at room temperature (22 to 23 ˚C). After 10 days, the resulting seedlings were transferred to the soil (Sunshine SMB-238) supplemented with Marathon pesticide and fungicide according to the manufacturer instruction. The plants were grown in growth chambers with temperature and light intensity of 22 ˚C and 130-150 μmol m^{-2} s^{-1}, respectively, for 16 h light and 8 h dark period.

For the hot/cold stress condition, see the Tunc-Ozdemir et al. (2013) with more details. In brief, the temperature inside the Percival growth chamber was cycling from the -1 ˚C from 6 AM in the morning, and increases gradually to reach 40 ˚C at noon. After 1 h at 40 ˚C, the temperature drops to 10 ˚C and stays at 10 ˚C until 10 PM, in which it drops to -1 ˚C until 6 AM in the morning. For all of the hot/cold crosses, plants were moved to the hot/cold stress chamber within 30 min after pollination between 3:00 to 5:00 PM in the afternoon.

T-DNA insertion alleles

For *ACA1* (At1g27770) and *ACA2* (At4g37640), we isolated two independent set of alleles for each gene including *aca1-7* (GABI_095C01; transgenic line no. 15528), *aca1-2* (Wis_J789 alpha; seed stock 28), *aca2-2* (SAIL_873_F03; seed stock 123), and *aca2-3* (SALK_082624; seed stock 493). For *ACA7*, we isolated 5 independent alleles; *aca7-5* (SALK_132552; seed stock 627), *aca7-7* (SALK_143504; transgenic line no.15752), *aca7-8* (GABI_452E05; transgenic line no. 15750), *aca7-9* (Wis_J3281 alpha; seed stock 49), and *aca7-10* (SALK_014124; seed stock 157). *aca7-7* and *7-10* are equal to *aca7-2* and *aca7-1* in the Lucca and Leon (2012) manuscript. All T-DNA insertion alleles were in the wild-type Col-0 ecotype except for *aca1-2* and *aca7-9*, which were in the wild-type Wassilewskija (Ws) ecotype. The selectable marker genes associated with each T-DNA insertion were sulfonosid for *aca1-7* and *aca7-8*; Basta for *aca2-2* and no selectable marker genes for the rest of alleles tested. The position of T-DNA insertions and the PCR primers used for genotyping are shown in Figure 1.

Plasmid construction and resulting transgenic lines

To create transgenic lines, ACAs full-length cDNA or genomic DNA were PCR amplified from either a cDNA library or genomic DNA derived from wild-type seedlings, and subcloned into the pGREEN binary vector under either the strong constitutive CaMV 35S promoter or the pollen- specific promoter from the autoinhibited Ca^{2+}-ATPase, ACA9. The resulting constructs were transformed into *Agrobacterium* GV3101 strain, and the obtained transformed *Agrobacterium* were used for plant transformation using the floral dip method as described (Clough and Bent 1998). Parallel transformations were done with the empty vector. The resulting seeds were harvested, and hygromycin (25 mg/ml)/ carbanicillin (200 mg/ml) resistant plants identified.

Transgenic lines created or used in this study include: *35Sp::ACA1-GFP* (plasmid no. 1294, transgenic line no. 15673-C/D/F), *35Sp::ACA2-GFP* (plasmid no. 660, transgenic line no. 15672-A/B/S), *35Sp::ACA7-YFP* (plasmid no. 2091 , transgenic line no. 15678-A/B/C),

35Sp::GFP (plasmid no. 346 , seed stock 1811), *ACA9p::ACA1-YFP* (plasmid no. 1295, transgenic line nos. 15718-1 to 15718-2, and 15721-2), *ACA9p::ACA2-GFP* (plasmid no. 585, transgenic line nos. 15266-A/B/C), *ACA9p::ACA7-YFP* (plasmid no. 1960, transgenic line nos. 15264-E/F/G and H), *ACA9p::ACA9-YFP* (plasmid no. 580, transgenic line no. 15729-15731), *ACA9p::YFP* (plasmid no. 532, transgenic line nos. 15720-1 to 4).

Quantitative RT-PCR

Total RNA was extracted from 10-day-old seedlings grown on the 0.5x Murashige and Skoog (MS) medium containing 1% sucrose, 0.05% MES, and 1% agar using the RNeasy

Plant Mini Kit (Qiagen). The resulting RNA samples were cleaned at least twice using RNase-free DNase to remove genomic DNA contamination. 1 µg of total RNA was reverse transcribed to cDNA using iScript cDNA Synthesis Kit (Catalogue#170-8891; Bio-RAD). 0.15 µg of the resulting cDNA was used in the real-time PCR reaction using SsoFast Probes Supermix (Catalog #172-5231; Bio-Rad) following the manufacturer's instructions. Taqman assays used in this study included *ef1-alpha* (*EF1-α*) and *pathogenesis-related protein* gene (*PR1*) with assay ID numbers At02337969_g1, and At02170748_s1, respectively, from the Applied Biosystems. *EF1-α* was used for normalization. Gene expression levels were quantified by real-time quantitative RT PCR using a thermocycler CFX96 (Bio-Rad laboratory). The PCR conditions were as follows: 2 min at 95 °C, 39 cycles of 95 °C for 15 s and 1 min at 60 °C. The delta Ct method was used for data normalization (Livak and Schmittgen, 2001).

In vitro pollen germination

Pollen from the open flowers (stage 13-14) were placed on the glass slides containing pollen germination media consist of 0.8 mM MES, 1 mM KCl, 9 mM $CaCl_2$, 1mM $Ca(NO_3)_2$, 0.8 mM $MgSO_4$, 1.5 mM Boric acid, and 16.6% (w/v) sucrose (Fan et al., 2001) with 1% low melting agar. The slides were then placed in square plates containing wet tissue paper to maintain humidity. Pollen tubes were grown at room temperature in the dark for almost 3 h.

Confocal microscopy

Confocal microscopy images were taken using an Olympus IX81 FV1000 confocal microscope equipped with the Olympus FluoView 1.07.03.00 software package

(Olympus, Center Valley, PA). For all images, a 60X objective was used unless otherwise stated. Excitation at wavelengths of 488nm (EGFP), 515nm (YFP), and 543nm (chlorophyll autofluorescence) were provided using an argon-ion laser. A spectral emission range of 500-530 nm for EGFP, 530-630 nm for YFP, and 687-787 nm for chlorophyll autofluorescence was used.

Seed set and top/middle/bottom analyses

For the seed set analysis, ten consecutive siliques were harvested from the primary bolt, and cleared in 70% ethanol. Four individual plants were used for each genotype. The cleared siliques were then scanned. The resulting images were used for seed counting.

For the top/middle/bottom analysis, pollen from either the *aca1-2*$^{-/-}$, *2-2*$^{+/-}$, *7-9*$^{-/-}$ or the *ACA9p:: ACA7-YFP* hemizygous transgenic lines was used to pollinate the pistil of the wild-type. Before drying, the resulting siliques were then nail polished to inhibit silique shatter. After drying, the siliques were divided into three equal pieces using scissor, and allowed to dry for a couple of days. The corresponding seeds from each piece were then plated on the 0.5x Murashige and Skoog (MS) medium containing appropriate selection marker followed by scoring of the transmission efficiency for each section individually.

Results

Loss of function of *ACA1, 2,* and *7* results in lesion-like phenotype

To determine the biological function of ACA1, 2, and 7, two different sets of triple knockouts were created (Fig. 1B). The triple knockout *aca1-7/2-3/7-5* was in a wild-type Col-0 background and *aca1-2/2-2/7-9* was in a mixed background resulting from

combining insertions identified in Wassilewskija (Ws) and Col-0 parental backgrounds. The resulting mutants both showed a similar lesion-like phenotype (Fig. 2A) and smaller leaf size (Fig. 2B) when compared to their wild-type backgrounds. The resulting phenotype looks similar to the lesion phenotype observed in the *aca4/11* mutant (Fig. 2C, Boursiac et al., 2010) thus called lesion-like, but with different degree, with *aca4/11* showing a stronger lesion phenotype compared to the *aca1/2/7* triple mutant. In addition, the RT-PCR results showed constitutive expression of *PR1* gene, a marker gene for the plant defense response, in the triple knockout plants (Fig. 2D).

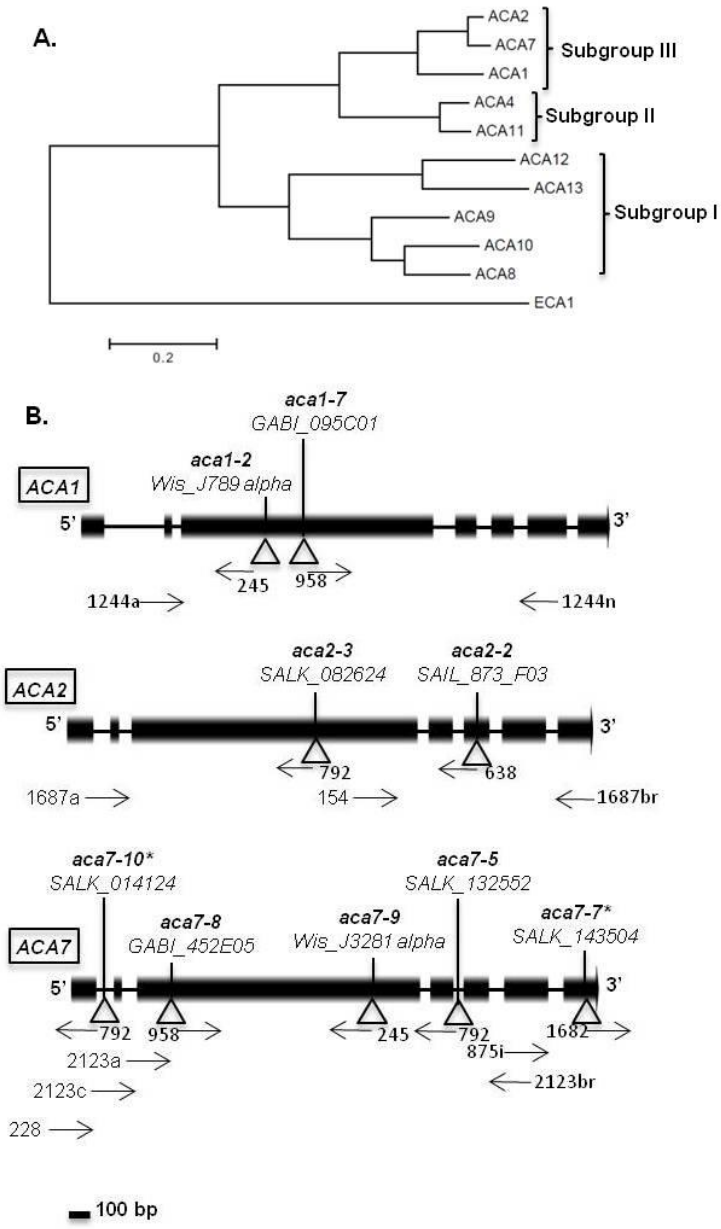

Figure 1. ACA family phylogenetic tree and schematic diagram of ACA1, 2 and 7 gene models**.** A) Phylogenetic tree of Arabidopsis ACAs family. ECA1 (ER Ca^{2+}-ATPase) was used as an outgroup. The tree was built using MEGA6.06 software. Scale bar = 0.2 showing the evolutionary distance using amino acid sequences.
B) Schematic diagram of gene models for *ACA1* (At1g27770), *ACA2* (At4g37640), and *ACA7* (At2g22950) are shown. The position of T-DNA insertions, and primers used for genotyping PCR are shown with triangles and arrows, respectively. Exons and introns are depicted by boxes and lines, respectively. Alleles marked by star (*) were studied by Lucca and Leon (2012). *aca7-10* and *7-7* are equal to *aca7-1* and *7-2* in Lucca and Leon (2012).

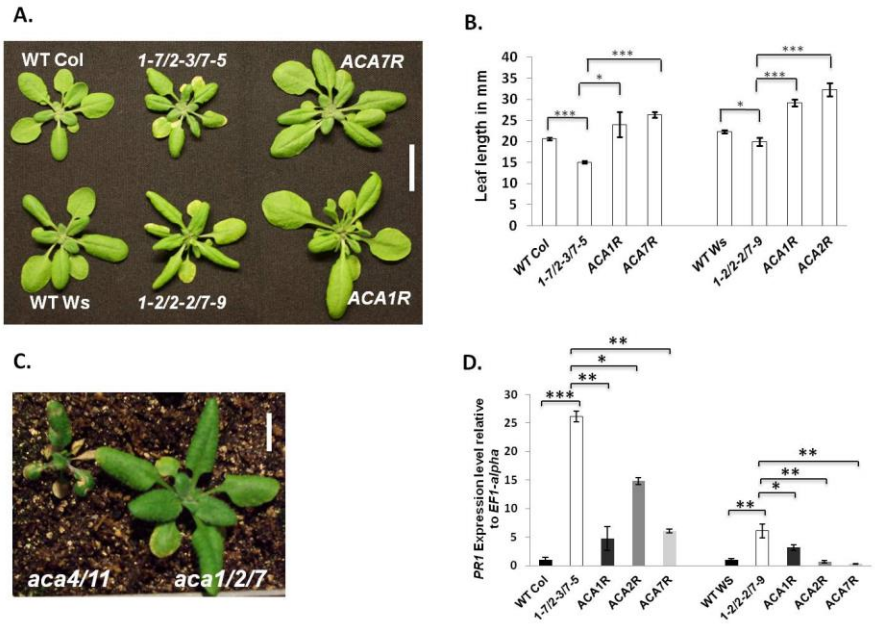

Figure 2. aca1/2/7 mutant showing lesion-like phenotype and reduced leaf size**.**
A) *aca1/2/7* knockouts showing lesion-like phenotype compared to their wild-type (WT) backgrounds, and expression of a *35Sp::ACA7-YFP* (top panel) or *35Sp::ACA1-GFP* (bottom panel) can reverse the lesion phenotype. *1-7/2-3/7-5* and *1-2/2-2/7-9* represent *aca1-7/2-3/7-5* and *aca1-2/2-2/7-9* triple knockout mutants. R refers to the rescued lines.
B) Leaf size measurement showing reduced leaf size for the *aca1/2/7* triple knockouts compared to the wild-type backgrounds. For leaf size measurement, three large rosette leaves were measured from each plant. Values shown are mean ± SE for representative of three independent experiments with at least three biological replicates in each experiment. Statistical significance was determined by the Student's t-test. The symbols * and *** represent Student's t-test significance at $p<0.05$ and $p<0.0001$, respectively.
C) Picture showing *aca4/11* and *aca1/2/7* mutants exhibiting lesion phenotypes.
D) *aca1/2/7* mutant shows increase in the expression of salicylic acid-dependent molecular marker gene, *PR1*. Quantitative PCR showing increase in the transcript level of *PR1* gene (AT2G14610) in the *aca1/2/7* mutants, in which vegetative expression of any of the three isoforms reduced the *PR1* level.
For all real-time PCR analyses, one-week-old seedlings grown in plate containing 0.5x Murashige and Skoog media plus 1% sucrose were used. Values represent means ± SE. qPCR experiments were performed twice with similar results. *EF1-alpha* (AT5G60390) was used for normalization. Statistical significance was determined by the Student's t-test. The symbols *, **, and *** indicate Student's t-test significance at $p\leq0.05$, ≤0.01, and $\leq0.000.1$, respectively. The scale bar is equal to 10 mm.

Vegetative expression of any of the three isoforms of ACA1 or 2 or 7 reverses the *aca1/2/7* lesion phenotype

To determine if the observed lesion phenotype is associated with the loss-of-functions of ACA1, 2, and 7, the triple knockout plants were stably transformed with transgenes encoding each of the ACAs; *ACA1-GFP*, or *ACA2-GFP*, or *ACA7-YFP* under the expression of the CaMV 35S promoter. Expression of any of the three ACAs reversed the lesion phenotype (Fig. 2A). In addition, expression of any of the three ACAs isoforms restores the leaf size (Fig. 2B). Further, the *PR1* transcript abundance was decreased to a great extent in all three rescued lines tested (Fig. 2D). Together, the results indicate that ACA1, 2, and 7 are functionally redundant, and loss of all three isoforms can be compensated by the expression of one of the three ACAs.

Disruption of *ACA1, 2,* and *7* activating a salicylic acid (SA)-dependent pathway

To determine the observed lesion phenotype of *aca1/2/7* is due to activation of a SA-dependent pathway, we analyzed the *aca1/2/7* mutant plant carrying the *NahG* transgene, a SA degradation enzyme (Gaffney et al., 1993; Delaney et al., 1994). Expression of the *NahG* transgene in the *aca1/2/7* mutant attenuated the lesion phenotype (Fig. 3A), indicating that *ACA1*, *2*, and *7* normally suppress a SA-dependent programmed cell death pathway.

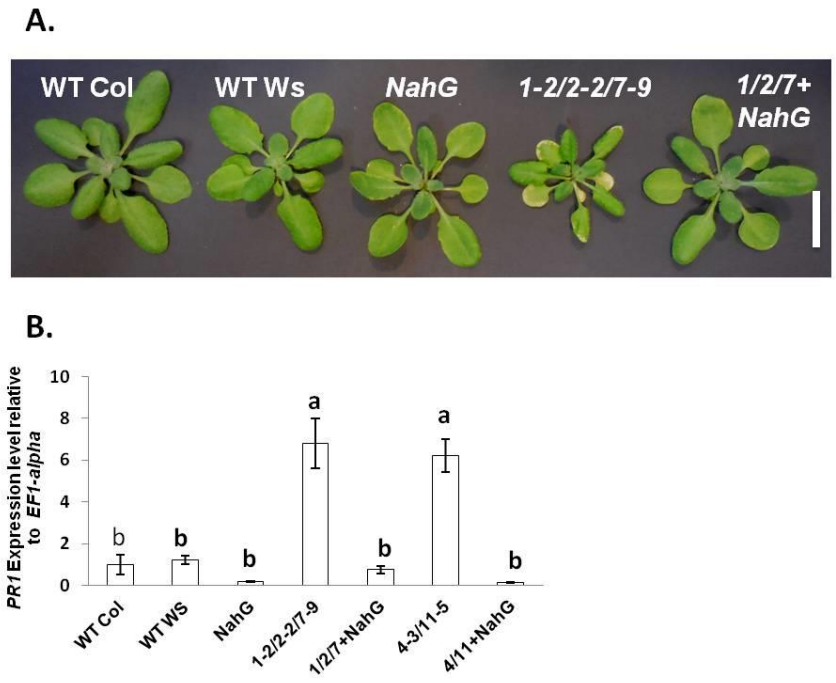

Figure 3. Expression of the NahG transgene in the aca1/2/7 mutant stops lesion phenotype**.**
A) Expression of a salicylic acid degradation enzyme gene, *NahG*, in the *aca1/2/7* mutant background stops lesion phenotype. All genotypes shown were grown in parallel under the same greenhouse condition, as explained in the material and methods section.
B) RT-PCR showing the *PR1* transcript abundance in different genotypes. Expression of the *NahG* transgene reduced the *PR1* expression level in both *aca1/2/7* and *aca4/11* mutants. The PCR condition was the same as described in Figure 2. Different letters consider to be statistically significant $P<0.05$. Scale bar is equal to 10mm.

To confirm a visual suppression of lesions through the expression of the *NahG* transgene, we measured the *PR1* transcript. The RT-PCR result showed the *PR1* level significantly decreased in the both *aca1/2/7* and *aca4/11* mutant plants harboring *NahG* (Fig. 3B). Together, these results indicate that both types of calcium pumps (ER *versus* vacuole) control PCD in a SA-dependent pathway.

Disruption of *ACA1, 2,* and *7* impairs pollen fitness in non- and stress-dependent way

To examine if the loss-of-function of each single ACA would affect the pollen transmission efficiency, segregation analyses were performed. The result showed no distortion associated with each single knockout (Table 1). However, the *aca1/2/7* triple knockout plants with a segregating wild-type ACA2 gene showed a decrease transmission efficiency of the mutant *aca2* allele from a 75% expected efficiency down to an average of 58% (Table 2). To determine if the observed distortion was due to a defect associated with male or female gametes, reciprocal crosses were performed. While transmission of the *aca2* allele appeared normal through the female parent, there was a deceased transmission through the pollen from a 50% expected down to an average of 31% (Table 2).

Table 1. Segregation analyses of single knockouts *aca1*, *aca2*, and *aca7* showing no deviation from normal Mendelian segregation.

	Cross	F1	Segregation of +/- T-DNA		Mutant allele	
KO assayed	Female x Male	total	Expected %	Observed %	scored by	P-value[a]
	aca1-7; Selfed	143,120	75	79,77	Sulfr marker	All 0.8
aca1	*aca1-7* X WT	1023	50	48	Sulfr marker	0.8
	WT X *aca1-7*	852	50	46	Sulfr marker	0.2
aca2	*aca2-2*; Selfed	489,447,105,120	75	78,76,73,79	Bastar marker	0.8,0.8,0.9,0.8
aca7	WT X *aca7-5*	104	50	54	PCR genotyping	0.8
	*aca7-7** X WT	40	50	55	PCR genotyping	0.7
	aca7-8; Selfed	247,173,262	75	70,70,69	Sulfr marker	All 0.8
	aca7-8 X WT	271,102,118,101	50	49,52,50,56	Sulfr marker	0.9,0.8,1,0.8
	WT X *aca7-8*	324,130,286,115	50	52,50,46,56	Sulfr marker	0.8,1,0.8,0.8
	aca7-9 X WT	33	50	48	PCR genotyping	0.95
	WT X *aca7-9*	50	50	62	PCR genotyping	0.8
	WT X *aca7-10**	112	50	53	PCR genotyping	0.8

a. Significance determined by the Pearson's chi-squared test.

WT and KO stand for the wild type and knockout,respectively.

* *aca7-10* and *7-7* are the same as *aca7-1* and *7-2* in Lucca and Leon (2012).

Table 2. Segregation analyses showing defect in pollen transmission of *aca1/2/7* but not for *aca4/11*.

Cross	Condition	F1	Segregation of Basta marker gene		
Female x Male		total	Expected %	Observed %	P-value[a]
aca1-2$^{(-/-)}$/*7-9*$^{(-/-)}$/*2-2*$^{(+/-)}$; Selfed	Control	219,204,199	75	61,57,57	<0.02,<0.005,<0.005
aca1-2$^{(-/-)}$/*7-9*$^{(-/-)}$/*2-2*$^{(+/-)}$ X WT	Control	56,83,47	50	48,44,49	0.9,0.8,0.95
WT X *aca1-2*$^{(-/-)}$/*7-9*$^{(-/-)}$/*2-2*$^{(+/-)}$	Control	215,97,121,674	50	25,35,35,29	<0.001,<0.05,<0.02,<0.0001
aca1-2$^{(-/-)}$/*7-9*$^{(-/-)}$/*2-2*$^{(+/-)}$; Selfed	Hot/Cold	140,203,233	75	43,52,53	All<0.001
MS1-1 X *aca1-2*$^{(-/-)}$/*7-9*$^{(-/-)}$/*2-2*$^{(+/-)}$	Hot/Cold	49,39,203	50	6,10,19	<0.001,<0.001,<0.0001
aca4-3$^{(-/-)}$/*11-5*$^{(+/-)}$; Selfed	Control	341,333,283	75	72,68,70	0.8,0.2,0.8
aca4-3$^{(-/-)}$/*11-5*$^{(+/-)}$; Selfed	Hot/Cold	257,303	75	70,75	0.8,0.95

a. Significance determined by the Pearson's chi-squared test.

WT and MS refer to the wild type and male steril plants, respectively.

To test whether the observed distortion of *aca1/2/7* is also stress-dependent, crosses were conducted under the conditions of hot days and cold nights as described. Segregation analyses indicated that pollen transmission of the segregating *aca2* allele is hyper-sensitive to stress, showing a decreased transmission from a 31% expected (under no stress) down more than two fold to an average of 12% (Table 2).

To determine if there are parallel deficiencies with knockouts of the vacuole ACA pumps, *aca4/11*, we conducted crosses with an aca4-*3/11-5* mutant plant that was segregating a wild-type ACA11 allele. The result showed no distortion associated with the *aca4/11* double mutant in either of condition tested (Table 2). This suggests that in contrast to the ER-ACA pumps, the vacuole ACA pumps do not appear to have significant functional role in the pollen.

Pollen-specific expression of any of the three ACAs isoforms can improve pollen fitness in *aca1/2/7* mutant plants

To corroborate that *aca1/2/7* triple knockout results in a decrease in pollen fitness, a homozygous triple mutant was separately and stably transformed with constructs

encoding *ACA1-YFP*, *ACA2-GFP* or *ACA7-YFP* under the control of either a pollen-specific promoter from autoinhibited Ca^{2+}-ATPase 9 (*ACA9*), or a promoter fragment corresponding to a 1.5 kb region upstream of *ACA7* gene (the later promoter was only used in case of *ACA7-YFP* transgene). Transgenic plants used for a segregation distortion analysis were shown to be heterozygous for a single copy transgene. As revealed by segregation analyses, expression of any one of the three ACAs improved pollen transmission efficiency in an *aca1/2/7* parental background, in which the average transmission efficiency increased from an expected 50% to 68% (*ACA1*), 63% (*ACA2*), or 77% (*ACA7*) (Figure 4 and Supplemental Table S2). Altogether, these results indicate that *ACA1*, *2*, and *7* are functionally redundant, and expression of any one of the three isoforms can compensate the loss-of-function of the other two genes.

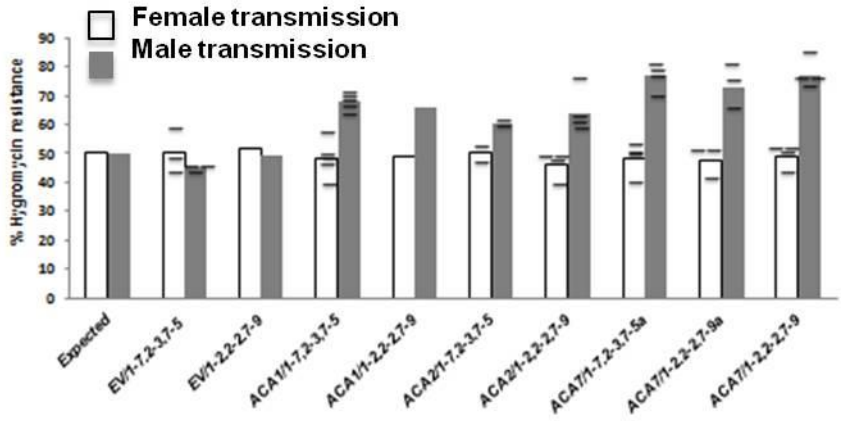

Figure 4. Pollen-specific expression of the ACA1 or ACA2, or ACA7 transgene can rescue the defect in pollen transmission of aca1/2/7 mutant**.**
Segregation analyses were performed on the progeny of reciprocal crosses between either male side of transgene with female side of *aca1/2/7* mutant or *vice versa*. The expectation from normal Mendelian segregation is 50%. Bar graphs are showing the average of individual lines being tested, and the dashes are showing number of lines tested with their

approximate values compared to the average. Female and male side crosses are shown in white and grey bars, respectively. All transgenes are expressed under control of the pollen specific promoter, *ACA9*, except for those that have been marked with letter a, which have the *ACA7* natural promoter. *1-7,2-3,7-5* refers to the aca*1-7,2-3,7-5* triple knockout, and *1-2,2-2,7-9* refers to the *aca1-2,2-2,7-9*. EV refers to empty vector which is a *ACA9promoter::YFP*. *ACA1* refers to the *ACA9promoter::ACA1-YFP*. *ACA2* refers to the *ACA9promoter::ACA2-GFP*. *ACA7* refers to either the *ACA9promoter::ACA7-YFP*, or the *ACA7promoter::ACA7-YFP* (marked with letter a). The complete list of crosses with statistical analyses were provided in Supplementary Table S2.

Transmission of *aca1/2/7* mutant through pollen is compromised at the top of the pistils

To determine possible mechanism(s) underlying the segregation distortion of *aca1/2/7* mutant pollen, we performed seed-set analysis to see if there is any missing seed in the *aca1/2/7* mutant silique. The seed-set analysis showed *aca1/2/7* mutants produce almost the same number of seeds per silique as the wild-type ecotypes (Fig. 5A).

Because there was no difference in terms of seed production between wild-type and the triple mutant, we hypothesized that the *aca1/2/7* mutant pollen tubes are simply deficient in their ability to compete with the wild-type pollen *in vivo.* To test this hypothesis, we conducted crosses in which 50% of the pollen were *aca1/2*(Basta^r)/*7*, and the other 50% had a functional *ACA2* and did not carry a Basta^r marker. The Basta^r marker allowed us to determine which pollen-phenotype was responsible for the fertilization event that gave rise to each seed in a silique. The relative distribution of Basta^r seed was determined by manually dividing siliques into three equal sections, and germinating the harvested seed on media containing Basta selection. Then, the transmission efficiency for each section was determined (Fig. 5B and Supplemental Table S3). Interestingly, this analysis showed

aca1/2/7 mutant transmission is less competitive at all 3 sections of silique with the top showing the most severe deficiency. The transmission efficiency for the mutant was 23% from the expected 50% (Fig. 5B and Supplemental Table S3).

To validate the *aca1/2/7* deficiency in fertilizing ovules especially at the top of the silique, we performed a top/middle/bottom segregation distribution analysis using siliques produced by outcrossing pollen from transgenic lines expressing the *ACA9P::ACA7-YFP* transgene. The result showed that the pollen harboring an *ACA9P::ACA7-YFP* transgene were more competitive in fertilizing ovules at the top of the ovary (Fig. 5C and Supplemental Table 3), suggesting that *aca1/2/7* mutant pollen are indeed specifically deficient in their ability to compete with wild-type pollen tube at the top of the ovary.

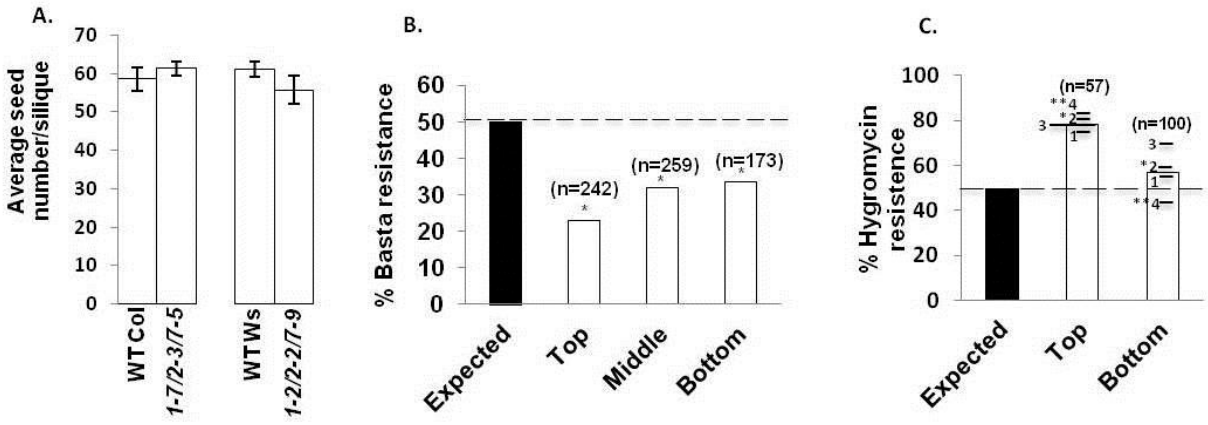

Figure 5. Transmission of aca1/2/7 through pollen is compromised at the top of the pistils**.**
A) Seed set analysis showing no difference in the number of seeds per silique for *aca1/2/7* mutants compared to the wild-type plants. Values are mean ± SE. Representative of two independent experiments with n=30 to 40 siliques are shown.

B) Transmission of *aca1/2/7* through pollen showing the mutant pollen is less competitive than wild-type pollen at all 3 sections of the silique, with most defects observed at the top. Wild-type pistils were fertilized with *aca1-2*$^{-/-}$,*2-2*$^{+/-}$,*7-9*$^{-/-}$ pollen and the resulting siliques were divided into 3 segments of equal length. The observed % was compared to an expected 50% for normal Mendelian segregation. Statistical significance was determined by the Pearson's Chi-Squared. * significant at $p \leq 0.05$. The seeds used for this analysis were transgenic line nos. 15776-15780.
C) Transmission of *ACA9p::ACA7-YFP* through pollen rescuing the defect observed for aca*1-7,2-3,7-5* more at the top of the silique. The observed % is compared to an expected 50%. Statistical significance was determined by the Pearson's Chi-Squared. *, and ** significant at $p \leq 0.05$ and ≤ 0.005, respectively. 1-*7,2-3,7-5* refers to the aca*1-7,2-3,7-5*, and *1-2,2-2,7-9* refers to the aca*1-2,2-2,7-9* mutants. The transgenic lines used for rescue experiment were nos. 16396-25, 16396-29, 16396-31, and 16396-19. n = total number of seeds counted. Dashes indicate different lines tested.
The corresponding table for the top/middle/bottom experiment in part B and C is in the Supplementary Table S3.

Confocal microscopy showing ACA1 localizes to the ER not the chloroplast envelope

To examine whether ACA1 localizes to the chloroplast envelope (as proposed by the Huang et al., 1993) or to the ER (as proposed by the Dunkley et al., 2006), stable transgenic lines were created which harboring the *35Sp::ACA1-GFP* construct. Using confocal microscopy, we examined the ACA1-GFP subcellular localization in both Arabidopsis root tips and guard cells. Multiple independent lines were examined, with similar localization patterns seen in cells showing strong GFP signals, as well as cells in which the GFP signal was weak and at its lower limit of detection. In all cases, the ACA1-GFP showed a subcellular localization pattern expected for the ER (Fig. 6). In the root tip (Fig. 6A), the ACA1-GFP signal was associated with a reticulated-like structure expected for the ER. In the guard cell (Fig. 6B), the ACA1-GFP signal appeared to wrap around the nucleus, which is often seen for the ER, and observed for an ACA2-GFP control. Importantly, the ACA1-GFP signal did not appear to colocalize with the red

autofluorescence of the chloroplast, providing evidence that ACA1 does not target to the chloroplast envelope, as proposed by Huang et al. (1993).

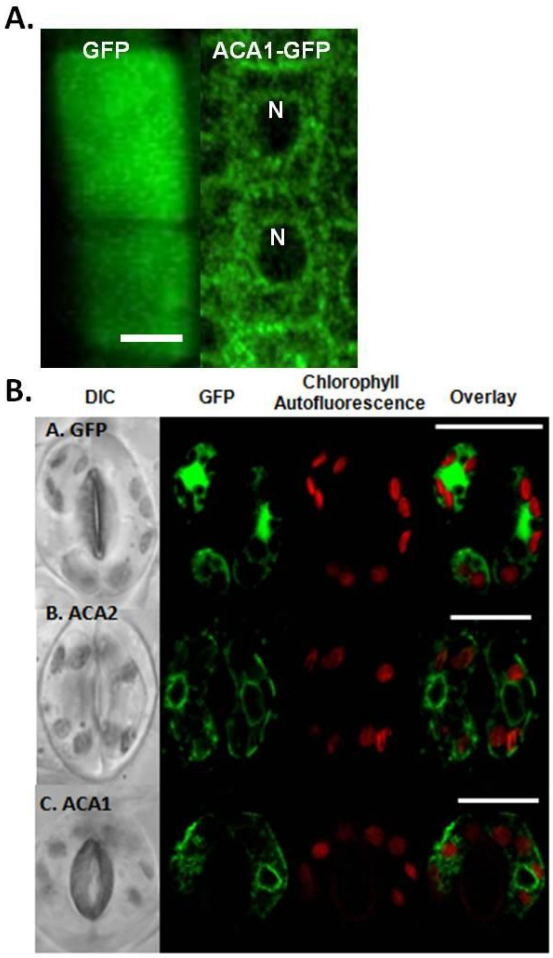

Figure 6. ACA1 showing endoplasmic reticulum (ER) localization**.**
A) Confocal microscopy showing ACA1-GFP localizes to the ER in two undifferentiated cells of the *Arabidopsis* root tips. GFP only is shown to the left and ACA1-GFP to the right. N refers to nucleus.
B) Confocal microscopy images showing ACA1-GFP localizes to the ER in the Arabidopsis guard cells. ACA1 localization was compared to the ACA2 as the ER marker. Scale bar is equal to 20 µm. For GFP only seed stock no.1811 was used. For each of the ACA1 and ACA2, three independent transgenic lines with different level of GFP expression from weak to strong were used. The seeds used were transgenic line nos. 15673-c, 15673-d, and 15673-f for ACA1-GFP and transgenic line nos. 15672-a, 15672-b, and 15672-s for ACA2-GFP.

Confocal microscopy showing endomembrane ER-like localization for ACA7

To further investigate the subcellular localization of ACA1, 2, and 7 in pollen, we created stable transgenic lines expressing each of the ACAs with a C-terminal YFP or GFP tag, under control of either the pollen specific promoter *ACA9*, or the natural promoter *ACA7*. Using confocal microscopy, we examined the subcellular localization of at least ten independent transgenic lines with equivalent localization patterns seen with cells showing strong YFP or GFP signals, or cells in which the YFP or GFP signal was weak and at its lower limit of detection. In all cases tested, *ACA7* showed an ER-like endomembrane localization similar to ACA1-YFP or ACA2-GFP, but it failed to show any evidence for localization to the plasma membrane (Fig. 7F), as previously proposed by the Lucca and Leon (2012). As a control, the plasma membrane localization is shown for ACA9-YFP (Schiott et al., 2004).

Genetic analysis confirming endomembrane localization of the ACA7

To functionally validate an ER-like localization for the ACA7, an *ACA9p::ACA7-YFP* transgene was stably transformed into an *aca9* knockout mutant (a pollen-specific plasma membrane Ca^{2+} pump) that displays a partial male sterile phenotype, with pollen that are short, slow, and deficient in their ability to discharge sperm (Schiott et al., 2004). The question being addressed was whether ACA7 could substitute for the plasma membrane Ca^{2+} pump ACA9. Segregation analyses were conducted with plants expressing *ACA7-YFP* transgenes at a level providing equal or greater amounts of YFP expression than a control *ACA9-YFP* (Fig. 8B). In contrast to the rescue provided by a control *ACA9-YFP*, neither *ACA7* nor *ACA1* provide any evidence of being able to rescue the *aca9* pollen

transmission defect (Fig. 8A). Limonta et al. (2014) reported similar result for ACA2 (in which ACA2 failed to rescue a loss-of-function of a plasma membrane Ca^{2+} pump ACA12). While the observed transmission for the rescue of *aca9* knockout with the *ACA9-YFP* transgene was 97% from the expected 50%, the average of the observed transmission for the *ACA7-YFP* transgene was around 72% (from the expected 75% in case of self-fertilization) and 45% (from the expected 50% in case of crosses). Together, these results in conjunction with the confocal microscopy indicate that the ACA1 and ACA7 (and ACA2 as shown by Limonta et al. 2014), as endomembrane Ca^{2+} pumps, cannot rescue the loss of function of the plasma membrane Ca^{2+} pump *ACA9*.

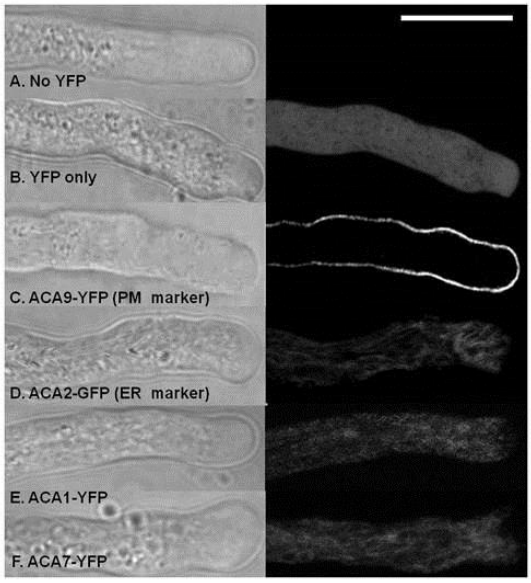

Figure 7. Confocal microscopy showing endomembrane localization for ACA7**.**
Pollen tubes were grown *in vitro and* imaged using confocal microscopy. Bright field and confocal fluorescence are shown to the right and left, respectively. Panel A showing wild-type pollen tube as a negative control without any YFP signal. Panel B showing ACA9promoter::YFP as a positive control with YFP signal only. Panel C and D showing ACA9promoter::ACA9-YFP and ACA9promoter::ACA2-GFP as plasma membrane and endoplasmic reticulum (ER) markers, respectively. Panel E showing

ACA9promoter::ACA1-YFP ER localization, as demonstrated in this study (and previous study conducted by Dunkley et al. 2006). Panel F showing ACA9promoter::ACA7-YFP endomembrane localization such as ER. Scale bar is equal to 10 µm. *For ACA7* subcellular localization, at least 20 independent transgenic lines with different expression levels were used. The same results obtained for all lines tested, no matter of the fluorescence level. Representative lines used for confocal microscopy were transgenic lines (TL) nos. 15728-1 to 15728-2 for empty vector, TL nos. 15729-15731 for ACA9, TL nos. 15266-A to 15266-C for ACA2, TL nos. 15718-1 to 15718-2, and 15721-2 for ACA1, and TL nos. 15264-E/F/G and H for ACA7.

A.

Segregation analysis showing expression of the pollen specific *ACA7* transgene can not rescue the defect in pollen transmission of *aca9* mutant.

Cross	F1	Segregation of Hyg^r marker		
Female x Male	total	Expected %	Observed %	P-value[a]
ACA9P::ACA9-YFP$^{(+/-)}$/aca9-8$^{(-/-)}$; Selfed	146[(1)],452[(2)],205[(3)]	75	92[(1)],85[(2)],93[(3)]	<0.02[(1,2)],<0.005[(3)]
ACA9P::ACA9-YFP/aca9-8$^{(-/-)}$ (TG) X Col WT	184[(1)]	50	57[(1)]	0.2[(1)]
aca9-8$^{(-/-)}$ X *ACA9P::ACA9-YFP/aca9-8$^{(-/-)}$* (TG)	71[(1)]	50	97[(1)]	<0.001[(1)]
ACA9P::YFP$^{(+/-)}$/aca9-8$^{(-/-)}$; Selfed	48[(1)],62[(2)],134[(3)]	75	67[(1)],82[(2)],66[(3)]	All 0.8
ACA9P::ACA1-YFP$^{(+/-)}$/aca9-8$^{(-/-)}$; Selfed	134[(1)],159[(2)],212[(3)],241[(4)]	75	76[(1)],68[(2)],76[(3)],65[(4)]	0.9[(1,3)],0.8[(2)],0.1[(4)]
ACA9P::ACA7-YFP$^{(+/-)}$/aca9-8$^{(-/-)}$; Selfed	226[(1)],161[(2)],300[(3)],299[(4)],269[(5)],77[(6)]	75	69[(1)],75[(2)],75[(3)],77[(4)],68[(5)],66[(6)]	0.8[(1,4,5,6)],1[(2)],0.95[(3)]
ACA9P::ACA7-YFP/aca9-8$^{(-/-)}$ (TG) X Col WT	135[(1)],89[(3)],259[(6)],98[(9)]	50	50[(1)],49[(3)],50[(6)],48[(9)]	0.97[(1)],0.95[(3)],0.9[(6)],0.8[(9)]
aca9-8$^{(-/-)}$ X *ACA9P::ACA7-YFP/aca9-8$^{(-/-)}$* (TG)	43[(1)],80[(3)],6[(6)],44[(9)]	50	44[(1)],40[(3)],50[(6)],50[(9)]	0.8[(1,3)],1[(6,9)]

a. Significance determined by the Pearson's chi-squared test. TG and WT refers to transgene and wild type respectively. The numbers shown as superscript refer to the line number in case of each transgene tested. These lines were the same as those tested for the YFP expression level. For the ACA9-YFP/aca9-8 transgeneic lines no. 15729-15731 was used. For the empty vector, transgenic lines no. 15728-2, tl15728-3, and tl15728-6 were used. For the ACA1-YFP/aca9-8 transgenic lines no. 15688-2, 15688-4, 15688-6 and 15722-7 were used. For the ACA7-YFP/aca9-8 transgenic lines no. 15727-1, 15727-3, 15727-4, 15727-6, 15727-7 and 15727-9 were used.

B.

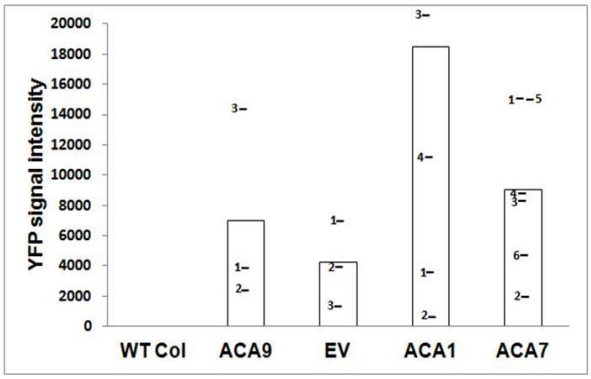

Figure 8. Segregation analysis showing expression of ACA7 in the aca9 mutant cannot rescue the pollen transmission defect of the aca9**.**

A) Segregation analysis showing expression of an endomembrane calcium pump, *ACA7*, cannot restore partial male sterility phenotype of the *aca9* mutant.

B) YFP signal intensity quantification in the pollen grains showing ACA1-YFP and ACA7-YFP transgenic lines that have the same or greater amounts of YFP expression compared to that ACA9-YFP still cannot rescue the partial male sterility phenotype of the *aca9*. All YFP quantification images were taken at the same time. The transgenic lines used for genetic crosses and YFP quantification are the same. For the *ACA9-YFP/aca9-8* transgenic lines no. 15729-15731 was used. For the empty vector, transgenic lines

no.15728-2, tl15728-3, and tl15728-6 were used. For the *ACA1-YFP/aca9-8* transgenic lines no. 15688-2, 15688-4, 15688-6 and 15722-7 were used. For the *ACA7-YFP/aca9-8* transgenic lines no. 15727-1, 15727-3, 15727-4, 15727-6, 15727-7 and 15727-9 were used.

Discussion

Disruption of *ACA1, 2,* and *7* Ca^{2+} pumps activates a programmed cell death (PCD) which depends on the activation of salicylic acid

While single knockouts of each ACAs did not show any observable phenotype, here we provide evidence for a salicylic acid-dependent PCD in *aca1/2/7* triple knockout. In addition to the current study, at least two other studies showed a connection between Ca^{2+} signaling pathway mediated by Ca^{2+} pumps and activation of PCD in plants. In the first study, Zhu et al. (2010) showed silencing of a tobacco ACA (NbCA1) can result in a high frequency of lesions from a PCD pathway. Based upon transient expression of a GFP-tagged enzyme, the tobacco NbCA1 was reported to be localized to the ER. Second, in Arabidopsis, using a gene knockout approach, Boursiac et al. (2010) demonstrated that the vacuolar ACA4 and 11 were essential for regulating a salicylic acid-dependent PCD pathway. The protein sequence of NbCA1 is more similar to two vacuolar ACAs (ACA4 and 11) that have been demonstrated to be localized to the vacuole using GFP-tagged enzymes expressed in stable transgenic plants. Thus, it is not yet clear if the silencing experiment in tobacco resulted in a lesion phenotype because of the loss of one or more ACAs localized to the ER or vacuole. Here using a gene knockout approach, we showed loss of all three ACAs (ACA1 and 2 were localized to the ER and ACA7 was localized to either the ER or ER-like structures such as trans-Golgi) results in mild-lesion phenotype

compared to the strong-lesion phenotype observed in the *aca4/11* double mutant. Figure 2C compares *aca4/11* to the *aca1/2/7* mutant, showing *aca4/11* mutant has overall smaller size and high frequency of lesion compared to that *aca1/2/7*. Further, the transcript abundance of *PR1* gene, a salicylic acid dependent molecular marker, increased in the *aca1/2/7* mutant (Fig. 2D), such as *aca4/11* (Fig. 3B). Together, the results here suggest both types of Ca^{2+} pumps *aca1/2/7 versus 4/11* control PCD in a SA-dependent manner. However, the resulting lesion phenotype differed between the two Ca^{2+} pumps, with loss of the vacuolar pumps resulting in the strong phenotype.

The resulting lesion phenotype was reversed when the *aca1/2/7* mutant plants were transformed by any one of the three isoforms, providing genetic evidence for the functional redundancy of *ACA1*, *2*, and *7* (Fig. 2A). This result was also supported by the reduced transcript abundance of the *PR1* gene in the rescued lines (Fig. 2D). In addition, the lesion phenotype was suppressed when the *aca1/2/7* mutant transformed with a *NahG* transgene (Fig. 3A), suggesting that the resulting lesion was dependent on SA production. Consistent with this, the expression level of the *PR1* gene was reduced in the *aca1/2/7* mutants harboring *NahG* (Fig. 3B).

***ACA1, 2,* and *7* calcium pumps are important for the pollen fitness**

While self-fertilization of each single knockout line did not show any changes in terms of transmission efficiency (Table 1), loss of function of all three Ca^{2+} pumps impaired pollen fitness with the average distortion of 58% from the expected 75% for the self-fertilized plants and of 31% from the expected 50% for the outcrosses (Table 2). The

observed distortion dropped to 49% and 8% from the expected 75% and 50% by performing the cross under hot/cold stress conditions.

Together, the results here provide evidence for the importance of ACA1, 2, and 7 calcium pumps in the overall health of pollen under unstressed and stressed conditions. The pollen-specific expression of any of the three isoforms improved pollen fitness, providing another layer of evidence for these three Ca^{2+} pumps being functionally redundant (Fig. 4 and Supplemental Table S2).

Conversely, no distortion was observed for the *aca4/11* double mutants, supporting the idea that the two Ca^{2+} pumps (vacuole *versus* ER type) have some unique feature for regulating cellular process such as pollen fitness.

Transmissions of the *aca1/2/7* mutant pollen tubes are impaired at the top of the pistils

Whereas the seed set analysis showed there was no differences in terms of seed production in the *aca1/2/7* mutants (Fig. 5A), the top/middle/bottom analysis revealed the *aca1/2/7* triple mutants defects in transmission of the pollen through all three parts of the pistils with the top part showing the most severe defect. In other words, the *aca1/2/7* mutant pollen were unsuccessful in competition with wild-type pollen to fertilize ovules in the pistil (Fig. 5B), as evidenced by the reduced transmission efficiency of the mutant pollen by fertilizing almost 30% of the ovules at all three sections of the pistils from the expected 50%. This is a unique type of pollen transmission defect, which has not been observed previously. In most cases, the defect in pollen transmission is associated with the slower growth rate of the pollen tube to fertilize the ovules near the bottom of the

pistils. For example, a double knockout of the *ala6/7* lipid flippases resulted in pollen tubes with shorter length and growth defects, in which the mutant pollen failed to compete with the wild-type pollen at the bottom of the pistils (McDowell et al., 2015).

We refer to this type of defect as the "blind defect", in which the mutant pollen fail to find ovules especially at the top. However, by approaching at the bottom of the pistils, finally the mutant pollen tubes fertilize ovules by chance, resulting in full seed set. This should be tested further by an aniline blue staining of the mutant pollen in a semi-*in vivo* experiment compared to the wild-type pollen.

A top/middle/bottom segregation distribution analysis using siliques produced by outcrossing pollen from transgenic lines expressing the *ACA9P::ACA7-YFP* transgene showed that the pollen harboring an *ACA9P::ACA7-YFP* transgene were more competitive in fertilizing ovules at the top of the ovary (Fig. 5C and Supplemental Table 3), suggesting that *aca1/2/7* mutant pollen are indeed (specifically) deficient in their ability to compete with wild-type pollen tube at the top of the ovary.

Confocal microscopy revealed ACA1 and ACA7 both targeting the ER and ER-like structure

ACA1, *2*, and *7* cluster together in the phylogenetic tree away from any other ACAs. A similarity analysis showed that they have high sequence similarity at the protein level. Here we provide at least three lines of evidence to support the functionally redundancy of ACA1, 2, and 7. First, while there was no phenotype with each single knockout, loss of all three genes together resulted in lesion production and a pollen transmission defects. Second, a vegetative expression of any of the three genes reversed the lesion phenotype.

Third, the pollen expression of any of the three isoforms improved the pollen fitness. Thus, because ACA1, 2, and 7 are functionally redundant, the speculation is they might have similar subcellular location such as ER.

Consistent with the study conducted by the Dunkley et al. (2006), using confocal microscopy, we provided the second layer of evidence for the ACA1 ER localization. Based upon the proteome study, ACA1 and ACA2 were found in the ER compartment (Dunkley et al., 2006). Here using the stably transgenic lines harboring the *35Sp::ACA1-GFP*, we looked at the ACA1 subcellular localization at the two different cell types in Arabidopsis: root tips and guard cells (Fig. 6). Our microscopy images indicate that in both cases, ACA1-GFP signals were found in the ER. The ACA1 localization in the root tips (Fig. 6A) looks similar to the ACA2 ER localization, as shown by the Harper et al. (1998). We further examined the ACA1 localization in the guard cells, the only epidermal cells containing chloroplasts. The result here showed no overlay between the ACA1-GFP and the chloroplast red autoflorescence (Fig. 6B), thus, ruling out the incorrect idea ACA1 localizes to the chloroplast envelope.

To re-examine the ACA7 localization, we utilized two independent approaches, confocal microscopy and genetic analysis. First, we created stable transgenic lines expressing ACA9p::ACA7-YFP or ACA7p::ACA7-YFP with the C-terminus end YFP tag to avoid possible interference of the fusion tagged protein with the N-terminus signal peptide required for the localization. Our confocal microscopy showed endomembrane ER-like localization for both of the constructs tested with different levels of YFP levels (Fig. 7). In the genetic approach, the segregation analysis indicated that expression of ACA7-YFP,

even with the same amounts of YFP expression level as the ACA9-YFP, cannot rescue the pollen transmission defect of the *aca9* mutant, a plasma membrane Ca^{2+} ATPase (Schiott et al., 2004, Fig. 8). Together, we provided two lines of evidence showing that ACA7 is localized to an endomembrane ER-like structure.

Conclusion and future direction

In this study, we had at least two major achievements. First of all, using genetic approach, we provided evidence for the importance of the ACA1, 2, and 7 in control of programmed cell death (PCD) and pollen fitness. Second, we provided evidence for the ER and endomembrane localization for the ACA1 and ACA7, respectively.

Although we provided evidence for the importance of the ACA1, 2, and 7 in PCD and pollen transmission, the mechanism by which a disruption of *ACA1*, *2*, and *7* activates PCD and impairs the pollen transmission are not yet clear. For example, in case of *aca1/2/7* "blind defect" phenotype, a semi-*in vivo* pollen tube growth assay would help in gaining insight into the mechanism that resulted in *aca1/2/7* pollen being less competitive at the top of the ovary.

Supplemental Data

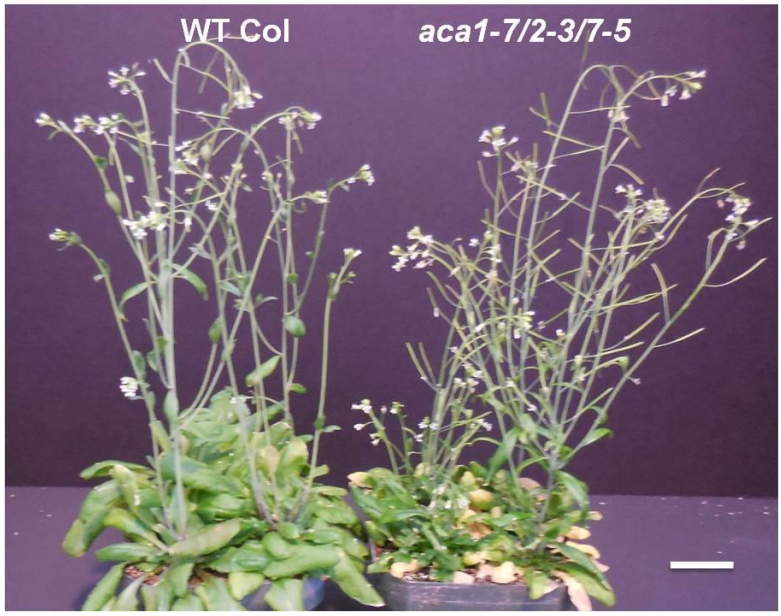

Supplemental Figure S1. *aca1/2/7* mutant showing lesion phenotype. Picture showing *aca1-7/2-3/7-5* mutant compared to the wild-type plant grown under the same greenhouse condition. Scale bar = 2 cm.

Supplementary table S2. Expression of *ACA1* or *ACA2*, or *ACA7* transgene in pollen can rescue the defect in pollen transmission of *aca1/2/7* mutant, indicating that *ACA1*, *2*, and *7* are functionally redundant.

Rescuing construct	Cross Female x Male	F1 total	Segregation of Hygromycin marker gene Expected %	Observed %	P-value[a]
Empty vector	*ACA9P::YFP/aca1-7(-/-)/2-3(-/-)/7-5(-/-)* (TG) X *aca1-7(-/-)/2-3(-/-)/7-5(-/-)*	75,49,67	50	43,49,58	0.8,0.9,0.8
	aca1-7(-/-)/2-3(-/-)/7-5(-/-) X *ACA9P::YFP/aca1-7(-/-)/2-3(-/-)/7-5(-/-)* (TG)	245,164,110	50	46,46,44	All 0.8
	ACA9P::YFP/aca1-2(-/-)/2-2(-/-)/7-9(-/-) (TG) X *aca1-2(-/-)/2-2(-/-)/7-9(-/-)*	117	50	52	0.8
	aca1-2(-/-)/2-2(-/-)/7-9(-/-) X *ACA9P::YFP/aca1-2(-/-)/2-2(-/-)/7-9(-/-)* (TG)	65	50	49	0.95
ACA1	*ACA9P::ACA1-YFP/aca1-7(-/-)/2-3(-/-)/7-5(-/-)* (TG) X *aca1-7(-/-)/2-3(-/-)/7-5(-/-)*	60,63,167,157,175	50	40,48,50,57,47	0.8,0.8,0.975,0.2,0.8
	aca1-7(-/-)/2-3(-/-)/7-5(-/-) X *ACA9P::ACA1-YFP/aca1-7(-/-)/2-3(-/-)/7-5(-/-)* (TG)	267,121,149,191,73	50	71,64,68,70,67	<0.0001,<0.025,<0.005,<0.0001,<0.05
	ACA9P::ACA1-YFP/aca1-2(-/-)/2-2(-/-)/7-9(-/-) (TG) X *aca1-2(-/-)/2-2(-/-)/7-9(-/-)*	45	50	49	0.95
	aca1-2(-/-)/2-2(-/-)/7-9(-/-) X *ACA9P::ACA1-YFP/aca1-2(-/-)/2-2(-/-)/7-9(-/-)* (TG)	107	50	66	<0.02
ACA2	*ACA9P::ACA2-GFP/aca1-7(-/-)/2-3(-/-)/7-5(-/-)* (TG) X aca1-7(-/-)/2-3(-/-)/7-5(-/-)	376,318	50	53,47	All 0.8
	aca1-7(-/-)/2-3(-/-)/7-5(-/-) X *ACA9P::ACA2-GFP/aca1-7(-/-)/2-3(-/-)/7-5(-/-)* (TG)	166,247	50	61,60	<0.05,<0.025
	ACA9P::ACA2-GFP/aca1-2(-/-)/2-2(-/-)/7-9(-/-) (TG) X *aca1-2(-/-)/2-2(-/-)/7-9(-/-)*	258,87,137,114	50	49,49,39,47	0.9,0.95,0.1,0.8
	aca1-2(-/-)/2-2(-/-)/7-9(-/-) X *ACA9P::ACA2-GFP/aca1-2(-/-)/2-2(-/-)/7-9(-/-)* (TG)	498,369,190,174	50	57,61,62,75	<0.05,<0.005,<0.02,<0.001
ACA7	*ACA7P::ACA7-YFP/aca1-7(-/-)/2-3(-/-)/7-5(-/-)* (TG) X *aca1-7(-/-)/2-3(-/-)/7-5(-/-)*	102,112,93,183	50	41,53,49,50	0.8,0.8,0.95,0.975
	aca1-7(-/-)/2-3(-/-)/7-5(-/-) X *ACA7P::ACA7-YFP/aca1-7(-/-)/2-3(-/-)/7-5(-/-)* (TG)	518,204,78,87	50	80,77,69,82	<0.0001,<<0.0001,<0.02,<0.0001
	ACA7P::ACA7-YFP/aca1-2(-/-)/2-2(-/-)/7-9(-/-) (TG) X *aca1-2(-/-)/2-2(-/-)/7-9(-/-)*	80,173,51	50	41,51,51	0.8,0.8,0.95
	aca1-2(-/-)/2-2(-/-)/7-9(-/-) X *ACA7P::ACA7-YFP/aca1-2(-/-)/2-2(-/-)/7-9(-/-)* (TG)	77,101,109	50	75,80,64	<0.005,<0.0001,<0.05
	ACA9P::ACA7-YFP/aca1-2(-/-)/2-2(-/-)/7-9(-/-) (TG) X *aca1-2(-/-)/2-2(-/-)/7-9(-/-)*	548,357,296,148	50	51,50,51,44	0.8,0.95,0.9,0.8
	aca1-2(-/-)/2-2(-/-)/7-9(-/-) X *ACA9P::ACA7-YFP/aca1-2(-/-)/2-2(-/-)/7-9(-/-)* (TG)	509,426,255,70	50	76,76,73,84	All<0.001

a. Significance determined by the Pearson's chi-squared test.

Supplementary Table S2. Expression of *ACA1* or *ACA2*, or *ACA7* transgene in pollen can rescue the defect in pollen transmission of *aca1/2/7* mutant, indicating that *ACA1*, *2*, and *7* are functionally redundant.

Supplementary table S3. Transmission of *aca1/2/7* through pollen is compromised at the top of the silique, which can be rescued by the *ACA7* transgene.

Male x Female	Expected %	observed %	P-value[a]	Total Top	Middle	Bottom	n	Total transmission % P-value[a]
aca1-2(-/-)/7-9(-/-)/2-2(+/-)[b] X WT	50			23	32	33	674	All <0.0001
Line#1; ACA9P::ACA7-YFP/aca1-7(-/-)/2-3(-/-)/7-5(-/-) (TG)[c] X WT	50	65	0.1	73	76	55	74	0.8,0.1,0.8
Line#2; ACA9P::ACA7-YFP/aca1-7(-/-)/2-3(-/-)/7-5(-/-) (TG)[c] X WT	50	73	<0.005	81	80	59	95	<0.05,<0.01,0.8
Line#3; ACA9P::ACA7-YFP/aca1-7(-/-)/2-3(-/-)/7-5(-/-) (TG)[c] X WT	50	70	0.1	78	65	69	44	0.2,0.8,0.8
Line#4; ACA9P::ACA7-YFP/aca1-7(-/-)/2-3(-/-)/7-5(-/-) (TG)[c] X WT	50	64	0.8	82	70	47	36	<0.005,<0.05,<0.8

a. Significance determined by the Pearson's chi-squared test.

b. Scored for Basta[r]

c. Scored for Hygromycin[r]

Supplementary Table S3. Transmission of *aca1/2/7* through pollen is compromised at all three sections of the ovary with the top showing the most severe defect, which can be rescued by the *ACA7* transgene.

References

Bonza MC, Morandini P, Luoni L, Geisler M, Palmgren MG, Michelis MID (2000) *At*-ACA8 encodes a plasma membrane-localized calcium-ATPase of Arabidopsis with a calmodulin-binding domain at the N-terminus. Plant Physiology 123: 1495-1506.

Bonza MC, Carnelli A, De Michelis MI, Rasi-Caldogno F (1998) Purification of the Plasma Membrane Ca-ATPase from Radish Seedlings by Calmodulin-Agarose Affinity Chromatography. Plant Physiology 116: 845–851.

Boursiac Y, Lee SM, Romanowsky S, Blank R, Sladek C, Chung WS, Harper JF (2010) Disruption of the vacuolar calcium-ATPases in Arabidopsis results in the activation of a salicylic acid-dependent programmed cell death pathway. Plant Physiology 154: 1158–1171.

Gaffney T, Friedrich L, Vernooij B, Negrotto D, Nye G, Uknes S, Ward E, Kessmann H, Ryals J (1993) Requirement of salicylic acid for the induction of systemic acquired resistance. Science 261: 754-756.

Harper JF, Hong B, Hwang I, Guo HQ, Stoddard R, Huang JF, Palmgren MG, Sze H (1998) A novel calmodulin-regulated Ca^{2+}-ATPase (ACA2) from Arabidopsis with an N-terminal autoinhibitory domain. The Journal of Biological Chemistry 273: 1099–1106.

Huang L, Berkelman T, Franklin AE, Hoffman NE (1993) Characterization of a gene encoding a Ca^{2+}-ATPase-like protein in the plastid envelope. Proceedings of the National Academy of Sciences of the United States of America 90: 10066–10070.

Iwano M, Igarashi M, Tarutani Y, Kaothien-Nakayama P, Nakayama H, Moriyama H, Yakabe R, Entani T, Shimosato-Asano H, Ueki M, Tamiya G, Takayama S (2014) A pollen coat-inducible autoinhibited Ca^{2+}-ATPase expressed in stigmatic papilla cells is required for compatible pollination in the Brassicaceae. The Plant Cell 26: 636-349.

Limonta M, Romanowsky S, Olivari C, Bonza MC, Luoni L, Rosenberg A, Harper JF, De Michelis MI (2014) ACA12 is a deregulated isoform of plasma membrane Ca^{2+}-ATPase of *Arabidopsis thaliana*. Plant Molecular Biology 84: 387-397.

Livak KJ, Schmittgen TD (2001) Analysis of relative gene expression data using real-time quantitative PCR and the 2(-Delta Delta C (T)) Method. Methods 4: 402-408.

Lucca N, León G (2012) Arabidopsis ACA7, encoding a putative auto-regulated Ca^{2+}-ATPase, is required for normal pollen development. Plant Cell Reports 31: 651-659.

McDowell SC, López-Marqués RL, Cohen T, Brown E, Rosenberg A, Palmgren MG, Harper JF (2015) Loss of the Arabidopsis thaliana P4-ATPases ALA6 and ALA7 impairs pollen fitness and alters the pollen tube plasma membrane. Frontiers in Plant Science 6:197-209.

Roh MH, Shingles R, Cleveland MJ, McCarty RE (1998) Direct measurement of calcium transport across chloroplast inner-envelope vesicles. Plant Physiology118: 1447–1454.

Schiøtt M, Romanowsky S, Baekgaard L, Jakobsen MK, Palmgren MG, Harper JF (2004) A plant plasma membrane Ca^{2+}-pump is required for normal pollen tube growth and fertilization. Proceedings of the National Academy of Sciences of the United States of America 101: 9502-9507.

Sousa AO, Assis ET, Pirovani CP, Alvim FC, Costa MG (2014) Phosphate-induced-1 gene from Eucalyptus (EgPHI-1) enhances osmotic stress tolerance in transgenic tobacco. Genetics and Molecular Research 13:1579-1588.

Chapter III.

Identification of heat stress responsive genes in Arabidopsis pollen: a transcriptome comparison between wild-type and the *cyclic nucleotide-gated channel 16* (*cngc16*) mutant

Abstract

Global warming is expected to have a major impact on crop loss around the world. In flowering plants, the male gametophyte (pollen), is one of the most vulnerable cells to temperature stress. In *Arabidopsis*, *Cyclic Nucleotide-Gated Channel 16* (*cngc16*), a pollen-specific calcium-conducting channel, is required for plant reproduction under temperature stress conditions. The *cncg16* mutant is nearly sterile under conditions of hot days and cold nights. To understand the mechanism(s) underlying the *cngc16* mutant pollen sensitivity to temperature stress conditions, RNA-Seq was used to compare the pollen transcriptomes of the wild-type and the *cngc16* mutant under normal and the hot/cold stress conditions. Here, we show that 641 (equal to 25%) of the stress-dependent changes (≥2-fold changes with adjusted *p*-value ≤0.01) in the wild-type pollen transcriptome fail to occur in the *cngc16* knockout, identifying a subset of failed responses that might contribute to the poor stress tolerance displayed by *cngc16* pollen. Of those 641 failed responses, 27 were transcription factors. In addition, there were two miRNAs (*MIR156A* and *MIR845A*) that were induced more than 7,000 fold in the wild-type pollen under the heat stress, but failed to express in the *cngc16* pollen. In addition to a failure to reproduce key wild-type responses, *cngc16* pollen showed a different set of 2,733 stress-dependent changes that remained unaltered in wild-type pollen. A metabolic pathways analysis based upon GO annotations suggested a high frequency of changes

associated with carbohydrate, lipid, and nucleotide biosynthesis pathways in the heat-stressed pollen. Taken together, these results support the hypothesis that the temperature-stress sensitivity displayed by *cngc16* pollen is due to a failure to coordinate global changes in the transcriptome because of a defect in a CNGC-calcium signaling pathway.

Introduction

Pollen, as a single cell, provide a unique opportunity in a plant system to examine genetic and physiology of a single cell during stresses. Plant reproductive system is the most vulnerable organ of the plant during stresses with most sensitivity associated with the male gametophyte during pollen development and seed formation (Zinn et al., 2010; Giorno et al., 2013). Mature pollen have specialized function in producing the proteins necessary for germination and pollen tube growth (Grennan, 2007). So, pollen would be expected to have a different set of transcriptome and metabolome than vegetative tissues. Thus, identification of uniquely expressed genes and metabolites in pollen during stresses will provide novel and fundamental insights into pollen viability in hostile environment during its lifespan.

Several experiments including microarray-based mRNA expression analysis showed transcriptome changes in pollen under heat stress in different plant species (Frank et al., 2009; Zang et al., 2012, Endo et al., 2009). However, only a few RNA-Seq experiments have been performed in pollen under heat stress. Recently an RNA-Seq experiment was done in rice to compare the transcriptome of spikelet at meiosis stage in response to heat and nitrogen stresses or a combination of both factors (Yang et al., 2015). The transcripts associated with heat-stress response include protein kinases, heat shock proteins, transcription factors, flavonoid, cytochrome, peroxidases, and ubiquitin. The other RNA-Seq experiment was performed in tomato pollen to compare transcript abundances of small non-coding RNAs (sncRNAs) with and without heat stress (Bokszczanin et al., 2015). In addition to other sncRNAs, two differentially expressed miRNAs in the pollen

expression profiles were reported with one being increased and the other being decreased under heat stress, suggesting the involvement of miRNAs in pollen thermotolerance.

Previous study from the Harper lab conducted by the Tunc-Ozdemir et al. (2013) identified Arabidopsis *Cyclic Nucleotide-Gated Channel 16* (*CNGC16*) as a necessary component for the plant reproductive system under the condition of hot days and cold nights. Loss of function of the *cngc16* resulted in 10-fold reduction in pollen transmission efficiency and seed production under hot/cold stress conditions. Q RT-PCR analysis showed the *cngc16* mutant showed reduced transcript abundances of heat stress marker genes including two heat shock transcription factors (*HsfA2* and *HsfB1*), and *BCL-2-associated athanogene 6* (*Bag6),* a downstream gene of the *HsfA2*. Several studies demonstrated that these three genes are required for plant thermotolerance (Charng et al., 2007; Ikeda et al., 2011; Nishizawa-Yokoi et al., 2009; Cartagena et al., 2008).

To gain insight into the mechanism(s) underlying the *cngc16* mutant hypersensitivity to hot/cold stress, we performed an RNA-Seq experiment to compare the transcriptome of the *cngc16* mutant pollen with the wild-type Col-0 pollen under control and the hot/cold stress conditions (as described in the Tunc-Ozdemir et al., 2013). Here, our RNA-Seq experiment identified that although *cngc16* mutant pollen showing higher number of statistically significant changes (4,705 differentially expressed transcripts) compared with the wild-type pollen (2,612 differentially expressed transcripts) under the hot/cold stress condition, the mutant lacks the proper induction of several key genes with potential function in the pollen thermotolerance under hot/cold stress. Among those are two miRNAs (*MIR156A* and *MIR845A*) and several transcription factors. These two miRNAs

are only induced in the wild-type pollen (log2-fold change of 13) under hot/cold stress, but not in the *cngc16* mutant pollen.

Unlike *MIR845A* with a putative target (a gene with role in DNA integration), *MIR156A* has been shown to be involved in a "heat stress memory" by repression of *SQUAMOSA PROMOTER BINDING PROTEIN-LIKE* (SPL) transcription factors in vegetative tissues. A heat-stress memory refers to a plant adaptation to recurring heat stress that allows improved survival to future heat stress (Stief et al., 2014). In contrast to the *cngc16* mutant, the SPL transcription factors transcript abundances in wild-type pollen did not decrease under the hot/cold stress. This is inconsistent with the idea that expression of *miRNAs* negatively regulates the target mRNAs. One possibility is that the same type of message will be transferred to downstream targets through SPL transcription factors that do not show changes in their steady-state transcript abundance. Overall, the results obtained here highlight that key components may be required for pollen thermotolerance under hot/cold stress condition.

Methods

Plant material and growth conditions

The *cngc16-2* (*SAIL_726_B04*, seed stock no. 91) mutant carries a glufosinate (Basta) resistance marker in the T-DNA insertion (Tunc-Ozdemir et al. (2013)). Following sterilization, seeds from both Arabidopsis Columbia wild-type (Col-0) and the *cngc16-2* mutant were sown on 0.5x Murashige and Skoog (MS) medium (pH=5.7) containing 1% agar with or without Basta (10 µg ml^{-1}). After 48 h of stratification at 4 °C, seedlings were grown at room temperature under constant light for 24 h for 10 days. The resulting

seedlings were then transferred to soil (Sunshine SMB-238; Hummert). Unless otherwise stated, seedlings were grown until maturity under controlled non-stress conditions in a growth chamber with a photoperiod of 16 h of light and 8 h of dark at 22 °C, 50% humidity, and light intensity of 125 µmol m^{-2} s^{-1}.

Stress condition

The hot days and cold night stress regime was performed as described (Tunc-Ozdemir et al., 2013). Briefly, flowering plants grown under controlled non-stress condition were transferred to the hot and cold stress regime when the chamber showing 10 °C, and grown for 1 to 2 more weeks to adapt to the condition (Figure 1).

Pollen collection

For both the wild-type and mutant, three biological replicates per each condition were used. All pollen samples were harvested at midday (12:00 pm). Pollen from open flowers were harvested in a 50 ml falcon tube containing water, and then vortexed for 10 to 20 sec followed by passing through a 70 µm nylon mesh (Becton Dickinson and Company). The pollen samples were centrifuged into a pellet at 14,000 rpm in a microfuge for 30 sec. The supernatant was discarded, and pollen pellets were frozen in liquid nitrogen and stored in -80 °C for future analyses. Pollen from hot and cold stress regime were harvested when the stress chamber temperature was preceded by 40 °C for 1 h (Figure 1). To evaluate possible contamination in the collected pollen samples, a suspension of pollen samples was inspected under the light microscope for each replicate (Supplemental Figure S2).

RNA extraction and library preparation

Total RNA was extracted from pollen samples using Plant Mini Kit (Qiagen, Invitrogen), and cleaned at least twice using RNase-free DNase to eliminate genomic DNA contamination. 1 µg of total RNA from each sample was sent in dry ice to the UCLA Neuroscience Genomic Core (UNGC) (Los Angeles, CA, USA) for library preparation using the TruSeq RNA kit and sequencing. The RNA samples were quantified using the RiboGreen assay, and the quality of the RNA was checked by the Agilent TapeStation 2200 and the visual inspection of the actual traces. Briefly, a 1 µg of total RNA was poly-A selected using oligo dT magnetic beads, fragmented, and random primed. Then double-stranded cDNA was phosphorylated, and A-tailed followed by adapter ligation, PCR amplification, and sequencing. The cDNA libraries were multiplexed and run on a single lane. The sequencing was performed on an Illumina HighSeq2500 with paired-end (PE) reads of 50 bp long (2 x 50 bp).

RNA-Seq data analysis

Sequence pairs were filtered to excise sequences containing sequencing adapters using NGS QC Toolkit, version 2.3 (Patel and Jian 2012). Sequence quality was visualized before and after adapter sequence removal using FastQC ver. 0.11.2 (http://www.bioinformatics.babraham.ac.uk/projects/fastqc/).

The filtered sequence pairs were aligned to the TAIR10 *Arabidopsis thaliana* reference genome (Swarbreck et al., 2008) sequence, using the spliced-read alignment tool Tophat2 (v. 2.0.13; Kim et al., 2013), which in execution employed Bowtie 2 (v. 2.2.4; Langmead and Salzberg 2012). The coordinates of known protein coding genes, exons, and splice

sites were obtained from the TAIR repository (www.arabidopsis.org), as a gene transfer format (GTF) file and provided to Tophat2.

The genome-aligned outputs of Tophat2 (bam-format files) were provided to the tools of the Cufflinks package (v.2.2.1) for transcript quantification (Trapnell et al., 2010). For each sample, the cufflinks executable was provided with the same GTF file as provided to Tophat2 to demarcate all known Arabidopsis gene models, with sequence bias correction enabled and maximum fragment bundle size increased to 10 million. Next, gene expression was estimated for all genes using the included cuffdiff tool. The effective library sizes (the number of reads successfully aligned by Tophat2) and transcript lengths were used to transform expression estimates from the cufflinks-native fragments-per-kilobase-per-million-reads (FPKM) format into a count-compatible format for downstream analyses. Specifically, the FPKMS value of each gene for each sample was multiplied by the gene length (in kilobases) and by the library size of the sample (in millions).

Counts were first transformed from isoform-level values to gene-level values by computing the sum of counts across all isoforms for each parent gene. Transcript counts were then filtered to exclude very low-count transcripts. Specifically, transcripts with counts equal to zero in all twelve samples were excluded from further analysis, as were those in which all four conditions had only one non-zero count replicate. Additionally, any transcript with count values less than 10 in all twelve samples were excluded. Filtering was performed to exclude transcripts with general low abundance that may affect the dispersion computations, following standard filtering protocols of (Chen 2015). Filtered count data were then normalized via the upper quartile method, one of the default

normalization methods of the edgeR package (Robinson 2010). Here normalization factors were computed to scale the raw library sizes to minimize the fold-changes of most tags between samples: scale factors were calculated from the 75% quantile of the counts for each sample. Normalization factors were then adjusted to multiply to 1.

Negative binomial models were then fitted and dispersion estimate were computed, after which the generalized model likelihood ratio test was performed with contrasts to determine differential expression. Details can be found in Robinson 2010 and Chen 2015. The p-value and log2-fold change were computed for each gene's statistical test of statistical differential expression between each pair of conditions. The p-values were then adjusted for the false discovery rate (Benjamini-Hochberg 1995). The count data presented in Supplemental Table S2 to Supplemental Table S12 are counts per million of the normalized filtered data, and averages thereof. Please note that these values do not translate directly into the estimated log2-fold changes as reported by edgeR. Sequence data generated by this study will be available in GenBank.

qRT-PCR validation of candidate genes

The same RNA samples used for RNA sequencing were used for qRT-PCR validation. First strand cDNA was synthesized using 1 µg of total RNA, iScript cDNA Synthesis Kit (Catalogue#170-8891; Bio-Rad laboratory). A fraction (0.14 μg) of the cDNA was used as the template in a total 20 µL reaction mixture in qRT-PCR using SsoFast Probes Supermix (Catalog # 172-5231; Bio-Rad laboratory) following the manufacturer's instructions. TaqMan assays were used for *HsfA2* (At2g26150; assay ID nos. At02302989_g1) and *Bag6 (*At2g46240; assay ID nos. At02256657_g1) from Applied

Biosystems Inc. Expression of target genes were normalized against *elongation factor1-α* (*EF1-α*) RNA levels (AT5G60390; assay ID no. At02337969_g1; Applied Biosystems). Gene expression levels were quantified by real-time quantitative RT PCR (CFX96; Bio-Rad laboratory). The PCR conditions were as follows: 2 minutes at 95 °C, 39 cycles of 95 °C for 15 sec. and 1 minute at 60 °C. The comparative cycle threshold method (delta Ct) was used to analyze the data (Livak and Schmittgen, 2001).

Gene ontology (GO) and metabolic pathway analyses

Differentially expressed transcripts showing ≥2-fold changes ($p<0.01$) were analyzed using AmiGO (Carbon et al., 2009). For mapping the differentially expressed transcripts to possible metabolic pathways, AraCyc (Plant Metabolic Network (PMN), http://www.plantcyc.org/tools/tools_overview.faces) was used.

Supplementary methods

Immune-labeling of pectins in the pollen tube cell wall

Pollen grains from both genotypes were mounted on the coverslip. Vaseline was used to make a ring around the pollen grains. Approximately 200 µl pollen germination growth media (Fan et al., 2001) was added to each coverslip to cover the pollen grains. The cover slips were then placed in the square plate containing wet tissue paper to maintain the humidity, and kept in dark at room temperature. For the immunolabeling, the method described in Chebli et al. (2012) was used with slight changes. After pollen tube formation, approximately between 3-4 hours, the pollen media were replaced by the 3.5% v/v formaldehyde in PIPES buffer. The PIPES buffer used included 50 mM PIPES, 1 mM EGTA, 5 mM $MgSO_4$, and 0.5 mM $CaCl_2$ with pH = 7 for 15 minutes. Then the samples

were briefly washed in the phosphate-buffered saline (PBS 1X) 3 times, followed by incubation with the monoclonal antibodies LM19 (for unesterified pectin) and LM20 (for methylesterified pectin) (Paul Knox, University of Leeds, UK). Both primary antibodies were diluted in 1:10 PBS 1X (according to the manufacturer's instruction) containing 3.5% (w/v) bovine serum albumin (BSA) for 45 minutes at 4 ˚C in the dark; followed by Alexa Fluor 555 goat anti-rat IgG secondary antibody (diluted 1:400 PBS 1X containing 3.5% (w/v) BSA; Life technologies) for 20 minutes at 37 ˚C in the dark. After three brief washes, 1-2 drops of antifade solution "Aua-mount" were added to the samples.

Fluorescence microscopy and fluorescence quantification

Confocal microscopy images were taken using an Olympus IX81 FV1000 confocal microscope equipped with the Olympus FluoView 1.07.03.00 software package (Olympus, Center Valley, PA). For all images, a 60X objective was used unless otherwise stated. Excitation at wavelength of 555 nm was provided using an argon-Ion laser. A spectral emission range of 550 to 600 nm was used.

ImageJ software (Rasband, W.S., ImageJ, U.S. National Institutes of Health, Bethesda, MD, http://rsb.info.nih.gov/ij/, 1997-2008) was used for quantification of fluorescence intensity based upon maximum projections of Z-stacks.

Mechanical test

Pollen grains from both wild-type and *cngc16* mutant were placed in the glass slide. About 50 µl pollen germination media (Fan et al., 2001) containing 1% agar was gently added on the top of the pollen grains on the slide. After one minute, the media were

solidified. Then, pollen germination media (Fan et al., 2001) containing 2% agar was added around the 1% solidified pollen media. The purpose here was to create a physical barrier to evaluate the pollen tube strength by passing through the 1% agar media to 2% agar media. After 3-4 h, light microscope was used to score for the number of pollen tubes that either passed through the 1% to 2% agar media, burst upon reaching the 2% agar, or turning around upon reaching the 2% agar.

Results

To compare *cngc16* and wild-type pollen for differences in their response to a temperature stress condition, the pollen transcriptome was analyzed for mature pollen harvested from plants grown under normal conditions with pollen harvested at the end of a heat period from plants grown under a diurnal cycle of hot and cold temperatures. A total of 12 pollen samples were sequenced with three independent biological replicates for each genotype and growth condition. Transcriptome sequencing was done with a single Illumina flow cell providing depth of 28 million reads for each sample (Supplementary Figure S1.A). A principal component analysis (PCA) of the raw, filtered data showed an almost perfect separation between the wild-type and *cngc16* knockout samples (Principal Component 1 is 97%, Supplementary Figure S1B).

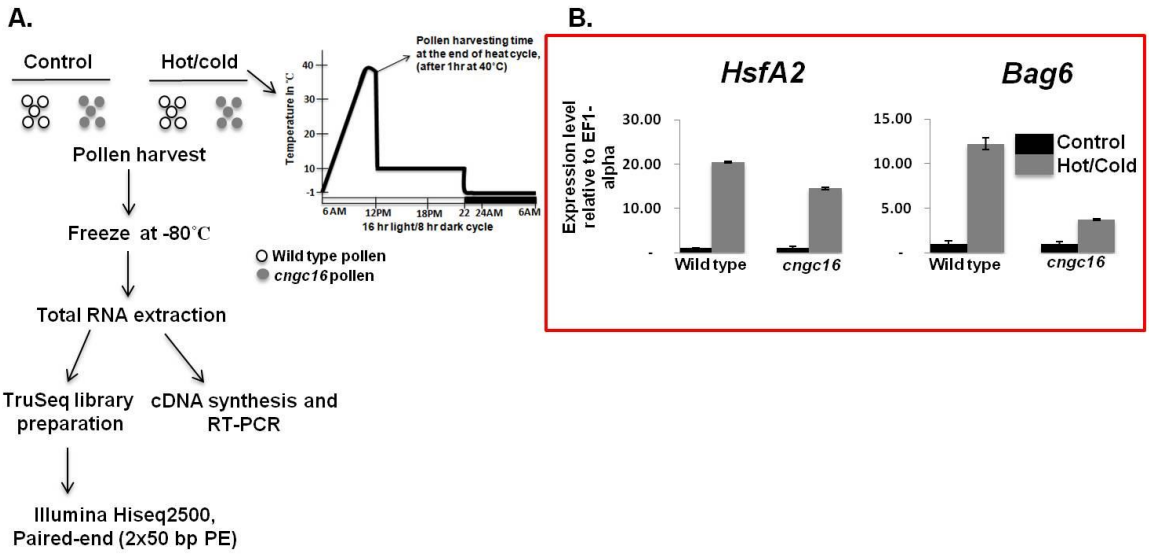

Figure 1. Experimental workflow and RT-PCR validation of RNA-Seq**.**
A) Schematic diagram of the experimental workflow.
B) Quantitative PCR for RNA-Seq validation. *HsfA2* and *Bag6* are two stress-related probe sets used in our previous study (Tunc-Ozdemir et al. 2013). After RNA extraction and cDNA synthesis, RT-PCR was performed to show that harvested pollen samples in the current study have the same expression pattern, as reported before.

To verify the equivalent purity of each pollen sample after filtering through a 70 µm nylon mesh screens, an aliquot of each suspension was examined under the light microscope (Supplementary Figure S2A). Visual inspection of the pollen samples indicated that they were free of any large fragments of vegetative tissues or non-plant debris. To confirm a high degree of purity, we examined our transcriptome data for the expression levels of a set of 29 known photosynthetic marker genes, such as chlorophyll a/b-binding proteins and light harvesting complex proteins (Umate 2010, Supplemental Figure S2B). To compare the purity of our pollen samples with other pollen transcriptome analyses (Qin et al., 2009; Frank et al., 2009; Loraine et al., 2013;

Bokszczanin et al., 2015), we calculated a ratio, in which the expression level of each photosynthetic gene from each experiment/condition was divided by the expression of related gene in semi-*in vivo* pollen tube experiment conducted by Qin et al. (2009), in which hand dissecting was used to isolate the pure pollen tube from a semi-*in vivo* growth experiment. This analysis showed a ratio of less than one for all four pollen libraries tested here (Supplemental Figure S2), indicating our pollen samples were free from any serious contamination. Although pollen grains do not photosynthesize, they contain plastids. Thus, a low but constant baseline expression of photosynthetic genes is possible in pollen plastids.

To ensure that *cngc16* samples showed a deficiency in *CNGC16* mRNA, the corresponding transcriptomes were analyzed for *CNGC16* transcripts. Although reads were detected for *CNGC16*, their alignment with the genome sequence (using the Integerative Genome Browser, IGB, bioviz.org) indicated that they were exclusively located upstream of the T-DNA insertion site, with only a few reads observed at two disconnected downstream positions (Supplemental Figure S4). Thus, there was no indication of any full-length *CNGC16* transcripts. Together, this transcriptome analysis along with transgene rescue experiment from Tunc-Ozdemir et al. (2013) corroborated that *cngc16-2* is a true knockout (i.e., null allele).

RT-PCR validation of two heat stress marker genes

To confirm that the heat stress in this study was similar to that previously used to document the heat stress sensitivity of a *cngc16* knockout (Tunc-Ozdemir et al., 2013), two heat stress marker genes, *HsfA2* and *Bag6*, were analyzed by qRT-PCR. Consistent

with previous results, both genes showed a significantly weaker heat-stress induction in *cngc16* mutant pollen compared to wild-type pollen (Figure 1B).

Heat stress results in more than 3,000 differences between wild-type and a *cngc16* knockout

To identify genes that show a statistically significant (≥2-fold changes and adjusted *p*-value <0.01) stress-dependent changes in transcripts abundance of the wild-type and *cngc16* mutant pollen, we compared the heat stress responses of these two genotypes at the end of the heat stress period. As a result, we identified 2,612 statistically significant changes (Figure 2 and Supplementary Table S3) that showed nearly equivalent increased and decreased in transcript abundances, with 55% of the changes observed being increased. The same comparison for the *cngc16* mutant identified 4,705 statistically significant changes (Figure 2 and Supplementary Table S5). Of those, increased transcripts were twice as the decreased ones by showing 65% of changes.

A comparison between the top 20 increased transcripts indicates that *cngc16* knockout has a different response to the heat stress (Table 1). Out of 20 genes in the Table 1, only five genes were found to have close ranking number in *cngc16* knockout compared to wild-type. For the four genes that show the greatest induction in wild-type, including *MIR845a* and *MIR156A*, their expression was not detectable in *cngc16* pollen. These specific examples were consistent with the indication of very different heat-stress transcriptome responses between pollen from wild-type and *cngc16* plants.

A. Total number of significant changes (≥2-fold changes and adjusted p<0.01) in the expression of annotated genes across different genotypes, conditions or interaction of both factors.

	Total changes	Number of increased transcript levels (%)	Number of decreased transcript levels (%)
Wild type control vs. stress condition	2612	1445 (55%)	1167 (45%)
cngc16 control vs. stress condition	4705	3041 (65%)	1664 (35%)
Wild type vs. *cngc16* under normal condition	74	23 (31%) in WT	51 (69%) in WT
Wild type vs. *cngc16* under stress condition	594	533 (90%) in *cngc16*	61 (10%) in *cngc16*

B.

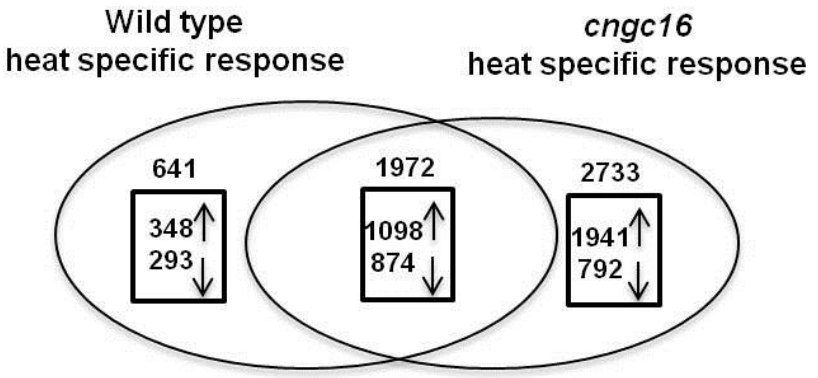

Figure 2. Number of statistically significant changes for differentially expressed transcripts**.**
A) Table showing total number of statistically significant changes (≥2-fold changes and adjusted p<0.01) in the expression of annotated genes across different genotypes, conditions or interaction of both factors.
B) A Venn diagram showing number of statistically significant changes (≥2-fold changes and adjusted p<0.01) under the hot/cold stress condition.

Table 1. Top 20 most up-regulated stress-dependent changes in *cngc16* and wild type pollen.

Gene ID	Description	Ranking nos. in wt	wt_Ctrl Expression Average	wt_Heat Expression Average	Log2-Fold change wt_Heat VS wt_Ctrl	Adjusted *p*-value wt_Heat VS wt_Ctrl	Ranking nos. in *cngc*	*cngc*_Ctrl Expression Average	*cngc*_Heat ExpressionAverage	Log2-Fold change *cngc*_Heat VS *cngc*_Ctrl	Adjusted *p*-value *cngc*_Heat VS *cngc*_Ctrl
AT4G23387	MIR845a	1	0	32.26	13.00	9.7E-09	NA	0	0	NA	NA
AT2G25095	MIR156A	2	0	29.28	12.86	1.2E-08	NA	0	0	NA	NA
AT1G53541	Unknown protein	3	0	9.04	11.17	1.9E-27	NA	0	0	NA	NA
AT5G41471	SNOR108	4	0	2.40	9.25	1.2E-06	NA	0	0	NA	NA
AT5G11920	Fructan exohydrolase	5	0	2.34	9.22	6.4E-20	5	0	1.58	8.66	2.04E-14
AT1G57550	Low temperature and salt responsive family	6	0	1.65	8.72	5.9E-16	2	0	1.94	8.95	4.22E-15
AT5G51440	HSP20-like chaperones superfamily	7	0	1.62	8.69	2.2E-16	361	0.04	1.43	4.73	3.86E-10
ATMG00690	Hypothetical protein	8	0	1.46	8.54	6.1E-09	6	0	1.30	8.37	7.28E-08
AT5G28824	Other RNA	9	0	0.93	7.90	4.8E-10	48	0	0.43	6.79	6.64E-06
AT5G41430	RING/U-box superfamily	10	0	0.80	7.67	1.4E-09	668	0.08	0.58	2.99	6.08E-04
AT5G41109	Unknown protein	11	0	0.75	7.58	6.7E-03	NS	0.54	0.22	-1.28	5.45E-01
AT2G03290	GOLD family protein	12	0	0.74	7.56	1.8E-12	304	0.03	1.49	5.29	2.03E-13
AT1G48770	Protein of unknown function 1639	13	0	0.72	7.53	4.8E-13	409	0.03	0.62	4.04	2.43E-07
AT5G35470	Unknown protein	14	0	0.70	7.49	4.1E-10	370	0.04	1.27	4.56	5.83E-09
AT1G31258	Other RNA	15	0	0.67	7.43	2.9E-03	65	0	0.37	6.58	9.97E-03
AT5G60978	Gametogenesis related family protein	16	0	0.62	7.30	1.4E-11	29	0	0.52	7.06	1.20E-08
AT1G56430	Nicotianamine synthase 4	17	0	0.61	7.28	3.8E-09	49	0	0.42	6.78	1.95E-06
AT4G19829	Unknown protein	18	0	0.60	7.27	2.3E-03	4704	0.48	0	-6.96	1.24E-03
ATMG01170	Subunit A of ATPase F0 complex	19	0	0.55	7.14	8.9E-05	NS	0.06	0.27	2.02	1.32E-01
AT4G10250	HSP20-like chaperones superfamily	20	0.06	9.33	7.14	2.0E-32	12	0.07	16.42	7.83	1.60E-36

The ranking number was based on a sorting of the log2-fold changes from ascending to descending order. NA and NS stand for not applicable and not statistically significant. The significant level was determined based on adjusted *p*-value <0.01.

Transcript comparison showing *cngc16* knockout does not have almost any pre-existing condition

To further gain insight into differences existing between wild-type and the *cngc16* mutant pollen, we compared the transcript abundance of the unstressed wild-type pollen with the transcript abundance of the unstressed *cngc16* mutant pollen. Our analysis showed only 74 genes that were statistically different (≥2-fold changes and adjusted *p*-value <0.01; Figure 2 and Supplementary Table S7) between the wild-type pollen and the *cngc16* mutant pollen under normal conditions. These few changes compared to those 594 changes under the heat stress suggest that the *cncg16* knockout has few pre-existing mRNA differences compared to wild-type plant. However, among the list of differentially expressed genes (Supplementary Table S7), there were some interesting

changes that caught our attention. They included the *ALA-interacting subunit 1* (AT5G46150), *CIPK11* (AT2G30360), and f *MIR780A* (AT4G14811), which showed 2-3-fold decrease in transcript abundance in the unstressed wild-type pollen compared to that of *cngc16*.

In contrast to the unstressed condition, transcript abundance comparison between heat-stressed wild-type pollen and the heat-stressed *cngc16* mutant pollen showed 594 statistically significant changes (Figure 2 and Supplementary Table S8). To further uncover differences between wild-type and the *cngc16* mutant pollen under the heat stress, we identified subsets of genes (Figure 2B, Venn diagram) that were differentially expressed either in the wild-type (herein referred to as "wild-type specific heat response") including 641 genes (Supplementary Table S9) or in the *cngc16* mutant pollen (herein referred to as "*cngc16* specific heat response") including 2,733 genes (Supplementary Table S10), or in both wild-type and the *cngc16* (herein referred to as "common heat response") pollen including 1,972 genes (Supplementary Table S11).

cngc16 showed 148 differences in the abundance of transcription factors

A comparison of changes in transcription factor was done to evaluate whether the nearly 2-fold increase in transcriptome changes in *cngc16* pollen might be related to an increase in the number of stress-dependent changes in transcription factors. While 81 transcription factor changes were common to both *cngc16* and wild-type, there were a greater number of differences (i.e., 148, Figure 3 and Supplementary Table S12). Of those, 27 were wild-type specific (Figure 3B), and 121 were *cngc16* specific (Supplementary Table S12). This supports a model in which the larger number of stress-dependent transcriptome changes

in *cngc16* pollen might result from the mis-regulation of a large subset of transcription factors, each of which could alter the expression of many downstream target genes.

A.

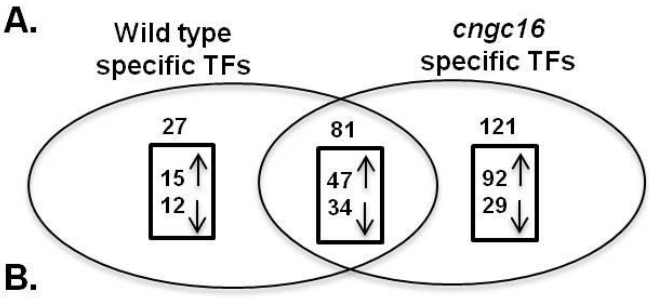

B.

Gene ID	Log2-Fold change	TF family	Gene name
AT5G06510	5	NF-YA	Nuclear factor Y, subunit A10
AT3G05860	4	M-type	MADS-box transcription factor family protein
AT4G38900	3	bZIP	Basic-leucine zipper transcription factor family protein
AT1G64380	3	ERF	Integrase-type DNA-binding superfamily protein
AT5G17320	2	HD-ZIP	Homeodomain GLABROUS 9
AT3G53790	2	MYB_related	TRF-like 4
AT5G50480	2	NF-YC	Nuclear factor Y, subunit C6
AT2G24681	2	B3	AP2/B3-like transcriptional factor family protein
AT1G03970	2	bZIP	G-box binding factor 4
AT2G24260	1	bHLH	LJRHL1-like 1
AT1G71130	1	ERF	Integrase-type DNA-binding superfamily protein
AT2G16400	1	TALE	BEL1-like homeodomain 7
AT5G59570	1	G2-like	Homeodomain-like superfamily protein
AT3G02830	1	C3H	zinc finger protein 1
AT2G20400	1	G2-like	myb-like HTH transcriptional regulator family protein
AT1G78540	-1	STAT	SH2 domain protein B
AT2G36400	-1	GRF	Growth-regulating factor 3
AT3G48430	-1	C2H2	Relative of early flowering 6
AT3G09600	-1	MYB_related	Homeodomain-like superfamily protein
AT3G06250	-1	FAR1	FAR1-related sequence 7
AT3G16870	-1	GATA	GATA transcription factor 17
AT4G14770	-1	CPP	TESMIN/TSO1-like CXC 2
AT1G05230	-2	HD-ZIP	Homeodomain GLABROUS 2
AT5G60910	-2	MIKC	AGAMOUS-like 8
AT5G19790	-2	ERF	Related to AP2 11
AT1G69180	-4	YABBY	Plant-specific transcription factor YABBY family protein
AT5G66300	-4	NAC	NAC domain containing protein 105

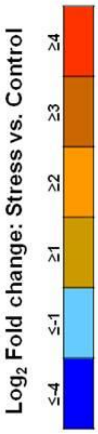

Figure 3. Differentially expressed transcription factors**.**
A) A Venn diagram showing number of statistically significant changes (≥2-fold changes and adjusted *p*-value <0.01) in the transcripts abundance of the transcription factors under the heat stress condition.
B) Differentially expressed transcription factors that are specific to the wild-type pollen.

cngc16 pollen showed twice as many stress-dependent changes in metabolic pathways compared to wild-type

To map expression data to the potential metabolic pathways, differentially expressed transcripts from both wild-type (Supplementary Table S3) and *cngc16* mutant (Supplementary Table S5) pollen were analyzed using the AraCyc (Plant Metabolic Network (PMN), http://www.plantcyc.org/tools/tools_overview.faces). This analysis revealed that several pathways were affected due to the heat stress in both genotypes. However, *cngc16* showed more changes (almost twice) compared to wild-type in every pathway. The top three altered metabolic pathways in wild-type (Table 2) were carbohydrates biosynthesis, nucleosides and nucleotides biosynthesis, and lipid biosynthesis.

Table 2. A comparison between the top 3 altered metabolic pathways showing global changes in the *cngc16* knockout metabolic pathways under the heat.

	wild type			*cngc16*		
Pathway	Total number of changes (%)	Up-regulated (%)	Down-regulated (%)	Total number of changes (%)	Up-regulated (%)	Down-regulated (%)
Carbohydrate biosynthesis	47(27%)	25(53%)	22(47%)	70(40%)	48(69%)	22(31%)
Nucleosides and nucleotides biosynthesis	40(26%)	6(15%)	34(85%)	56(37%)	33(59%)	23(41%)
Lipid biosynthesis	40(11%)	28(70%)	12(30%)	81(22%)	64(79%)	17(21%)

Transcripts with significant changes (≥2-fold changes and adjusted *p*-value <0.01) were used to map on the metabolic pathways by the AraCyc

(Plant Metabolic Network (PMN), http://www.plantcyc.org/tools/tools_overview.faces). Number of altered transcripts are shown in percentage.

Pectin content comparison between wild-type and *cncg16* knockout

To understand possible mechanisms underlying the *cngc16* mutant hypersensitivity, we focused on the overall changes in transcript abundance for genes involved in cell wall modification. These included pectin methylesterase inhibitors (PMEIs), pectin methylesterases (PMEs), and pectin acetylesterases (PAEs) (Supplementary Figure S3A).

Among these three gene families, PMEs and PAEs showed higher transcript abundances under heat stress compared to the wild-type under the same condition. Using immunological approach, we compared pectin content (de-esterified and methylesterified) in the wild-type and the *cngc16* mutant pollen tubes. The result showed no detectable differences in these two forms of pectin in pollen tubes from *cngc16* compared to wild-type pollen (Supplementary Figure S3C).

We also performed a mechanical test to evaluate the cell wall strength of the *cngc16* mutant pollen tube compared with the wild-type pollen tube. The result of mechanical test also showed the *cngc16* pollen tube is flexible (or stiff) enough to pass through a physical barrier, the same as wild-type pollen tube (Supplementary Figure S3D).

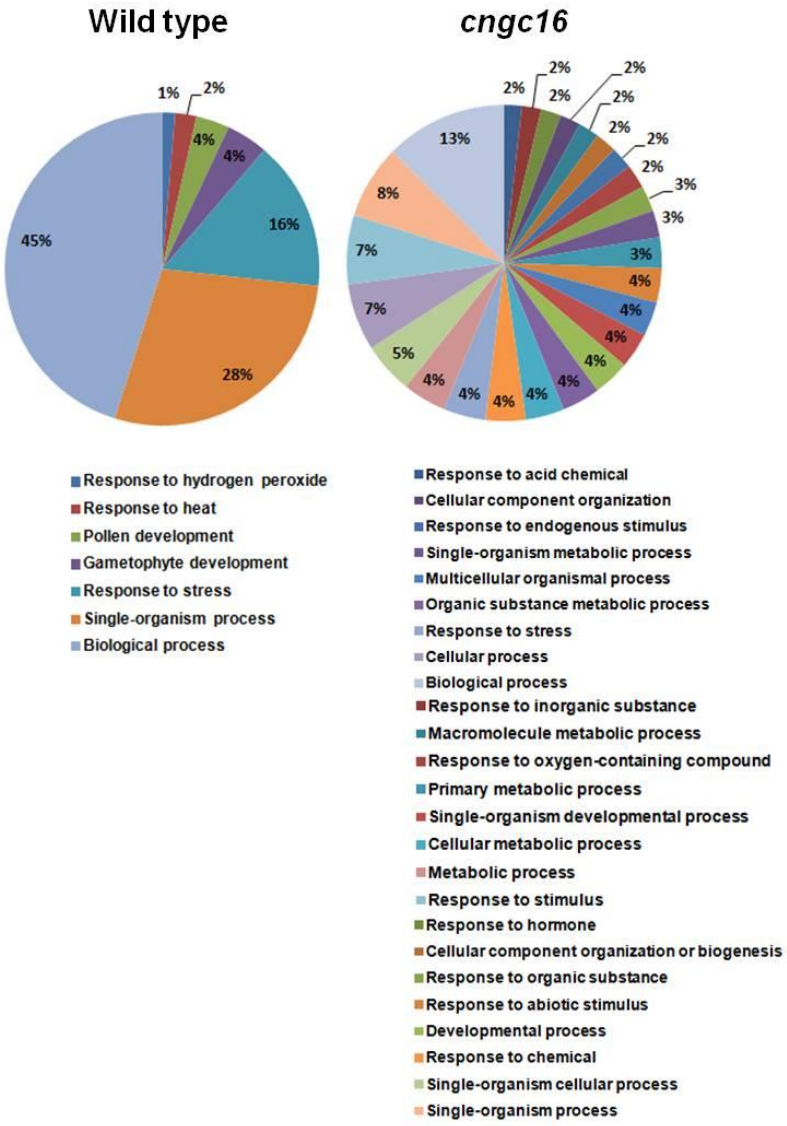

Figure 4. GO biological process comparison between cngc16 and wild-type pollen showing global changes in the mutant. GO biological process for the statistically significant changes (≥2-fold changes and adjusted *p*-value <0.01) are shown. AmiGO was used to identify gene enrichment categories in the GO Biological Processes (Carbon et al., 2009). Only overrepresented terms are shown.

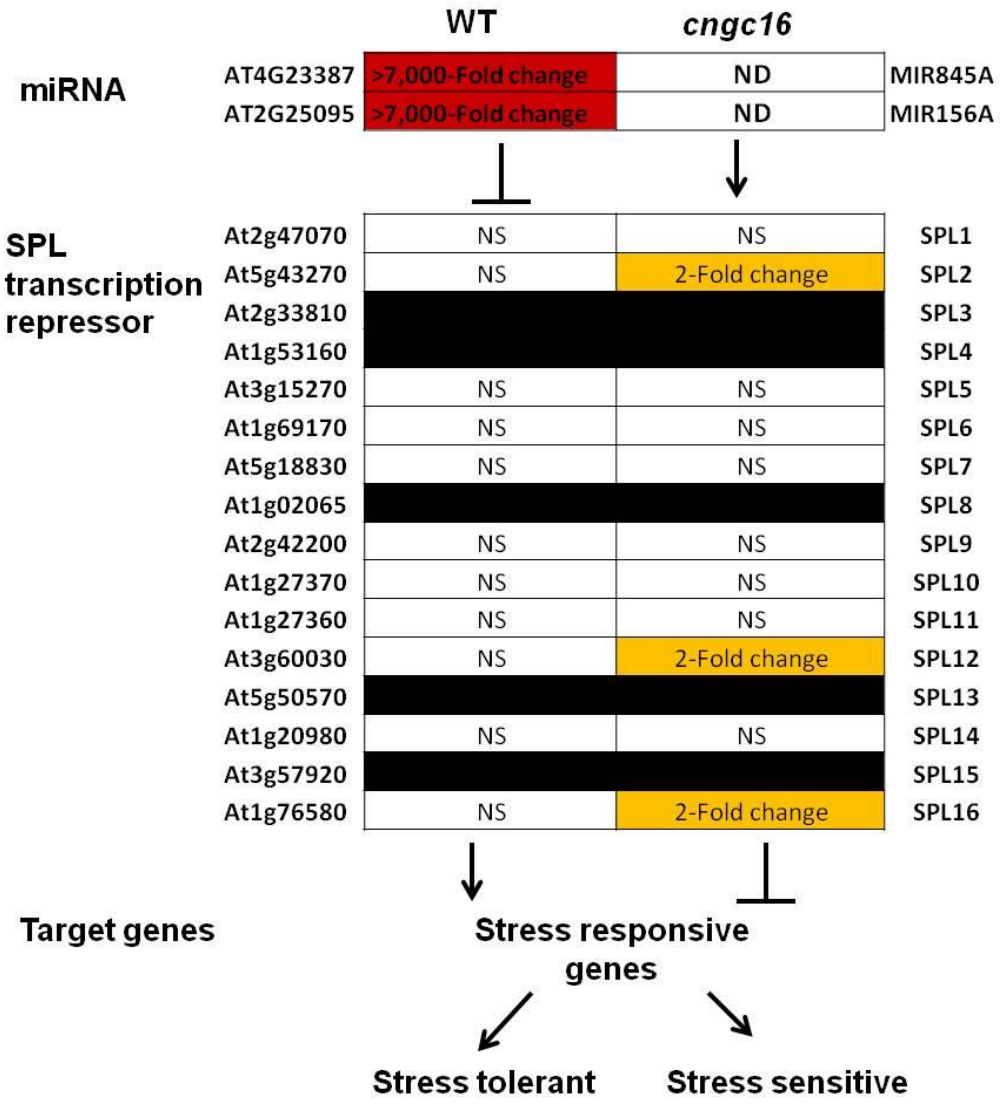

Figure 5. Proposed working model showing cngc16 mutant lacks heat stress memory. A model showing two miRNA genes (*MIR845A* and *MIR156A*) are only induced (>7,000-fold changes) in the wild-type pollen under the hot/cold stress but not in the *cngc16* mutant pollen. The induced miRNAs, in turn, inhibit expression of SPL transcription factors *SPL2*, *12*, and *16* in the wild-type. Suppression of these transcription factors seem to be required for the heat stress memory in the wild-type, and in turn, result in induction of stress responsive genes. ND and NS refer to as not detected and not significant. However, in the *cngc16* knockout, absence of these two miRNAs resulted in increased transcript abundances of SPL transcription factors *SPL2*, *12* and *16*, which in turn, inhibited the downstream stress-responsive genes.

Discussion

This study provides the first analysis of a temperature-stress response in pollen from the model plant Arabidopsis, and the first comparison of this response with a mutant with defective temperature stress response. The two primarily objectives of this study were: 1) to gain insight into the mechanisms involving in pollen thermotolerance, and 2) to uncover the mechanisms underlying the *cngc16* mutant hypersensitivity under heat stress. Here we provide multiple lines of evidence for a defective temperature-stress response in pollen harboring a knockout of *cngc16*. First, the mutant failed to show 641 of the stress-dependent changes observed in the wild-type. Second, the mutant showed more than twice the number of overall stress-dependent changes in mRNA expression patterns, and more than twice the number of changes in transcription factor mRNA abundance, which suggests a significant mis-regulation of a stress-dependent transcriptional response. Third, an examination of the top-ranked changes in both wild-type and mutant showed very few similarities (Table 1), and instead highlighted examples such as the top-four transcripts with increased abundance in wild-type being undetectable in a *cngc16* mutant. Fourth, in the *cngc16* knockout, almost 60% of the transcription factors changed. Fifth, metabolic pathway analysis showed metabolic pathways in the *cngc16* knockout have twice as many changes as the wild-type, with the largest number of changes observed in lipid biosynthesis pathways (Table 2). Sixth, the GO term analysis (Figure 4) showed *cngc16* having statistically significant changes in 25 categories compared to only seven in wild-type.

Transcriptome analysis comparison between wild-type and *cngc16* knockout showed the mutant failed to induce key components required for pollen thermotolerance

While a total of 2,612 transcripts were affected by the heat stress in the wild-type pollen (Supplemental Tables S3), *cngc16* knockout showed almost two-fold more changes than wild-type (Supplemental Tables S5). At the same time, many of the changes that occurred with wild-type, failed to change in *cngc16*. For example, in a comparison of the top 20 biggest changes (Table 1) showed the top-four largest changes in wild-type were not even detectable in the *cngc16* knockout. These examples included two miRNAs *MIR845A* and *MIR156A*, each with more than 7,000-fold changes, and one small nuclear RNA (snoRNA) called *SNOR108* with a 500-fold-change. The fact that these RNAs were strongly induced under the heat stress in the wild-type pollen suggests a potentially important function in a pollen heat stress response that failed to occur in *cngc16* pollen.

Many studies have documented the role of miRNAs in plant stress tolerance. For example, *MIR845A* has been shown to be increased in response to drought stress in rice seedling (Sunkar et al., 2008; Zhou et al., 2010) and in response to fungus *Exserohilum turciucum* in maize (Wu et al., 2014). The predicted target for maize *MIR845* is a gene with DNA integration function. *MIR156A* has been shown to play role in flowering time (Serivichyaswat et al., 2015) and tolerance to the recurring stress in Arabidopsis seedlings (Steif et al., 2014) by suppression of the *SQUAMOSA PROMOTER BINDING PROTEIN-LIKE* (*SPL*) transcription factors. In addition to heat stress, *MIR156A* has been shown to be up-regulated in many other stresses such as cold, drought, salt, and oxidative stresses, indicating it has a key role in stress adaptation (Sunkar et al., 2012). Recently, a study conducted in heat-stressed tomato pollen in different developmental stages showed induction of sncRNAs (Bokszczanin et al., 2015). As a part of heat-stress responses, they

found two miRNAs that were differentially expressed under the heat, wherein one was increased and the other was decreased.

Consistent with evidence for negative regulatory effects of miRNAs on their target genes, the stress-dependent increases observed in wild-type pollen for *MIR156A* and *MIR845A* are expected to suppress the expression of a subset of downstream transcription factors. For *MIR156A,* there is evidence that they can suppress the expression of a set of SPL transcriptional suppressors. When an SPL is down-regulated, this results in a subset of SPL-suppressed genes experiencing a release from suppression. Thus, for *MIR156A*, the expectation is that an increase in this negative regulator will ultimately result in a reduction of an SPL and the subsequent up-regulation of some subset of genes. The observation that *MIR156A* fails to be induced in *cngc16* predicts that a subset of SPL transcriptional suppressors might be able to increase in abundance and thereby suppress the induction of some subset of specific genes. In agreement, the transcript abundance for SPL2, 12, and 16 increased by more than two-fold in the *cngc16* knockout. While it is not clear which target genes might be suppressed as a result of this increase in SPL2, 12, and 16, it is noteworthy that *cngc16* failed to up-regulate the abundance of 348 genes that in wild-type showed a stress-dependent increase in abundance (Figure 2B and Figure 5).

In terms of small nuclear RNAs (snoRNAs), Bokszczanin et al. (2015) identified six isoforms in the heat-stressed tomato pollen, in which two snoRNAs U1 and U3 were up-regulated in mature pollen. snoRNAs have been linked to the splicing of mRNA transcripts (Jurica et al., 2003; Staiger et al., 2013) as well as processing of ribosomal RNA transcripts (rRNAs, Brown et al., 2003), and therefore, they might play a key role in protein biosynthesis under stress. Taken together, consistent with the evidence provided

from tomato study, our study also highlights the potential importance of miRNAs and other small RNAs in the regulation of pollen heat-stress tolerance.

As a part of general heat-stress response (Table 1), transcript abundances of fructan exohydrolase, low temperature/salt responsive family and HSP20-like chaperones superfamily were increased in both wild-type and *cngc16* knockout, suggesting a potential importance of these genes in pollen heat stress tolerance. For example, fructan exohydrolase, which hydrolyses the last fructose from fructans (Roy et al., 2007), may function in thermotolerance by providing more soluble sugars as osmoprotectant.

The second evidence showing *cngc16* failed to response to heat stress came from the transcription factor analysis. This analysis showed in *cngc16* about 60% of transcription factors (=121) showing changes, which are not required for the pollen heat stress response, as evidenced by the wild-type specific heat stress response (Figure 3B, and supplementary Table S12). This might explain why *cngc16* knockout showed a more than 2-fold increase in the number of stress-dependent transcript abundance changes.

Unlike the stress condition, a transcript comparison between wild-type and *cngc16* mutant under non-stress condition only showed a few changes, 74 (Figure 2A and Supplementary Table S7) compared to that 3374 changes (equal to 2733+641 from Venn diagram in Figure 2B) under the heat stress condition. This relatively low number of pre-existing differences is consistent with the observation that under optimal plant growth condition, there is no evidence of any difference in pollen fitness between wild-type and mutant pollen during self-fertilization of a heterozygous *cngc16* plant (Tunc-Ozdemir et al., 2013). While this might suggest that *cngc16* does not have any serious pre-existing condition that would make it hypersensitive to a stress, we cannot exclude the possibility

that one or more of these 74 differences could directly or indirectly interfere with the induction of an appropriate transcriptional stress-response. For example, we identified some genes with possible function in transport and Ca^{2+} signaling. They were *ALA-interacting subunit 1* (AT5G46150), *CIPK11* (AT2G30360), and *MIR780A* (AT4G14811) each with 2-3 fold reduction in the unstressed wild-type pollen compared to that *cngc16* knockout. In case of *ALA-interacting subunit 1*, *CIPK11* and *MIR780A*, it seems that disruption of *CNGC16* gene resulted in enhancement of transcript abundances. Biological function for *ALA-interacting subunit 1* has not been assigned yet. By potential interaction with membrane lipid flippases such as *ALA6* and *7*, which are speculated to change membrane stability (McDowell et al., 2015).

CIPK 11 which encoding a SOS2-like protein kinase (also known as *PKS5*) has been known as a negative regulator of the plasma membrane H^+-ATPase AHA2 (Fuglsang et al., 2007). Loss-of-function of *pks5* increased tolerance to high external pH. This might explain *cngc16* hypersensitivity phenotype during *in vitro* growth germination assay. Tunc-Ozdemir et al. (2013) reported a high percentage of dead pollen for *cngc16* mutant by increasing concentrations of exogenous Ca^{2+}. By repression of plasma membrane H^+-ATPases or other transport systems, such as cation/proton exchanger, *CIPK11* might result in hypersensitivity of *cngc16* due to changes in membrane potential. We did not detect transcript for the *AHA2* gene in our RNA-Seq data, and this is consistent with microarray data (based upon Pollen RCN website, http://pollennetwork.org/content/bioinformatics-tools). The transcript abundance of *AHA8* (with high expression in pollen) also did not show any statistically significant changes.

MIR780A encodes a miRNA with prediction to target a cation/proton exchanger 18 (CHX18). Enhanced transcript level of *MIR780A* in *cngc16* knockout might suggest that *cngc16* has altered membrane property compared to that wild-type pollen. However, transcript abundance of CHX18 did not show any changes in pre-existing condition between wild-type and *cngc16*. Together, increased transcript abundances of *ALA-interacting subunit 1, CIPK11* and *MIR780A* would suggest *cngc16* has altered membrane potential, which makes it more vulnerable to bursting *in vitro*.

Metabolic pathway and GO term analyses showing global changes in *cngc16* knockout

The third line of evidence showing *cngc16* knockout failed to respond to heat stress is from the metabolic pathway comparison. Carbohydrate biosynthesis pathway is one of the well-known metabolic pathways affected by temperature extremes such as heat (Rizhsky et al., 2002; Rizhsky et al., 2004; Wan et al., 2015). A study in tomato (Pressman et al., 2002) has shown that exposure of tomato plants to heat stress resulted in decrease in starch concentration before anthesis followed by decrease in soluble sugars in mature pollen grain. The reduced amount of soluble sugar in pollen grain, in turn, resulted in reduced pollen viability in tomato under the heat stress. The RNA-Seq data show 70 of the *cngc16* transcripts were active in carbohydrate biosynthesis pathway while in wild-type, almost half of the transcripts were involved (Table 2).

Nucleosides and nucleotides biosynthesis pathway are major source of energy, building blocks for nucleic acid biosynthesis, and cofactor for several proteins and enzymes (Moffatt and Ashihara 2002). The altered nucleotide biosynthesis pathway under the heat

stress is consistent with the previous study conducted by the Tunc-Ozdemir et al. (2013) in which cGMP level increased in both pollen and leaves, supporting this idea that cyclic nucleotides are key player in heat stress tolerance in pollen and other tissues. A metabolic pathway comparison again showed *cngc16* has more changes than the wild-type in terms of nucleotides biosynthesis pathway (Table 2).

Another altered metabolic pathway due to the heat stress was lipid biosynthesis pathway (Table 2). One explanation would be lipids (such as alpha-tocopherol) help to maintain membrane integrity during heat stress. Another explanation would be lipids serve as signaling molecules (such as phosphatidic acid) under heat stress, which, in turn, are required for the activation of stress response pathway. Again *cncg16* showed more changes in lipid biosynthesis pathway related genes compared to that of wild-type.

The fourth line of evidence showing global changes in *cngc16* transcriptome was provided by a GO term enrichment analysis (Figure 4, AmiGO; Carbon et al., 2009). Consistent with metabolic pathway analysis, the GO analysis also showed global changes in the transcriptome of the *cngc16* knockout due to heat stress. This analysis showed wild-type was enriched in response to hydrogen peroxide, heat stress/and other stresses and also enriched in pollen and gametophyte development. However, *cngc16* showed enrichment in almost every GO term, indicating global changes, which are not required for the pollen heat stress tolerance.

Common and unique pollen stress-responsive transcripts

To answer this question “does the pollen respond differently to stresses than vegetative tissues”, we searched the literature for vegetative heat stress responses (Rizhsky et al.,

2002; Rizhsky et al., 2004; Bhardwaj et al., 2015; Wan et al., 2015) to compare with the pollen heat stress response in our study. In general, vegetative and pollen have several common heat responses such as the induction of small *HSPs*, *HSFs* (e.g. *HsfA2*), *BAG6* (Nishizawa-Yokoi et al., 2009; Tunc-Ozdemir et al., 2013), *WRKY* transcription factors, *Mbf1C* (Suzuki et al., 2008), dehydrogenases, phospholipases, hormone signaling pathway such as ethylene (AT1G64380 and AT5G47230) and auxin (AT3G23050)-responsive transcription factors. Among the common heat stress responses were also antioxidant enzymes such as ascorbate peroxidase 2, peroxidase, and glutathione S-transferase.

However, pollen also displayed some unique responses. As documented here, the pollen heat response (Table 1 and Supplemental Table S3) included genes with roles in RNA processing, cell wall modification (such as invertase/pectin methylesterase inhibitor), and embryogenesis/gametogenesis (such as GAMETE EXPRESSED 2 (*GEX2)*). However, the vegetative heat specific response usually comprises of response to a variety of stresses including biotic stress and also response to hormones (such auxin, salicylic acid, jasmonic acid, and ABA) (Bhardwaj et al., 2015).

The top three transcription factor families that were differentially expressed under the heat in vegetative tissues based upon the Bhardwaj et al. (2015) included MYB (26 isoforms), HSF (23 isoforms), and ERF (15 isoforms). In addition, protein kinases, such as receptor-like kinase family, MAP kinases, casein kinases, calcium-dependent protein kinases, CBL-interacting protein kinases, and cyclin-protein kinases were part of the vegetative heat response (Bhardwaj et al., 2015). In pollen, the top three differentially expressed transcription factors under the heat stress were MYB and MYB-related (13

isoforms), bHLH (7 isoforms), and ERF, G2-like, MIKC, and WRKY (each with six isoforms). In terms of protein kinases, unclassified protein kinases (20 isoforms) were the overrepresented class in the heat stressed pollen followed by leucin-rich repeat protein kinases (five isoforms). The other protein kinases, such as AGC kinases and CDPKs, were present in the heat-stressed pollen with two isoforms. Taken together, although vegetative and pollen have many common heat responses, each utilizes a unique set of stress response genes.

Conclusion and Future perspective

This study has at least two major impacts. First, it provided the first comprehensive transcriptome analysis of the heat stressed wild-type pollen in the model plant, Arabidospsis. Knowing the differentially expressed transcripts in pollen would help understanding their biological functions in terms of engineering plants with increased tolerance to heat stress. Second, it suggested a mis-regulated transcriptional response as possible mechanism underlying the *cngc16* mutant pollen sensitivity under the stress.

As a future direction, some candidate genes with potential importance in pollen heat stress tolerance were isolated for further characterization.

Supplemental Data

The supplemental tables are available in the online version of this manuscript.

Supplemental figures and tables

Supplemental Figure S1. Library size and principal component analysis

Supplemental Figure S2. Examining pollen purity samples used for RNA-Seq

Supplemental Figure S3. Pectin content comparison between wild-type and *cncg16* knockout

Supplemental Figure S4. IGB screenshot showing raw reads associated with the *CNGC16* gene in the wild-type and the *cngc16* mutant

Supplemental Table S1. Expression count estimates from the cufflinks-native fragments-per-kilobase-per-million-reads (FPKM) format transformed into a count-compatible format

Supplemental Table S2. Master table

Supplemental Table S3. Differentially expressed transcripts in wild-type pollen

Supplemental Table S4. GO term for differentially expressed transcripts in wild-type pollen

Supplemental Table S5. Differentially expressed transcripts in *cngc16* pollen

Supplemental Table S6. GO term for differentially expressed transcripts in *cngc16* pollen

Supplemental Table S7. Transcript comparison between unstressed wild-type and unstressed *cngc16* mutant pollen

Supplemental Table S8. Transcript comparison between heat stressed wild-type and heat stressed *cngc16* mutant pollen

Supplemental Table S9. Wild-type heat specific response

Supplemental Table S10. *cngc16* heat specific response

Supplemental Table S11. Common heat response

Supplemental Table S12. Differentially expressed transcription factors

Supplemental Data

A. Library size

Library size based on raw reads.

	Raw reads
Wild type-Control1	32213076
Wild type-Control2	30690445
Wild type-Control3	30793566
Wild type-Heat1	31450178
Wild type-Heat2	30839854
Wild type-Heat3	27968364
cngc16-Control1	22391055
cngc16-Control2	27790750
cngc16-Control3	23086919
cngc16-Heat1	21941025
cngc16-Heat2	26069550
cngc16-Heat3	24886408

B. PCA analysis

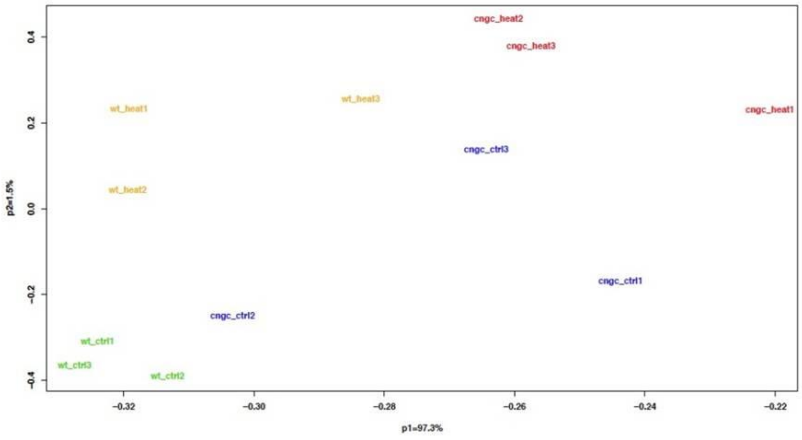

Supplemental Figure S1. RNA-Seq library size and principal component analysis**.**

A.

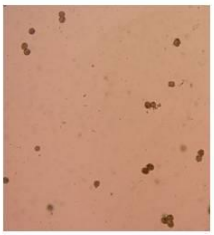

B. **Table showing expression level as ratio for all transcripts of the light harvesting complex genes, based on Umate (2010). For the ratio calculation, the expression values in each group was divided by the expression average from semi-*in vivo* pollen tube experiment from Qin et al. (2009), as the cleanest sample.**

Gene ID	Symbol based on Umate (2010)	Expression Average in semi *in-vivo* pollen tubes (Q)	Ratio of wt_ctrl Expression Average (R)/ Expression Average in semi *in-vivo* pollen tubes (Q)	Ratio of wt_Heat Expression Average (R)/ Expression Average in semi *in-vivo* pollen tubes (Q)	Ratio of *cngc*_ctrl Expression Average (R)/ Expression Average in semi *in-vivo* pollen tubes (Q)	Ratio of *cngc*_heat Expression Average (R)/ Expression Average in semi *in-vivo* pollen tubes (Q)	Ratio of pollen Expression (L)/ Expression Average in semi *in-vivo* pollen tubes (Q)	Ratio of seedling Expression Average (L)/ Expression Average in semi *in-vivo* pollen tubes (Q)
AT1G15820	Lhcb6 protein	67.160	0.026	0.024	0.028	0.082	0.208	970.862
AT1G19150	Lhca2*1 mRNA	51.645	0.002	0.004	0.003	0.005	0.019	62.106
AT1G29910	chlorophyll a/b-binding protein	44.806	0.037	0.051	0.079	0.146	0.089	2362.487
AT1G29920	Lhcb1.1	44.806	0.068	0.049	0.161	0.167	0.089	1551.646
AT1G29930	LHCII	44.806	0.167	0.076	0.293	0.292	0.513	13060.403
AT1G34000	One-helix protein 2	104.970	0.001	0.001	0.001	0.004	0.010	19.387
AT1G44575	PsbS	86.280	0.013	0.017	0.014	0.062	0.023	396.905
AT1G45474	Lhca5	43.364	0.004	0.004	0.004	0.009	2.790	87.792
AT1G61520	Lhca3*1	104.379	0.018	0.021	0.026	0.066	0.077	1053.339
AT1G76570	chlorophyll a/b-binding protein	42.569	0.075	0.031	0.047	0.020	1.316	18.171
AT2G05070	Lhcb2.2	79.262	0.014	0.010	0.013	0.036	0.063	375.642
AT2G05100	Lhcb2.1	79.262	0.013	0.007	0.020	0.036	0.000	519.071
AT2G21970	stress-enhanced protein 2	36.750	0.005	0.007	0.004	0.009	0.218	203.076
AT2G34420	chlorophyll a/b-binding protein	38.886	0.078	0.081	0.122	0.270	0.257	6592.710
AT2G34430	chlorophyll a/b-binding protein	38.886	0.009	0.003	0.012	0.005	0.000	1366.711
AT2G40100	Lhcb4.3	48.395	0.004	0.005	0.006	0.017	0.021	67.021
AT3G08940	Lhcb4.2	48.747	0.020	0.018	0.034	0.052	0.103	946.247
AT3G22840	early light-inducible protein 1	113.188	0.004	0.005	0.004	0.008	0.000	44.470
AT3G27690	Lhcb2.4	31.069	0.015	0.006	0.017	0.009	0.064	327.514
AT3G47470	chlorophyll a/b-binding protein	48.622	0.090	0.097	0.138	0.294	0.247	2348.025
AT3G54890	LHCA1	79.236	0.033	0.040	0.040	0.114	0.101	1368.873
AT3G61470	LHCA2	90.316	0.015	0.014	0.027	0.061	0.022	1593.394
AT4G10340	LHCB5/CP26	144.770	0.019	0.018	0.041	0.056	0.028	712.330
AT4G14690	early light-inducible protein 2	75.328	0.000	0.001	0.002	0.003	0.000	3.279
AT4G17600	light-harvesting like	39.697	0.004	0.005	0.011	0.019	0.101	122.138
AT4G34190	stress-enhanced protein 1	377.956	0.008	0.007	0.016	0.010	0.352	14.716
AT5G01530	LHCB4/CP29	91.194	0.019	0.021	0.027	0.063	0.197	1348.877
AT5G02120	One-helix protein	23.631	0.003	0.007	0.013	0.017	0.042	65.233
AT5G54270	Lhcb3	88.550	0.049	0.031	0.080	0.093	0.723	672.026

Q refers to Qin et al. (2009); R refers to the current study by Rahmati Ishka et al. (2016); and L refers to Loraine et al. (2013).

Supplemental Figure S2. Testing pollen samples purity**.**

A) Image showing a suspension of pollen samples under the light microscope.

B) Table showing chloroplast-related transcript abundances in different transcriptome data analyses. The numbers presented showing ratio of expression average in each group divided by expression level of semi-*in vivo* pollen tube experiment, as the cleanest sample.

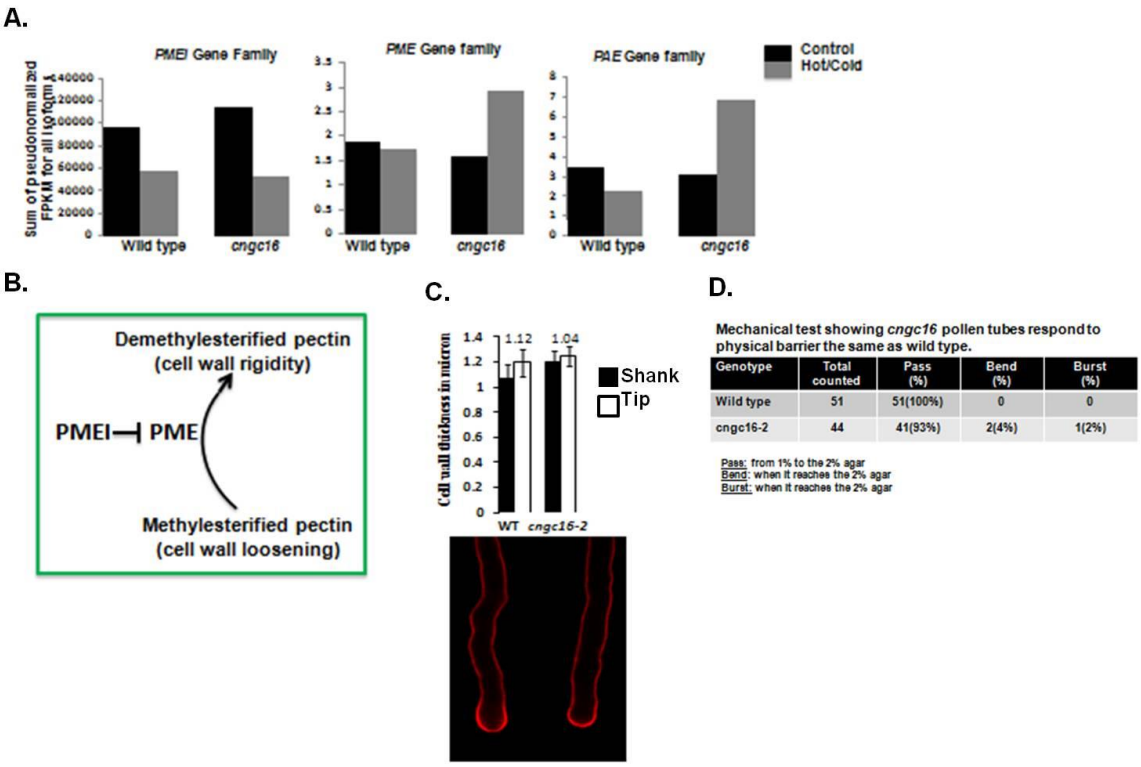

Supplemental Figure S3. Pectin content comparison between wild-type and cncg16 knockout. A) Transcripts abundance of all isoforms of Pectin methylesterase inhibitors (*PMEIs*), Pectin methylesterases (*PMEs*), and Pectin acetylesterases (*PAEs*) in the wild-type and *cngc16* pollen under control and hot/cold stress conditions.
B) A reaction showing PMEs are involved in the cell wall modification by converting the methylesterified pectin to the de-esterified pectin, which make the cell wall rigid. PMEIs inhibit PMEs.
C) Cell wall thickness quantification was done using the LM19 antibody which stains de-esterified pectin. The cell wall thickness measurement was done in both tip and shank areas, and the resulting ratio are shown on the graph for both wild-type and *cngc16* knockout.
D) Mechanical test showing pollen tubes from both wild-type and *cngc16* mutant behave similarly when they reach the 2% agar barrier.

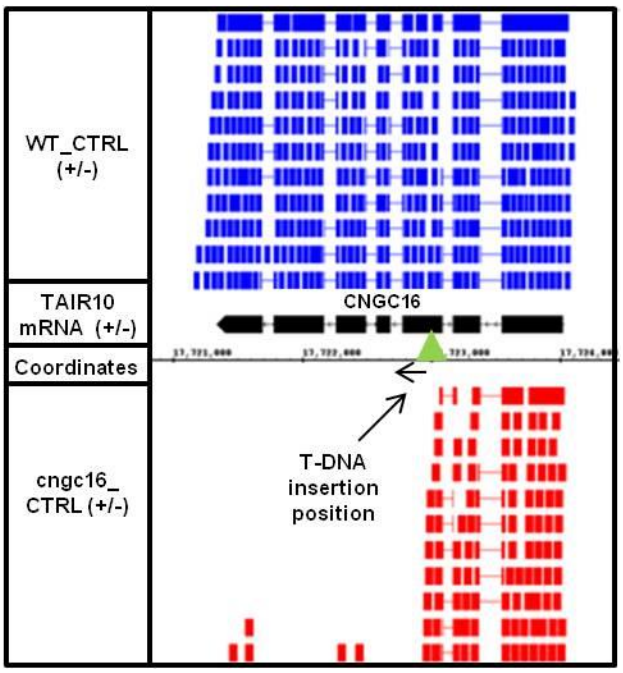

Supplemental Figure S4. Integerated Genome Browser (IGB) screenshot showing CNGC16 (AT3G48010) transcript abundance in the wild-type and cngc16 mutant. The green triangle shows the position of *T-DNA* insertion in *CNGC16* gene. The observed transcripts in the *cngc16* mutant in the RNA-Seq data correspond to the 5' end of the gene before the *T-DNA* interruption.

References

Benjamini Y and Hochberg Y (1995) Controlling the false discovery rate: a practical and powerful approach to multiple testing. Journal of the Royal Statistical Society Series B 57: 289–300.

Bhardwaj AR, Joshi G, Kukreja B, Malik V, Arora P, Pandey R, Shukla RN, Bankar KG, Katiyar-Agarwal S, Goel S, Jagannath A, Kumar A, Agarwal M (2015) Global insights into high temperature and drought stress regulated genes by RNA-Seq in economically important oilseed crop *Brassica juncea.* BMC Plant Biology 15: 9-24.

Bokszczanin KL, Krezdorn N, Fragkostefanakis S, Müller S, Rycak L, Chen Y, Hoffmeier K, Kreutz J, Paupière MJ, Chaturvedi P, Iannacone R, Müller F, Bostan H, Chiusano ML, Scharf K, Rotter B, Schleiff E, Winter P, SPOT-ITN Consortium (Solanaceae Pollen Thermotolerance Initial Training Network Consortium) SPOT-ITN Consortium (Solanaceae Pollen Thermotolerance Initial Training Network Consortium) (2015) Identification of novel small ncRNAs in pollen of tomato. BMC Genomics 16: 714-733.

Brown JW, Echeverria M, Qu LH, Lowe TM, Bachellerie JP, Huttenhofer A, Kastenmayer J P, Green PJ, Shaw P, Marshall DF (2014) Plant snoRNA database. Nucleic Acids Research 31: 432-435.

Carbon S, Ireland A, Mungall CJ, Shu S, Marshall B, Lewis S (2009) AmiGO: online access to ontology and annotation data. Bioinformatics 25: 288-289.

Cartagena JA, Matsunaga S, Seki M, Kurihara D, Yokoyama M, Shinozaki K, Fujimoto S, Azumi Y, Uchiyama S, Fukui K (2008) The Arabidopsis SDG4 contributes to the regulation of pollen tube growth by methylation of histone H3 lysines 4 and 36 in mature pollen. Developmental Biology 315: 355-368.

Charng YY, Liu HC, Liu NY, Chi WT, Wang CN, Chang SH, Wang TT (2007) A Heat-Inducible Transcription Factor, HsfA2, Is Required for Extension of Acquired Thermotolerance in Arabidopsis. Plant Physiology 143: 251-262.

Chebli Y, Kaneda M, Zerzour R, Geitmann A (2012) The cell wall of the Arabidopsis pollen tube--spatial distribution, recycling, and network formation of polysaccharides. Plant Physiology 160: 1940-1955.

Chen Y, McCarthy D, Robinson M, Smyth GK. edgeR: differential expression analysis of digital gene expression data: User's Guide, https://www.bioconductor.org/packages/3.3/bioc/vignettes/edgeR/inst/doc/edgeRUsersGuide.pdf

Endo M, Tsuchiya T, Hamada K, Kawamura S, Yano K, Ohshima M, Higashitani A, Watanabe M, Kawagishi-Kobayashi M (2009) High temperatures cause male sterility in rice plants with transcriptional alterations during pollen development. Plant and Cell Physiology 50: 1911-1922.

Fan LM, Wang YF, Wang H, Wu WH (2001) In vitro Arabidopsis pollen germination and characterization of the inward potassium currents in Arabidopsis pollen grain protoplasts. Journal of Experimental Botany 52: 1603-1614.

Firon N, Pressman E, Meir S, Khoury R, Altahan L (2012) Ethylene is involved in maintaining tomato (*Solanum lycopersicum*) pollen quality under heat-stress conditions. AoB Plants pls024.

Frank G, Pressman E, Ophir R, Althan L, Shaked R, Freedman M, Shen S, Firon N (2009) Transcriptional profiling of maturing tomato (*Solanum lycopersicum* L.) microspores reveals the involvement of heat shock proteins, ROS scavengers, hormones, and sugars in the heat stress response. Journal of Experimental Botany 60: 3891-3908.

Giorno F, Wolters-Arts M, Mariani C, Rieu I (2013) Ensuring Reproduction at High Temperatures: The heat stress response during anther and pollen development. Plant 2: 489-506.

Grennan AK (2007) An Analysis of the Arabidopsis Pollen Transcriptome. Plant Physiology 145: 3-4.

Ikeda M, Mitsuda N, Ohme-Takagi M (2011) Arabidopsis HsfB1 and HsfB2b act as repressors of the expression of heat-inducible Hsfs but positively regulate the acquired thermotolerance. Plant Physiology 157: 1243-1254.

Kim D, Pertea G, Trapnell C, Pimentel H, Kelley R, Salzberg SL (2013) TopHat2: accurate alignment of transcriptomes in the presence of insertions, deletions and gene fusions. Genome Biology 14: 36-49.

Langmead B and Salzberg SL (2012) Fast gapped-read alignment with Bowtie 2. Nature Methods 9: 357-359.

Livak KJ, Schmittgen TD (2001) Analysis of relative gene expression data using real-time quantitative PCR and the 2(-Delta Delta C (T)) Method. Methods 4: 402-408.

Loraine AN, McCormick S, Estrada A, Patel K, Qin P (2013) RNA-Seq of Arabidopsis Pollen Uncovers Novel Transcription and Alternative Splicing. Plant Physiology 162: 1092-1109.

McDowell SC, López-Marqués RL, Cohen T, Brown E, Rosenberg A, Palmgren MG, Harper JF (2015) Loss of the Arabidopsis thaliana P4-ATPases ALA6 and ALA7 impairs pollen fitness and alters the pollen tube plasma membrane. Frontiers in Plant Science 6:197-209.

Moffatt BA, Ashihara H (2002) Purine and Pyrimidine Nucleotide Synthesis and Metabolism. The Arabidopsis Book 1: e0018.

Nishizawa-Yokoi A, Yoshida E, Yabuta Y, Shigeoka S (2009) Analysis of the Regulation of Target Genes by an Arabidopsis Heat Shock Transcription Factor, HsfA2. Bioscience Biotechnology and Biochemistry 73: 890-895.

Patel RK and Jain M (2012) NGS QC Toolkit: a toolkit for quality control of next generation sequencing data. PloS one 7: e30619.

Qin Y, Leydon AR, Manziello A, Pandey R, Mount D, Denic S, Vasic B, Johnson MA, Palanivelu R (2009) Penetration of the stigma and style elicits a novel transcriptome in pollen tubes, pointing to genes critical for growth in a pistil. PLoS Genetics 5: e1000621.

Rizhsky L, Liang H, Mittler R (2002) The combined effect of drought stress and heat shock on gene expression in tobacco. Plant Physiology 130: 1143-1151.

Rizhsky L, Liang HJ, Shuman J, Shulaev V, Davletova S, Mittler R (2004) When defense pathways collide. The response of Arabidopsis to a combination of drought and heat stress. Plant Physiology 134: 1683-1696.

RNA-Seq reveals differentially expressed genes of rice (*Oryza sativa*) spikelet in response to temperature interacting with nitrogen at meiosis stage. BMC Genomics 16: 959-977.

Robinson MD, McCarthy DJ, Smyth GK (2010) edgeR: a Bioconductor package for differential expression analysis of digital gene expression data. Bioinformatics 26: 139-140.

Roy KL, Lammens W, Verhaest M, De Coninck B, Rabijns A, Van Laere A, Van den Ende W (2007) Unraveling the Difference between Invertases and Fructan Exohydrolases: A Single Amino Acid (Asp-239) Substitution Transforms Arabidopsis Cell Wall Invertase1 into a Fructan 1-Exohydrolase. Plant Physiology 145: 616-625.

Serivichyaswat P, Ryu HS, Kim W, Kim S, Chung KS, Kim JJ, Ahn JH (2015) Expression of the Floral Repressor miRNA156 is Positively Regulated by the AGAMOUS-like Proteins AGL15 and AGL18. Molecules and Cells 38: 259–266.

Staiger D, Brown JWS (2013) Alternative Splicing at the Intersection of Biological Timing, Development, and Stress Responses. The Plant Cell 25: 3640-3656.

Stief A, Altmann S, Hoffmann K, Datt Pant B, Scheible W, Bäurle I (2014) *Arabidopsis miR156* Regulates Tolerance to Recurring Environmental Stress through *SPL* Transcription Factors. The Plant Cell 26: 1792-1807.

Stief A, Altmann S, Hoffmann K, Pant BD, Scheible W, Bäurle I (2014) *Arabidopsis miR156* Regulates Tolerance to Recurring Environmental Stress through *SPL* Transcription Factors. The Plant Cell 26: 1792-1807.

Sunkar R, Li Y, Jagadeeswaran G (2012) Functions of microRNAs in plant stress responses. Trends in Plant Cell 17: 196-203.

Sunkar R, Zhou X, Zheng Y, Zhang W, Zhu JK (2008) Identification of novel and candidate miRNAs in rice by high throughput sequencing. BMC Plant Biology 8: 25-42.

Suzuki N, Bajad S, Shuman J, Shulaev V, Mittler R (2008) The transcriptional co-activator MBF1c is a key regulator of thermotolerance in *Arabidopsis thaliana*. The Journal of Biological Chemistry 283: 9269-9275.

Swarbreck D, Wilks C, Lamesch P, Berardini TZ, Garcia-Hernandez M, Foerster H, Li D, Meyer T, Muller R, Ploetz L et al (2008) The Arabidopsis Information Resource (TAIR): gene structure and function annotation. Nucleic Acids Research 36: 1009-1014.

Trapnell C, Williams B, Pertea G, Mortazavi A, Kwan G, van Baren J, Salzberg S, Wold B, Pachter L (2010) Transcript assembly and quantification by RNA-Seq reveals unannotated transcripts and isoform switching during cell differentiation. Nature Biotechnology 28: 511-515.

Tunc-Ozdemir M, Tang C, Rahmati Ishka M, Brown E, Groves NR, Myers CT, Rato C, Poulsen LR, McDowell S, Miller G, Mittler R, Harper JF (2013) A cyclic nucleotide-gated channel (CNGC16) in pollen is critical for stress tolerance in pollen reproductive development. Plant Physiology 16: 1010-1020.

Umate P (2010) Genome-wide analysis of the family of light-harvesting chlorophyll a/b-binding proteins in arabidopsis and rice. Plant Signaling and Behavior 12: 1537-1542.

Wan XL, Zhou Q, Wang YY, Wang WN, Bao MZ, Zhang JW (2015) Identification of heat-responsive genes in carnation (*Dianthus caryophyllus* L.) by RNA-seq. Frontiers in Plant Science 6: 519-532.

Wu F, Shu J, Jin W (2014) Identification and Validation of miRNAs Associated with the Resistance of Maize (*Zea mays L*.) to *Exserohilum turcicum*. PLoS ONE 9: e87251.

Zhou L, Liu Y, Liu Z, Kong D, Duan M, Luo L (2010) Genome-wide identification and analysis of drought-responsive microRNAs in *Oryza sativa*. Journal of Experimental Botany 61: 4157-4168.

Zinn KE, Tunc-Ozdemir M, Harper JF (2010) Temperature stress and plant sexual reproduction: uncovering the weakest links. Journal of Experimental Botany 61: 1959-1968.

Chapter IV.

Improving pollen stress tolerance in Arabidopsis

(This chapter is the follow-up of RNA-Seq experiment presented in chapter III)

Abstract

Global warming is a threat for all living organisms including plants. Many studies have documented the deleterious effects of high temperature to plant development. One of the most vulnerable stages is during pollen development when pollen have a limited window of opportunity to grow tubes into the ovary and fertilize egg cells. Based upon the RNA-Seq experiment in Arabidopsis wild-type pollen from Harper lab (unpublished result), we identified several candidate genes, including two miRNAs (*MIR156A* and *MIR845A*) and many transcription factors of potential importance to regulating a transcriptional response to a hot/cold temperature stress. In wild-type pollen, the expression of *MIR156A* and *MIR845A* were induced by more than 7,000-fold by the end of heat stress period. In contrast, these miRNAs failed to show any detectable induction in a *cngc16* mutant that shows an attenuated heat-stress response. Here we used both loss-of-function and gain-of-function approaches to characterize the function of these two miRNAs and other gene candidates in pollen thermotolerance. The results obtained here will provide valuable information for engineering of the crop plants with improved thermotolerance.

Introduction

Unlike animals, plants are sessile. Therefore, to counter environmental challenges, they need physiological and behavioral adaptation. A series of events are required during stresses to prevent oxidative damage, and maintain the native structure of macromolecules and membranes. Global climate change will influence all aspects of life on earth including agriculture and food supply in many ways. Higher temperatures and changing rainfall patterns could make the environment harsh enough to impede crops to grow.

Most agricultural regions would experience environmental fluctuations during global climate change. In the United States during August 2000, approximately US $4.2 billion in agricultural losses were caused by the combination of high temperature and drought (Mittler 2006).

In many crop species, pollination is the most stress sensitive part of the life cycle (Zinn et al., 2010; Bokszannin 2013). Because the vast majority of our food supply is a result of sexual reproduction in flowering plants, decoding how different plants face stress conditions during the reproductive stage is critical for the future of agriculture. For many food crops such as corn, tomato, and *Brassica napus* (canola), pollen growth and fertilization appear to be particularly sensitive to heat stress (Zinn et al., 2010; Firon et al., 2009). The current Midwest maximum daytime temperature in the United States based upon "Assessing 2012 Crop Heat Damage" report (http://seekingalpha.com/article/698041-assessing-2012-crop-heat-damage) is around 29-32 °C. Temperatures above 32 °C result in leaf rolling, pollen kill, and silk desiccation in

corn, and lastly, result in hindering successful plant fertilization, which is critical to crop yield.

Several studies showed pollen sensitivity during various stresses. Pressman et al. (2002) showed exposure of tomato plants to high temperature (32 ˚C) caused reduction in the number of viable pollen grains. Young et al. (2004) showed that heat stress applied to the pollen of the donor plant before and during pollen release decreased seed number (in both tomato and canola), and fruit set (in tomato) more severely than heat stress applied to the developing ovule and style. Tunc-Ozdemir et al. (2013) showed more than ten-fold decrease in the male transmission efficiency of *cngc16* (Cyclic Nucleotide-Gated Channel 16) *T-DNA* knockout mutations, when the outcross was done between *cngc16*$^{(+/-)}$ pollen (male) and wild-type plant (female) under hot/cold stress regime.

In addition to well-characterized genes conferring heat-stress tolerance, recent studies have indicated an important role of small non-coding RNAs (Stief et al., 2014; Bokszannin 2013). For example, Stief et al. (2014) demonstrated that *MIR156A* is a key player in heat-stress memory to recurring stress. Arabidopsis seedlings overexpressing this miRNA showed increased tolerance to heat stress compared to that of wild-type seedling. Furthermore, an RNA-Seq experiment in tomato pollen exposed to high temperature showed increase and decrease in transcript abundances of two miRNAs (Bokszannin et al., 2015). This is consistent with the result obtained in our RNA-Seq data (Chapter 3, unpublished), in which two miRNAs were strongly induced under a heat stress condition in Arabidopsis wild-type pollen. Thus, we speculate that these miRNAs are part of the pollen thermotolerance pathway.

Understanding the regulatory network involved in pollen thermotolerance will help to develop strategies for improving crop plants. From our RNA-Seq experiment (chapter 3), we identified more than 2,600 heat-stress dependent statistically significant changes (≥2-fold changes and adjusted *p*-value <0.01) in Arabidopsis wild-type pollen. Among those, 27 were transcription factors that were strongly increased in the wild-type pollen, but not in the *cngc16* knockout. Cyclic nucleotide-gated channel 16 is a pollen-specific channel required for plant fertility under hot/cold stress condition.

Figure 1 shows genes that have been selected for further characterization in this study. Using a gain-of-function approach, we over-expressed the two identified miRNAs in the wild-type and *cngc16* knockout background. Using a loss-of-function approach, we analyzed *mir845a*, *myb-related*, *pmei*, and *yabby* knockouts. For miRNAs, usually a target-mimicry approach is used (Gupta 2015). However, we isolated a T-DNA insertion allele for *mir845a*. So far, no functional analysis has been reported for this gene. The transcript abundance of *MIR845A* has been shown to be increased in salt and drought stresses in rice (Sunkar et al., 2008; Zhou et al., 2010) and in response to fungus (Wu et al., 2014).

Arabidopsis genome encodes 97 *MYB-related* transcription factors (based upon Plant Transcription Factor Database v3.0) with several functions in plant development and stress responses (Yanhui et al., 2006; Ambawat et al., 2013; Xiong et al., 2014). For example, *MYB-related* transcription factors 26 and 103 have been shown to function in plant reproduction and trichome development, respectively (Steiner-Lange et al., 2003; Higginson et al., 2003). A gene disruption of *myb-related 26* resulted in male sterility phenotype due to non-dehiscent anthers (Steiner-Lange et al., 2003). In rice,

overexpression of the *MYB48-1* resulted in increased tolerance to drought and salt stresses (Xiong et al., 2014). Functional analysis for *TRF-like 3 MYB-related* transcription factor has not yet been conducted. Up-regulation of this gene under the hot/cold stress condition in both wild-type and *cngc16* knockout suggests it might play a role in pollen thermotolerance.

Pectin methylesterase inhibitors (PMEIs) in combination with pectin methylesterases (PMEs) are important for cell wall formation and modification. PMEIs regulate PMEs by reversibly inhibiting PMEs activity. So a balance between PMEIs and PMEs activities is key for cell wall modification. For example, a disruption of *VANGAURD1* gene, an Arabidopsis PME, resulted in decreased pollen tube growth through style and transmitting tract, which finally caused a significant reduction in male fertility (Jiang et al., 2005). Among 70 PMEIs genes in Arabidopsis, 60 have detectable expression in pollen, based upon our RNA-Seq analysis. Of those 60 genes, 10 showed high expression in pollen comparable to one of the highly expressed pollen specific gene autoinhibited Ca^{2+} ATPAses 9, *ACA9*. Although *PMEI* (AT2G31425) that has been chosen here for functional analysis, does not belong to the ten highly abundant *PMEIs* in pollen, it showed almost an eight-fold increase in transcript abundance under the hot/cold stress condition, suggesting a potential role in heat stress tolerance in pollen.

YABBY transcription factors comprised of eight members in Arabidopsis. YABBY1, 2, and 3 are involved in cell fate determination (Siegfried et al., 1999). Still, functional analysis for the CRABS CLAW (CRC) transcription factor is lacking. Based upon the RNA-Seq data (Figure 1), the CRC transcript reduction seems to be important for pollen fitness under hot/cold stress condition.

Methods

Growth condition and stress treatment

Seeds from both Arabidopsis Columbia wild-type (Col-0) and the mutants following surface-sterilization, were sown on 0.5x Murashige and Skoog (MS) medium (PH = 5.7) containing 1% agar with or without selectable marker. After 48 h of stratification at 4 °C, seedlings were grown at room temperature under constant light for 24 h for ten days. The resulting seedlings were then transferred to the soil (Sunshine SMB-238; Hummert). Unless otherwise stated, seedlings were grown until maturity under controlled non-stress condition in growth chambers with a photoperiod of 16 h light and 8 h dark at 22 °C, 50% humidity, and light intensity of 125 µmol m^{-2} s^{-1}.

The hot days and cold nights stress regime was explained in detail in the Tunc-Ozdemir et al. (2013). For all crosses performed on the stress condition, the pollinated plants were moved to the hot/cold stress chamber within 30 minutes after pollination, when the chamber temperature was 10 ˚C (Chapter 3-Figure 1).

T-DNA insertions

Except for *mirna845a* knockout, we isolated two independent alleles for each gene. For *miRNA845A* (At4g23387), the single allele isolated was Gabi_106_F07 (transgenic line no. 15766). The two independent set of alleles for *MYB-related* (At1g17460) included *myb-related 1-1* (Gabi_406G11; transgenic line no. 15586) and *myb-related 1-2* (*Gabi_453B02;* transgenic line no. 15600).

For *PMEI* (At2g31425), the two independent alleles were *pmei1-1* (Sail_669_H08; transgenic line no. 15580) and *pmei1-2* (Sail_1147_G11; transgenic line no. 15581). For

YABBY (At1g69180), the two independent set of alleles were *yabby1-1* (Sail_686_A03; transgenic line no. 15582) and *yabby1-3* (WiscDSLox382C6; transgenic line no. 15584). All T-DNA insertion alleles were in the wild-type Col-0 background. The selectable marker gene associated with the *mirna845a, myb-related 1-1* and *myb-related 1-2* were sulfonosid. For the *pmei and yabby T-DNA* insertions, a glufosinate (Basta) resistance marker was used.

PCR-based genotyping was used to verify the *T-DNA* insertion position followed by sequencing. The schematic diagram of the gene models, and the corresponding primer positions were shown in Figure 2.

Plasmid construction

To create miRNA overexpressor, around 1 Kb of the DNA sequences surrounding the mature miRNAs were PCR amplified from the genomic DNA derived from the wild-type seedling, and subcloned into a pGREEN binary vector harboring a hygromycin resistance gene marker for selection in plants (Hellens et al., 2000) under the pollen-specific promoter autoinhibited Ca^{2+} ATPAase 9, *ACA9* (plasmid nos. 2213-2216). The resulting constructs were then transformed into the *Agrobacterium* GV3101 strain and the obtained transformed *Agrobacterium* were used for the wild-type Col-0 transformation using the floral dip method (Clough and Bent 1998). Parallel transformations were done with the empty vector (plasmid no. 532). The resulting seeds were harvested, and Hygromycin (25 mg/ml)/Carbanicillin (200 mg/ml)-resistant plants identified.

The resulting transgenic lines (TL) were TL nos. 15789-1-12 for empty vector, TL nos. 15790-1-28 and TL nos. 15791-1-22 for miRNAs overexpressors.

Segregation distortion assay

Heterozygous transgenic lines were used for reciprocal crosses to either wild-type or *cngc16* knockout backgrounds for segregation distortion analyses. For segregation analyses of single knockouts, reciprocal crosses were done with wild-type Col. For the hot/cold stress crosses, plants were moved to the stress chamber 30 minutes after pollination when the temperature inside the chamber was 10 ˚C.

Results

To gain insight into function of genes that were differentially expressed under the condition of hot days and cold nights from our RNA-Seq data (Chapter 3), we selected *MIR845A*, pectin methylesterase inhibitor (*PMEI*), and two transcription factors including *MYB-related* and *YABBY* for further analyses. The expression profiles of these genes (based upon unpublished RNA-Seq data from Harper lab) were shown in the Figure 1. When grown under normal condition, these mutants did not show any visible phenotype, except for *yabby1-1* which showed short, but fat siliques.

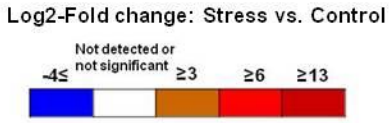

	WT	*cngc16*		Gene name
AT2G25095		ND	MIR156A	
AT4G23387		ND	MIR845A	
AT1G17460			MYB_related	TRF-like 3
AT2G31425			PMEI	
AT1G69180		NS	YABBY	CRC

Figure 1. Heat map showing expression pattern of five genes selected from the RNA-Seq data for further characterization. *MYB-related* and *YABBY* are transcription factors. ND and NS refer to as not detected and not significant, respectively.

A.

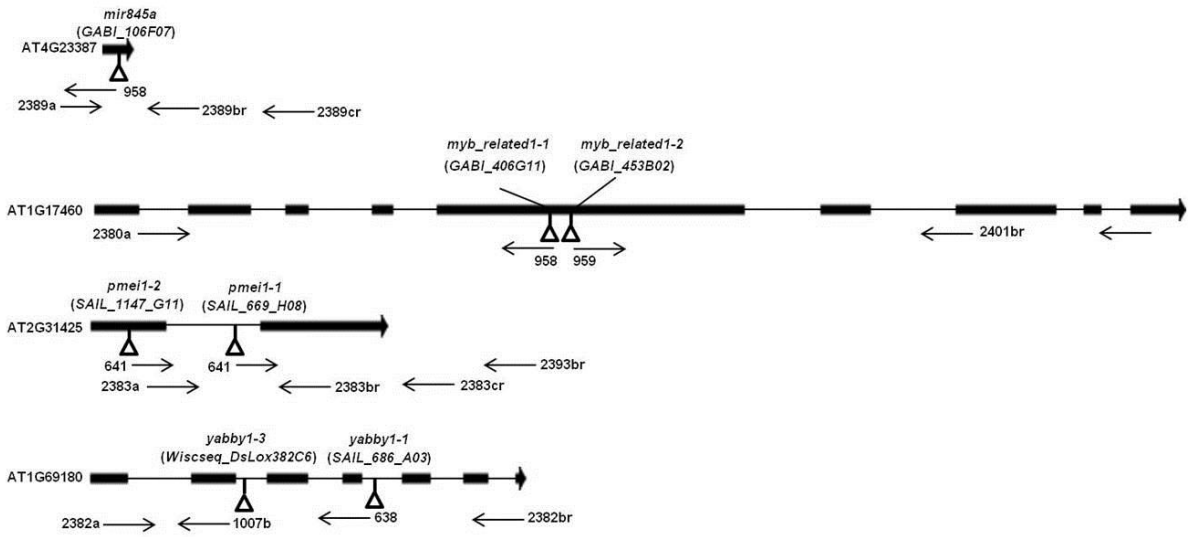

B.

Primer	Sequence (5' to 3' direction)	Purpose
2377h	TTT GGC GCG CCC GGCATTGTTCACTCTCAAATCTCA	Overexpression of MIR156A
2377i	TTT TTCGAA GGCATTGTTCACTCTCAAATCTCA	Overexpression of MIR156A
2377br	CCCGAGCTCGCCAGCTAATCATGCACCTCATGG	Overexpression of MIR156A
2378b	TTT GGC GCG CCC GGC ATTGCACGATTTCTCAATAGTTCCGTCGCT	Overexpression of MIR845A
2378h	TTT TTCGAA GGC ATTGCACGATTTCTCAATAGTTCCGTCGCTG	Overexpression of MIR845A
2378gr	CCCGAGCTCGCCCAGACCATCTAATTTCTGATTTTCATCTC	Overexpression of MIR845A
2389a	TAAGCAGATAAGGGATTGCACG	mir845a T-DNA diagnostics
2389br	CTTCTAGATCTTCAAGAC	mir845a T-DNA diagnostics
2389cr	CGTATCTACCTCTCTGC	mir845a T-DNA diagnostics
2380a	GACTATGGAGAGACGTTTCAAG	myb-related1(-1,-2) T-DNA diagnostics
2380br	CGTGTTTCTTCAGACCTCCTTC	myb-related1(-1,-2) T-DNA diagnostics
2401br	AGCTCTGGCTCCATCATCTCTTGATC	myb-related1-2 T-DNA diagnostics
2383a	CAATGCCAATCTCAGACGTAC	pmei1(-1,-2) T-DNA diagnostics
2383br	GAAAGTGAGAGGAGACTCTTG	pmei1(-1,-2) T-DNA diagnostics
2383cr	CGGGTTTACAACTAGAAGCAG	pmei1-1 T-DNA diagnostics
2393br	CCTTTTTTTATGGATAGGAAATTGTCCTC	pmei1-2 T-DNA diagnostics
2382a	CCATGAACCTAGAAGAGAAACC	yabby1(-1,-3) T-DNA diagnostics
2382br	TTCTTCTCACCGAATCCCAAGC	yabby1(-1,-3) T-DNA diagnostics
958	ATATTGACCATCATACTCATTGC	Gabi T-DNA left border
959	CGCCAGGGTTTTCCCAGTCACGACG	Gabi T-DNA right border
638	GCCTTTTCAGAAATGGATAAATAGCCTTGCTTCC	SAIL T-DNA left border

PCR primer used for overexpression of miRNAs and genotyping of T-DNA insertion lines.

Figure 2. Schematic diagram of gene models and the position of T-DNA insertions.
A) Schematic diagram of gene models were shown. Exons and introns are depicted by boxes and lines, respectively. The positions of *T-DNA* were shown by triangles. Arrows showing the PCR primers used for genotyping.
B) Primer sequences used for PCR-based genotyping and over-expression of two miRNAs are shown.

mir845a disruption showing non-stress and (potential) stress-dependent segregation distortion

To gain insight into function of *MIR845A* which showed an estimated 8,000-fold induction in pollen in response to a heat stress, a *T-DNA* disruption of the gene was obtained and used to conduct a segregation analysis under normal and temperature stress conditions. As evidenced by the segregation analysis (Table 1), *mir845a*$^{(+/-)}$ mutant, which self-fertilized under non-stress condition showed deviation from the normal Mendelian segregation. The observed distortion was 64% from the expected 75%.

To find out the resulting distortion was due to a defect in the male or female side gametophyte, reciprocal crosses were performed, which showed the observed distortion was associated with the female side, but not the male side (38% transmission efficiency instead of the expected 50%, Table 1). While a potential pollen-side distortion was suggested by an outcross done with a hot/cold stress, additional crosses are needed to determine if this distortion is statistically significant.

A disruption of *myb-related transcription factor* failed to show any significant difference to pollen fitness

To determine the role of a *MYB-related* gene in pollen thermotolerance, a segregation analysis was performed for two independent *myb-related-1* T-DNA insertion alleles. Under the normal condition, no deviation was observed from normal Mendelian segregation in cases of both self-fertilization event and reciprocal crosses (Table 1). While a potential pollen-side distortion was suggested by an outcross done with *myb-related1-1* under the conditions of a hot/cold stress, no distortion was observed for the second set of allele *myb-related1-2* tested. Because the two *T-DNA* insertions are very

close together, suggesting they may be a single insertion. Additional crosses are needed to determine if the distortion associated with *myb-related1-1* is statistically significant.

pmei and *yabby* disruptions showing no deviation from normal Mendelian segregation

To determine role of *PMEI* and *YABBY* genes in pollen, a segregation analysis was conducted on *T-DNA* insertions in each gene. Results indicated normal Mendelian segregation under normal or stress condition for single allele tested, which suggest that these genes do not make a significant contribution to pollen fitness under the conditions of tested here. However, in both *pmei1-1* and *yabby1-1*, the *T-DNA* insertion positions are located in an intron, which may be spliced out, and thus may still provide some level of functional transcript. Another possibility is that loss-of-function of these genes may be compensated by the other gene family members. For example, out of 70 *PMEIs* in Arabidopsis, 60 isoforms have detectable mRNA expression in pollen, and thus might provide some level of functional redundancy.

Improving pollen thermotolerance by overexpression of miRNAs

To identify function of the two miRNAs *MIR156A* and *MIR845A* (Figure 1) in pollen, we over-expressed these two genes under the control of the pollen-specific promoter that drives the expression of an autoinhibited Ca^{2+}-ATPase 9 (*ACA9*). The first generation of transgenic lines was used for reciprocal crosses with either the wild-type plant or *cngc16* knockout. Male-sterile (*ms-1*) plants were used for hot/cold stress crosses. The preliminary results suggest *MIR156A*-dependent improvement in pollen fitness in both wild-type and *cngc16* backgrounds under the hot/cold stress condition. Additional crosses

are needed to determine if the preliminary results are statistically significant. Whereas hot/cold stress crosses for *MIR845A* overexpressor lines in both backgrounds have thus far failed for technical reasons, additional crosses are in progress.

Table 1. Segregation analyses of pollen knockouts.

	Cross	Condition	F1	Segregation of T-DNA marker gene		
KO analyzed	Female x Male		total	Expected %	Observed %	*P*-value[a]
mir845a	*mir845a*$^{(+/-)}$; Selfed[b]	Control	661	75	64	<0.0001
	mir845a$^{(+/-)}$ X WT[b]	Control	196	50	38	0.05
	WT X *mir845a*$^{(+/-)}$[b]	Control	181,171,175,248	50	50,47,44,55	1,0.8,0.8,0.8
	ms-1 X *mir845a*$^{(+/-)}$[b]	Hot/Cold	62	50	39	0.8
myb_related1-1	*myb1-1*$^{(+/-)}$; Selfed[b]	Control	104,122	75	78,74	0.8,0.9
	myb1-1$^{(+/-)}$ X WT[b]	Control	383	50	49	0.9
	WT X *myb1-1*$^{(+/-)}$[b]	Control	211	50	49	0.8
	ms-1 X *myb1-1*$^{(+/-)}$[b]	Hot/Cold	5	50	0	0.2
myb_related1-2	*myb1-2*$^{(+/-)}$ X WT[b]	Control	451	50	49	0.9
	ms-1 X *myb1-2*$^{(+/-)}$[b]	Hot/Cold	478	50	53	0.8
pmei1-1	*pmei1-1*$^{(+/-)}$; Selfed[c]	Control	179,167,163	75	70,83,76	0.8,0.8,0.9
	pmei1-1$^{(+/-)}$ X WT[c]	Control	221	50	49	0.9
	WT X *pmei1-1*$^{(+/-)}$[c]	Control	675	50	48	0.8
	ms-1 X *pmei1-1*$^{(+/-)}$[c]	Hot/Cold	101	50	43	0.8
yabby1-1	*yabby1-1*$^{(+/-)}$; Selfed[c]	Control	220,373	75	79,78	All 0.8
	yabby1-1$^{(+/-)}$ X WT[c]	Control	259	50	49	0.9
	WT X *yabby1-1*$^{(+/-)}$[c]	Control	415	50	44	0.2
	ms-1 X *yabby1-1*$^{(+/-)}$[c]	Hot/Cold	21	50	48	0.9

a. Significance determined by the Pearson's chi-squared test and degree of freedom one.

b. Scored for Sulf^{r}

c. Scored for Bast$^{a r}$

WT and ms-1 refer to the wild type and male sterile plants, respectively.

Table 2. Over-expression of *MIR156A* in wild type and *cngc16* suggesting hint of improvement in pollen thermotolerance.

Cross		F1	Segregation of Hygromycin marker gene		
Female x Male	Condition	total	Expected %	Observed %	*P*-value[a]
ACA9P::YFP/WT Col (TG) X WT Col	Control	44	50	52	0.9
WT Col X *ACA9P::YFP/WT Col* (TG)	Control	118	50	50	1
***ms-1* X *ACA9P::YFP/WT Col* (TG)**	**Hot/cold**	**13**	**50**	**46**	**0.9**
ACA9P::MIR156A/WT Col (TG) X WT Col	Control	74,112,127	50	50,46,49	All 0.8
WT Col X *ACA9P::MIR156A/WT Col (TG)*	Control	160,95,87	50	54,54,46	All 0.8
ms-1* X *ACA9P::MIR156A/WT Col (TG)	**Hot/cold**	**19,7,18**	**50**	**63,71,61**	**All 0.8**
ACA9P::MIR845A/WT Col (TG) X WT Col	Control	46	50	48	0.9
WT Col X *ACA9P::MIR845A/WT Col (TG)*	Control	74	50	43	0.8
ACA9P::MIR156A/cngc16$^{(-/-)}$ (TG) X *cngc16*$^{(-/-)}$	Control	102	50	50	1
cngc16$^{(-/-)}$ X *ACA9P::MIR156A/cngc16*$^{(-/-)}$*(TG)*	Control	164	50	55	0.8
ms-1* X *ACA9P::MIR156A/cngc16*$^{(-/-)}$ *(TG)	**Hot/cold**	**6**	**50**	**67**	**0.8**
ACA9P::MIR845A/cngc16$^{(-/-)}$ (TG) X *cngc16*$^{(-/-)}$	Control	72,57,20	50	47,49,55	0.8,0.95,0.8
cngc16$^{(-/-)}$ X *ACA9P::MIR845A/cngc16*$^{(-/-)}$*(TG)*	Control	145,114,64	50	47,49,47	0.8,0.95,0.8

a. Significance determined by the Pearson's chi-squared test.

WT, ms, and TG refer to wild type, male sterile, and transgenic line respectively.

Hot/cold crosses are shown in bold.

Discussion

The RNA-Seq experiment (chapter 3) identified numerous genes of potential importance to thermotolerance in pollen. Here, we chose candidate genes and initiated experiments to evaluate their individual contribution to pollen fitness under a hot/cold stress regime. These genes included two miRNAs (*MIR156A* and *MIR845A*), *PMEI*, and two transcription factors *MYB-related* and *YABBY*.

Although the transcript abundances of *MYB-related*, *PMEI* and *YABBY* showed big changes under the hot/cold stress condition used here (64- and 8-fold induction for *MYB-related* and *PMEI*, and 16-fold reduction for the *YABBY*), corresponding gene knockouts tested failed to show any evidence of their importance to pollen fitness under normal or stress conditions. However, as explained earlier, this might be due to either leaky mutation or functional redundancy. More crosses are in progress for further analyses.

Disruption of *MIR845A* seems to impair plant reproductive systems

MIR845A is a non-conserved miRNA that lacks a functional target (Qin et al., 2014). So far, only a study in rice proposed the predicated target for *MIR845A* as a gene with DNA integration function.

A plant line harboring *mir845a*$^{(+/-)}$ was allowed to self-fertilize under control condition and showed a segregation distortion in which the observed transmission was 64% compared to the expected 75% (Table 1). As evidenced by the reciprocal crosses, this defect was due to reduced transmission efficiency of the female side rather than the male gametophyte. This implies that the *MIR845A* gene might also be expressed in the female gametophyte under normal conditions, and a loss-of-function results in a reduced

transmission efficiency through the female gametophyte. However, the pollen outcross to a *ms-1* plant under the hot/cold stress condition also showed a hint of a pollen deficiency with a reduced transmission efficiency from an expected 50% down to 39%.

Over-expression of *MIR156A* seems to be improving pollen heat stress response in wild-type and *cngc16* knockout

The over-expression of both miRNAs in the wild-type and *cngc16* knockout pollen did not show any changes in transmission efficiency of pollen under non-stress condition (Table 2). However, over-expression of *MIR156A* in the wild-type and *cngc16* mutant under the temperature stress condition seems to be improving the pollen transmission efficiency by an average of 65% from the expected 50%. To corroborate the preliminary results, more crosses are needed to see statistically significant changes.

The preliminary results obtained here are in agreement with previous studies showing role of miRNAs in plant heat stress tolerance. For example, over-expression of *MIR156A* has been shown to confer stress tolerant to the recurring heat stress through suppression of the plant SPL transcription factors in Arabidopsis seedlings (Stief et al., 2014). Plant thermotolerance has also been observed due to overexpression of the Arabidopsis *MIR173* (Li et al., 2014).

Conclusion and Future direction

Taken together, our preliminary results suggest the potential importance of *MIR845A* and *MIR156A* in pollen heat stress response. A loss-of-function of *mir845a* resulted in reduced transmission efficiency due to female side defect. The outcross to *ms-1* plant suggests *MIR845A* might be also important for pollen transmission under hot/cold stress condition. We isolated only one *T-DNA* insertion allele for the *mir845a* (there was not

any other *T-DNA* insertion in the Salk site in *MIR845A* gene), it requires a rescue approach to verify that the observed phenotype was due to a loss-of-function of the *MIR845A* gene.

Overexpression of *MIR156A* also seems to improve pollen fitness under temperature stress. Second generations of crosses are in progress to corroborate these preliminary results.

Segregation analyses have been so far suggested *PMEI* and transcription factors *MYB-related* and *YABBY* are not critical for pollen heat stress tolerance. However, for all three genes more crosses need to be performed to confirm these preliminary results.

References

Bokszczanin KL, Solanaceae Pollen Thermotolerance Initial Training Network (SPOT-ITN) Consortium, Fragkostefanakis S (2013) Perspectives on deciphering mechanisms underlying plant heat stress response and thermotolerance. Frontiers in Plant Science 4: 1-20.

Clough SJ, Bent AF (1998) Floral dip: a simplified method for Agrobacterium-mediated transformation of *Arabidopsis thaliana*. The Plant Journal 16: 735-743.

Firon N, Shaked R, Peet MM, Pharr DM, Zamski E, Rosenfeld K, Althan L, Pressman E (2006) Pollen grains of heat tolerant tomato cultivars retain higher carbohydrate concentration under heat stress conditions. Scientia Horticulturae 109: 212-217.

Fourquin C, Primo A, Martínez-Fernández I, Huet-Trujillo E, Ferrándiz C (2014) The CRC orthologue from Pisum sativum shows conserved functions in carpel morphogenesis and vascular development. Annals of Botany 114: 1535-1544.

Gupta PK (2015) MicroRNAs and target mimics for crop improvement. Current Science 108: 1624-1633.

Hellens RP, Edwards EA, Leyland NR, Bean S, Mullineaux PM (2000) pGreen: a versatile and flexible binary Ti vector for Agrobacterium-mediated plant transformation. Plant Molecular Biology 42: 819-832.

Hopf N, Plesofsky-Vig N, Brambl R (1992) The heat shock response of pollen and other tissues of maize. Plant Molecular Biology 19: 623-630.

Hothorn M, Wolf S, Aloy P, Greiner S, Scheffzek K (2004) Structural insights into the target specificity of plant invertase and pectin methylesterase inhibitory proteins. The Plant Cell 16: 3437-3447.

Li S, Liu J, Liu Z, Li X, Wu F, He Y (2014) HEAT-INDUCED TAS1 TARGET1 mediates thermotolerance via HEAT STRESS TRANSCRIPTION FACTOR A1a-directed pathways in Arabidopsis. The Plant Cell 26: 1764–1780.

Lionetti V, Raiola A, Camardella L, Giovane A, Obel N, Pauly M, Favaron F, Cervone F, Bellincampi D (2007) Overexpression of Pectin Methylesterase Inhibitors in Arabidopsis Restricts Fungal Infection by *Botrytis cinerea*. Plant Physiology 143: 1871-1880.

Mittler R (2006) Abiotic stress, the field environment and stress combination. Trends in Plant Science 11: 15-19.

Pressman E, Peet MM, Pharr DM (2002) The Effect of Heat Stress on Tomato Pollen Characteristics is Associated with Changes in Carbohydrate Concentration in the Developing Anthers. Annals of Botany 90: 631-636.

Qin Z, Li C, Mao L, Wu L (2014) Novel insights from non-conserved microRNAs in plants. Frontiers in Plant Science 5: 586-596.

Röckel N, Wolf S, Kost B, Rausch T, Greiner S (2008) Elaborate spatial patterning of cell-wall PME and PMEI at the pollen tube tip involves PMEI endocytosis, and reflects the distribution of esterified and de-esterified pectins. The Plant Journal 53: 133-143.

Saidi Y, Finka A, Muriset M, Bromberg Z, Weiss YG, Maathuis FJM, Goloubinoff P (2009). The eat shock response in moss plants is regulated by specific calcium-permeable channels in the plasma membrane. The Plant Cell 21: 2829–2843.

Steiner-Lange S, Unte US, Eckstein L, Yang C, Wilson ZA, Schmelzer E, Dekker K, Saedler H (2003) Disruption of *Arabidopsis thaliana MYB26* results in male sterility due to non-dehiscent anthers. The Plant Journal 34: 519-528.

Stief A, Altmann S, Hoffmann K, Pant BD, Scheible W, Bäurle I (2014) *Arabidopsis miR156* Regulates Tolerance to Recurring Environmental Stress through *SPL* Transcription Factors. The Plant Cell 26: 1792-1807.

Tunc-Ozdemir M, Tang C, Rahmati Ishka M, Brown E, Groves NR, Myers CT, Rato C, Poulsen LR, McDowell S, Miller G, Mittler R, Harper JF (2013) A cyclic nucleotide-gated channel (CNGC16) in pollen is critical for stress tolerance in pollen reproductive development. Plant Physiology 161: 1010-1020.

Volkov RA, Panchuk II, Schöffl F (2005) Small heat shock proteins are differentially regulated during pollen development and following heat stress in tobacco. Plant Molecular Biology 57: 487-502.

Xiong H, Li J, Liu P, Duan J, Zhao Y, Guo X, Li Y, Zhang H, Ali J (2014) Overexpression of OsMYB48-1, a Novel MYB-Related Transcription Factor, Enhances Drought and Salinity Tolerance in Rice. PLoS ONE 9: e92913.

Yanhui C, Xiaoyuan Y, Kun H, Meihua L, Jigang L, Zhaofeng G, Zhiqiang L, Yunfei Z, Xiaoxiao W, Xiaoming Q, Yunping S, Li Z, Xiaohui D, Jingchu L, Xing-Wang D, Zhangliang C, Hongya G, Li-Jia Q (2006) The MYB transcription factor superfamily of Arabidopsis: expression analysis and phylogenetic comparison with the rice MYB family. Plant Molecular Biology 60: 107-124.

Young LW, Wilen RW, Bonham-Smith PC (2004) High temperature stress of Brassica napus during flowering reduces micro- and megagametophyte fertility, induces fruit abortion, and disrupts seed production. Journal of Experimental Botany 55: 485-495.

Zinn KE, Tunc-Ozdemir M, Harper JF (2010) Temperature stress and plant sexual reproduction: uncovering the weakest links. Journal of Experimental Botany 61: 1959-68.

Ambawat S, Sharma P, Yadav NR, Yadav RC (2013) MYB transcription factor genes as regulators for plant responses: an overview. Physiology and Molecular Biology of Plants 19: 307–321.

Steiner-Lange S, Unte US, Eckstein L, Yang C, Wilson ZA, Schmelzer E, Dekker K, Saedler H (2003) Disruption of *Arabidopsis thaliana* MYB26 results in male sterility due to non-dehiscent anthers. Plant Journal 34: 519–528.

Higginson T, Li SF, Parish RW (2003) AtMYB103 regulates tapetum and trichome development in Arabidopsis thaliana. Plant Journal 35: 177–192.

Jiang L, Yang SL, Xie LF, Puah CS, Zhang XQ, Yang WC, Sundaresan V, Ye D (2005) VANGUARD1 encodes a pectin methylesterase that enhances pollen tube growth in the Arabidopsis style and transmitting tract. Plant Cell 17: 584-596.

Siegfried KR, Eshed Y, Baum SF, Otsuga D, Drews GN, Bowman JL (1999) Members of the YABBY gene family specify abaxial cell fate in Arabidopsis. Development 126: 4117-4128.

Chapter V.

Conclusion and Future Direction

Ca^{2+} circuits, which are created by action of Ca^{2+} influx and Ca^{2+} efflux systems, are critical for all types of living organisms. Heat stress senesced by the plasma membrane, which in turn results in increase in Ca^{2+} influx, and finally activation of Ca^{2+} sensors such as Ca^{2+}-dependent protein kinases (Saidi 2009). The rise in cytosolic Ca^{2+} is restored to basal levels by Ca^{2+} transporters such as ACAs. In the preceding chapters, we addressed two main subjects: functional characterization of Ca^{2+} ATPases 1, 2, and 7 (ACA1, 2, and 7) and a transcriptome comparison of wild-type pollen with *cngc16* knockout pollen under the condition of a hot/cold stress condition.

Functional analysis of Arabidopsis Ca^{2+}-ATPases

In chapter II, we described the results of functional analysis of a subgroup of Ca^{2+}-ATPases with 3 members: ACA1, 2 and ACA7. In addition, we reexamined ACA1 and ACA7 subcellular localization.

Because ACA1, 2, and 7 branch together in phylogenetic tree, the speculation is that they provide some level of redundancy. Based upon this, we created a triple knockout plant. Using two different sets of *T-DNA* alleles (Chapter 2- Figure 1), we created two triple knockouts. Both triple knockout plants showed a leaf lesion phenotype (Chapter 2- Figure 2). Both triple mutants showed reduction in their leaf size compared to their wild-type backgrounds. Vegetative expressions of any of the three ACAs isoforms precluded the lesion phenotype and restored leaf size (Chapter 2- Figure 2). In addition, we further examined lesion suppression in the rescued lines by measuring the transcript abundances

of a *PR1* gene, which has been used as a marker for the activation of a pathogen defense response. The RT-PCR results showed *PR1* level decreased in the rescued lines to a greater extent, indicating suppression of lesion phenotype (Chapter 2- Figure 2).

The link between the ACA4 and 11 vacuole Ca^{2+} pumps and salicylic acid (SA)-dependent lesion phenotype has been described in a previous study (Boursiac et al., 2010). To determine the observed lesion phenotype of *aca1/2/7* is also dependent on SA production, we expressed the *NahG* transgene (Gaffney et al., 1993; Delaney et al., 1994), a SA degradation enzyme. The result showed expression of *NahG* transgene can reverse the *aca1/2/7* lesion phenotype (Chapter 2- Figure 3). To further verify the result, we measured *PR1* level in the *aca1/2/7* mutant harboring a *NahG* transgene. The results showed *PR1* transcript abundance was significantly reduced in triple knockout plants carrying the *NahG* gene (Chapter 2- Figure 3), indicating ACA1, 2, and 7 control an SA-dependent programmed cell death pathway.

A phenotypic comparison of *aca1/2/7* triple knockout with *aca4/11* double knockout suggests that although a loss of either group of Ca^{2+} pumps results in lesions, the type of lesion is different. This was evidenced by high frequency of rapidly expanding lesions in *aca4/11,* but not in *aca1/2/7* (Chapter 2- Figure 2). The *PR1* expression level did not show any differences between *aca1/2/7* and *aca4/11* mutant (Chapter 2- Figure 3), indicating *PR1* marker is being expressed systemically after lesion initiation, and it is not dependent upon the degree of lesion. Boursiac et al. (2010) showed *aca4/11* lesion phenotype was suppressed by growing double knockout plants in high concentrations of anions such as 15 mM NO_3^-. Thus, it will be important for the future to test hypothesis concerning the differences in the lesion phenotypes caused by *aca1/2/7* compared to

aca4/11. The fact that loss of *aca4/11* Ca^{2+} pumps do not impair pollen fitness (Chapter 2- Table 2), in contrast to *aca1/2/7*, supports the idea that *aca12/7* and *aca4/11* have different roles, consistent with the idea that different Ca^{2+} stores (ER vs vacuole) are used for different signaling pathways in plant cells. One interesting experiment to consider is whether the lesions associated with the *aca1/2/7* triple knockout can be suppressed by high concentrations of anions, such as 15 mM NO_3^- , as observed for the aca4/11 phenotype.

Whereas loss of function of each individual gene (*aca1, or 2, or 7* alone) did not show any deviation from Mendelian segregation (Chapter 2- Table 1), loss of function of all three isoforms compromised pollen fitness as evidenced by segregation distortion analyses (Chapter 2- Table 2). Pollen-specific expression of any of the three isoforms improved *aca1/2/7* pollen fitness to a greater extent (Chapter 2- Figure 4). Together these results suggest that ACA1, 2, and 7 provide some level of functional redundancy.

Segregation analysis showed *aca1/2/7* mutants have reduced pollen transmission efficiency (30% from the expected 50%). Thus, to get more insight into the mechanisms underlying the *aca1/2/7* pollen transmission defect, we performed a competition assay in which an outcross was done with a 1:1 ratio of mutant and wild-type pollen, and the resulting seeds from the fertilized siliques harvested by dividing siliques into three sectors, a top, middle and bottom. The resulting seed were germinated and scored for Basta-resistance, which is diagnostic of fertilization by a *aca1/2/7* triple knockout pollen. While each sector showed a significant reduction of Basta-resistant seed from an expected 50%, the top sector (nearest the stigma end) showed the greatest distortion (Chapter 2- Figure 5). This poor success in competing for successful fertilization at the

top of the silique was corroborated with an independent strategy in which all of the pollen were mutant, and half the pollen harbored a rescue construct. In this case, the rescued pollen showed a competitive advantage in fertilizing the top of the silique. It is not clear why mutant pollen are less competitive in fertilizing ovules at the top of the ovary. One possible explanation is that mutant pollen tubes might be slower in changing directions in response to a guidance cue released from the ovule. While this slow response might contribute to a reduced level of competitiveness throughout the ovary, this deficiency might be more pronounced at the top of ovary where a mutant might have to turn around and grow back to find the ovule that it missed. By the time the tube turns around, there is an increased chance that a wild-type tube will have targeted and fertilized the 1st few ovules in the ovary. One way to examine this hypothesis is to use aniline blue staining method to visualize pollen tube growth patterns near the top of the ovary.

Lastly, using confocal microscopy and genetic approaches, we showed ACA1 and ACA7, the close homologues of ACA2, target ER and endomembrane-ER like structure, respectively.

Comparing Ca^{2+} signatures created due to loss of Ca^{2+} pumps (vacuole *vs.* ER) is one goal for future research. To determine whether the shape of a Ca^{2+} signature is different in the *aca1/2/7* mutant compared to the vacuolar *aca4/11* mutant, a good experimental approach is to transform mutant and wild-type plants with Ca^{2+} reporters such as Yellow Cameleon-Nano65 (YC-Nano65) (Horikawa et al., 2010), which is sensitive to subtle changes in intracellular Ca^{2+}.

Transcriptome comparison of Arabidopsis wild-type pollen and *cngc16* knockout pollen under hot/cold condition

In chapter III and IV, we presented the results from a pollen transcriptome analysis that compared wild-type pollen with *cngc16* knockout pollen under the conditions of hot/cold stress, and a functional characterization of some gene candidates, respectively.

Our transcriptome analysis is unique at least in two aspects. First, it is the first RNA-Seq experiment done in heat-stressed Arabidopsis pollen, which represents a cell-autonomous system for exploring how a plant cell responds to stress. Second, it is the first RNA-Seq experiment conducted to compare a wild-type stress response with a mutant that has an attenuated heat stress response (i.e., *cngc16* as described in Tunc-Ozdemir et al., 2013). The results showed *cngc16* knockout failed to show 25% (= 641 changes, Chapter 3-Figure 2) of the stress-dependent responses of transcript abundances observed in wild-type. In addition, 148 transcription factors (Chapter 3-Figure 3 and Supplementary Table S12) showed mis-regulation under the heat stress in *cngc16* knockout. These mis-regulated transcription factors might contribute to causing the additional 2,733 transcriptome changes in *cngc16* pollen that are not present in wild-type.

Many studies have shown the importance of small non-coding RNAs (sncRNAs) such as miRNAs in plant adaptation to different environmental stimuli including both biotic and abiotic stresses. *MIR845A* has been shown to be up-regulated in drought stress in rice (Sunkar et al., 2008; Zhou et al., 2010) and in response to fungus *Exserohilum turciucum* in maize (Wu et al., 2014).

MIR156A is one of the well-studied miRNAs. Its role in plant adaptation in different plant species has recently been documented (Serivichyaswat et al., 2015; Steif et al.,

2014; Sunkar et al., 2012). During stresses, transcript abundance of *MIR156A* increases, and in turn, suppresses a group of transcription factors known as *SQUAMOSA PROMOTER BINDING PROTEIN-LIKE* (*SPL*). Recently, a study in heat stressed tomato pollen suggested role of miRNAs in pollen heat stress response (Bokszczanin et al., 2015).

To get more insight into mechanisms underlying the *cngc16* mutant hypersensitivity, we used loss-of-function and gain-of-function approaches to characterize biological function of the two identified miRNAs as well as other gene candidates with potential of importance in pollen adaptation to heat stress. In Chapter IV, we discussed the preliminary results from the functional analyses of RNA-Seq experiment.

Wild-type and *cngc16* knockout were stably transformed with a pollen-specific expression of the two miRNAs *MIR156A* and *MIR845A*. To determine whether these two miRNAs could improve the pollen fitness under the heat stress, segregation analyses were done. The preliminary results suggest *MIR156A* might have function in pollen heat stress response in both wild-type and *cngc16* (Chapter 4-Table 2). However, more crosses will be needed to corroborate the preliminary results.

We also isolated *T-DNA* knockouts for *mir845a*, *myb-related*, *pmei*, and *yabby*. For all knockouts, except for *mir845a*, two independent sets of alleles were examined for their potential defect in pollen transmission. Among all of those knockouts tested, our preliminary results showed *mir845a* knockout has reduced transmission efficiency due to a female-side defect (Chapter 4-Table 1). The hot/cold stress cross suggests it may also

have a defect in male transmission efficiency (Chapter 4-Table 1). More hot/cold crosses will be needed to confirm these initial results.

From > 2,000 differentially expressed transcripts identified in heat-stressed wild-type pollen, we selected a subset of genes for further characterization. All those statistically significant changes have potential to play a role in pollen heat-stress response. Most of genes belong to gene families that might encode isoforms with redundant functions. Thus, for functional analyses, it might be necessary to knockout related genes. For example, one possible reason that we did not observe any defect associated with the *pmei1-1* knockout would be compensation by other family members expressed in pollen. Out of 70 *PMEIs* in Arabidopsis, 60 had detectable expression in our RNA-Seq data, suggesting possible functional redundancy, at least, for some of these isoforms.

Preliminary analysis of our RNA-Seq data (not shown in this dissertation) revealed 317 putative genes that have not yet been identified and annotated in the Arabidopsis reference genome (TAIR10). Of these, 133 showed stress-dependent changes in transcript abundances. As a future direction, more in-depth analyses such as Integrative Genome Browser (IGB) inspection will be required to verify these new genes. Our primary investigation showed at least some of these putative novel genes contain *T-DNA* insertions which provide valuable source for future functional analyses.

Another important goal for future research will be to determine the functions for almost 1,500 genes with unknown functions, which comprise of almost 60% of the pollen transcriptome. Together, these RNA-Seq data provide a valuable resource for the research community to explore genes function in the plant male reproductive system.

References

Bokszczanin KL, Krezdorn N, Fragkostefanakis S, Müller S, Rycak L, Chen Y, Hoffmeier K, Kreutz J, Paupière MJ, Chaturvedi P, Iannacone R, Müller F, Bostan H, Chiusano ML, Scharf K, Rotter B, Schleiff E, Winter P, SPOT-ITN Consortium (Solanaceae Pollen Thermotolerance Initial Training Network Consortium) SPOT-ITN Consortium (Solanaceae Pollen Thermotolerance Initial Training Network Consortium) (2015) Identification of novel small ncRNAs in pollen of tomato. BMC Genomics 16: 714-733.

Boursiac Y, Lee SM, Romanowsky S, Blank R, Sladek C, Chung WS, Harper JF (2010) Disruption of the vacuolar calcium-ATPases in Arabidopsis results in the activation of a salicylic acid-dependent programmed cell death pathway. Plant Physiology 154: 1158-1171.

Delaney TP, Uknes S, Vernooji B, Friedrich L, Weymann K, Negrotto D, Gaffney T, Gut-Rella M, Kessmann H, Ward E, Ryals J (1994) A central role in salicylic acid in plant disease resistance. Science 266: 1247-1250.

Gaffney T, Friedrich L, Vernooij B, Negrotto D, Nye G, Uknes S, Ward E, Kessmann H, Ryals J (1993) Requirement of salicylic acid for the induction of systemic acquired resistance. Science 261: 754-756.

Serivichyaswat P, Ryu HS, Kim W, Kim S, Chung KS, Kim JJ, Ahn JH (2015) Expression of the Floral Repressor miRNA156 is Positively Regulated by the AGAMOUS-like Proteins AGL15 and AGL18. Molecules and Cells 38: 259–266.

Stief A, Altmann S, Hoffmann K, Datt Pant B, Scheible W, Bäurle I (2014) *Arabidopsis miR156* Regulates Tolerance to Recurring Environmental Stress through *SPL* Transcription Factors. The Plant Cell 26: 1792-1807.

Sunkar R, Li Y, Jagadeeswaran G (2012) Functions of microRNAs in plant stress responses. Trends in Plant Cell 17: 196-203.

Sunkar R, Zhou X, Zheng Y, Zhang W, Zhu JK (2008) Identification of novel and candidate miRNAs in rice by high throughput sequencing. BMC Plant Biology 8: 1-17.

Tunc-Ozdemir M, Tang C, Rahmati Ishka M, Brown E, Groves NR, Myers CT, Rato C, Poulsen LR, McDowell S, Miller G, Mittler R, Harper JF (2013) A cyclic nucleotide-gated channel (CNGC16) in pollen is critical for stress tolerance in pollen reproductive development. Plant Physiology 16: 1010-1020.

Wu F, Shu J, Jin W (2014) Identification and Validation of miRNAs Associated with the Resistance of Maize (*Zea mays L.*) to *Exserohilum turcicum*. PLoS ONE 9: e87251.

Zhou L, Liu Y, Liu Z, Kong D, Duan M, Luo L (2010) Genome-wide identification and analysis of drought-responsive microRNAs in *Oryza sativa*. Journal of Experimental Botany 61: 4157-4168.

Saidi Y, Finka A, Muriset M, Bromberg Z, Weiss YG, Maathuis FJM, Goloubinoff P (2009). The eat shock response in moss plants is regulated by specific calcium-permeable channels in the plasma membrane. The Plant Cell 21: 2829–2843.

Kazuki Horikawa K, Yamada Y, Matsuda T, Kobayashi K, Hashimoto M, Matsu-ura T, Miyawaki A, Michikawa T, Mikoshiba K, Nagai T (2010) Spontaneous network activity visualized by ultrasensitive Ca^{2+} indicators, yellow Cameleon-Nano. Nature Methods 7: 729–732.